

Available online at [www.sciencedirect.com](http://www.sciencedirect.com)

SCIENCE @ DIRECT®

Ore Geology Reviews xx (2005) xxx–xxx

ORE GEOLOGY  
REVIEWS[www.elsevier.com/locate/oregeorev](http://www.elsevier.com/locate/oregeorev)

## Precambrian geodynamics and ore formation: The Fennoscandian Shield

Pär Weihed<sup>a,\*</sup>, Nicholas Arndt<sup>b</sup>, Kjell Billström<sup>c</sup>, Jean-Clair Duchesne<sup>d</sup>, Pasi Eilu<sup>e</sup>,  
Olof Martinsson<sup>a</sup>, Heikki Papunen<sup>f</sup>, Raimo Lahtinen<sup>e</sup>

<sup>a</sup> Division of Ore Geology and Applied Geophysics, Luleå University of Technology, SE-971 87 Luleå, Sweden

<sup>b</sup> LGCA, Université Joseph Fourier, Grenoble, Maison des Géosciences 1381, rue de la Piscine 38400 Saint Martin d'Heres, France

<sup>c</sup> Swedish Museum of Natural History, Stockholm, Box 50007, SE-10405, Sweden

<sup>d</sup> University of Liège Bat. B20, B-4000 Sart Tilman, Belgium

<sup>e</sup> Geological Survey of Finland, PO Box 96, FIN-02151 Espoo, Finland

<sup>f</sup> Department of Geology, University of Turku FIN-20014 Turku, Finland

Received 2 July 2004; accepted 6 July 2005

### Abstract

Compared with present-day global plate tectonics, Archaean and Palaeoproterozoic plate tectonics may have involved faster moving, hotter plates that accumulated less sediment and contained a thinner section of lithospheric mantle. This scenario also fits with the complex geodynamic evolution of the Fennoscandian Shield from 2.06 to 1.78 Ga when rapid accretion of island arcs and several microcontinent–continent collisions in a complex array of orogens was manifested in short-lived but intense orogenies involving voluminous magmatism. With a few exceptions, all major ore deposits formed in specific tectonic settings between 2.06 and 1.78 Ga and thus a strong geodynamic control on ore deposit formation is suggested.

All orogenic gold deposits formed syn- to post-peak metamorphism and their timing reflects the orogenic younging of the shield towards the SW and west. Most orogenic gold deposits formed during periods of crustal shortening with peaks at 2.72 to 2.67, 1.90 to 1.86 and 1.85 to 1.79 Ga.

The ca. 2.5 to 2.4 Ga Ni–Cu ± PGE deposits formed both as part of layered igneous complexes and associated with mafic volcanism, in basins formed during rifting of the Archaean craton at ca. 2.5 to 2.4 Ga. Svecokarelian ca. 1.89 to 1.88 Ga Ni–Cu deposits are related to mafic–ultramafic rocks intruded along linear belts at the accretionary margins of microcratons.

All major VMS deposits in the Fennoscandian Shield formed between 1.97 and 1.88 Ga, in extensional settings, prior to basin inversion and accretion. The oldest “Cyprus-type” deposits were obducted onto the Archaean continent during the onset of convergence. The Pyhäsalmi VMS deposits formed at 1.93 to 1.91 Ga in primitive, bimodal arc complexes during extension of the arc. In contrast, the Skellefte VMS deposits are 20 to 30 million years younger and formed in a strongly extensional intra-arc region that developed on continental or mature arc crust. Deposits in the Bergslagen–Uusimaa belt are similar in age to the Skellefte deposits and formed in a microcraton that collided with the Karelian craton at ca. 1.88 to 1.87 Ga. The Bergslagen–

\* Corresponding author.

E-mail address: [par.weihed@ltu.se](mailto:par.weihed@ltu.se) (P. Weihed).

33 Uusimaa belt is interpreted as an intra-continental, or continental margin back-arc, extensional region developed on older  
34 continental crust.

35 Iron oxide–copper–gold (IOCG) deposits are diverse in style. At least the oldest mineralizing stages, at ca. 1.88 Ga, are  
36 coeval with calc-alkaline to monzonitic magmatism and coeval and possibly cogenetic subaerial volcanism more akin to  
37 continental arcs or to magmatic arcs inboard of the active subduction zone. Younger mineralization of similar style took place  
38 when S-type magmatism occurred at ca. 1.80 to 1.77 Ga during cratonization distal to the active N–S-trending subduction zone  
39 in the west. Possibly, interaction of magmatic fluids with evaporitic sequences in older rift sequences was important for ore  
40 formation.

41 Finally, the large volumes of anorthositic magmas that characterize the Sveconorwegian Orogeny formed a major  
42 concentration of Ti in the SW part of the Sveconorwegian orogenic belt under granulite facies conditions, about 40 million  
43 years after the last regional deformation of the Sveconorwegian Orogeny, between ca. 930 and 920 Ma.

44 © 2005 Elsevier B.V. All rights reserved.

45 *Keywords:* Palaeoproterozoic; Fennoscandian Shield; VMS; Orogenic gold; Iron oxide–copper–gold (IOCG); Anorthosite; Titanium deposit

46

## 47 1. Introduction

48 The Fennoscandian Shield forms the north-wes-  
49 ternmost part of the East European craton and con-  
50 stitutes large parts of Finland, NW Russia, Norway,  
51 and Sweden (Fig. 1). The oldest rocks yet found in the  
52 shield have been dated at 3.5 Ga (Huhma et al., 2004)  
53 and major orogenies took place in the Archaean and  
54 Palaeoproterozoic. Younger Meso- and Neoprotero-  
55 zoic crustal growth took place mainly in the western  
56 part, but apart from the anorthositic Ti-deposits  
57 described in this paper, no major ore deposits are  
58 related to rocks of this age. The western part of the  
59 shield was reworked during the Caledonian Orogeny.

60 Economic mineral deposits are largely restricted to  
61 the Palaeoproterozoic parts of the shield. Although  
62 Ni–PGE deposits, orogenic gold deposits, and some  
63 very minor VMS deposits occur in the Archaean,  
64 virtually all economic examples of these deposit  
65 types are related to Palaeoproterozoic magmatism,  
66 deformation and fluid flow. Besides these major  
67 deposit types, the Palaeoproterozoic part of the shield  
68 is also known for its Fe-oxide deposits, including the  
69 famous Kiruna-type Fe-apatite deposits. The genesis  
70 of these deposits is still much debated and both mag-  
71 matic segregation (e.g., Nyström and Henriquez,  
72 1994) and hydrothermal (e.g., Hitzman et al., 1992)  
73 origin have been advocated. The Kiruna-type Fe-apa-  
74 tite deposits have recently also been suggested to form  
75 an end member of the disparate family of iron oxide–  
76 copper–gold (IOCG) deposits (cf. Hitzman et al.,  
77 1992; Hitzman, 2000; Porter, 2000; Williams et al.,

2003). Cu–Au deposits, with a large tonnage and low  
grade (e.g., Aitik), are associated with intrusive rocks  
in the northern part of the Fennoscandian Shield.  
These deposits have been described as porphyry  
style deposits or as hybrid deposits with features  
that also warrant classification as iron oxide–cop-  
per–gold (IOCG) deposits (Weihed, 2001; Wanhainen  
et al., 2003).

In this paper, we discuss the deposit types men-  
tioned above, including the important Mesoprotero-  
zoic anorthosite-hosted Ti deposits. Although still  
much debated both the Kiruna-type Fe-apatite depos-  
its and the intrusion related Cu–Au deposits are here  
discussed as IOCG deposits. The emphasis is on the  
geodynamic aspects of ore formation. The deposits are  
discussed in terms of their tectonic setting and rela-  
tionship to the overall geodynamic evolution of the  
shield. Also considered are deposit-scale structural  
features and their relevance for the understanding of  
the ore genesis.

## 2. The geodynamics of ore formation in the Precambrian

Precambrian ore deposits have much in common  
with more recent deposits. There are some notable  
differences, such as the virtual restriction of komatiite-  
hosted deposits to the Archaean and Early Protero-  
zoic, and the absence of Pb-rich VMS deposits and the  
scarcity of economic porphyry copper deposits in  
Archaean and Palaeoproterozoic granite–greenstone

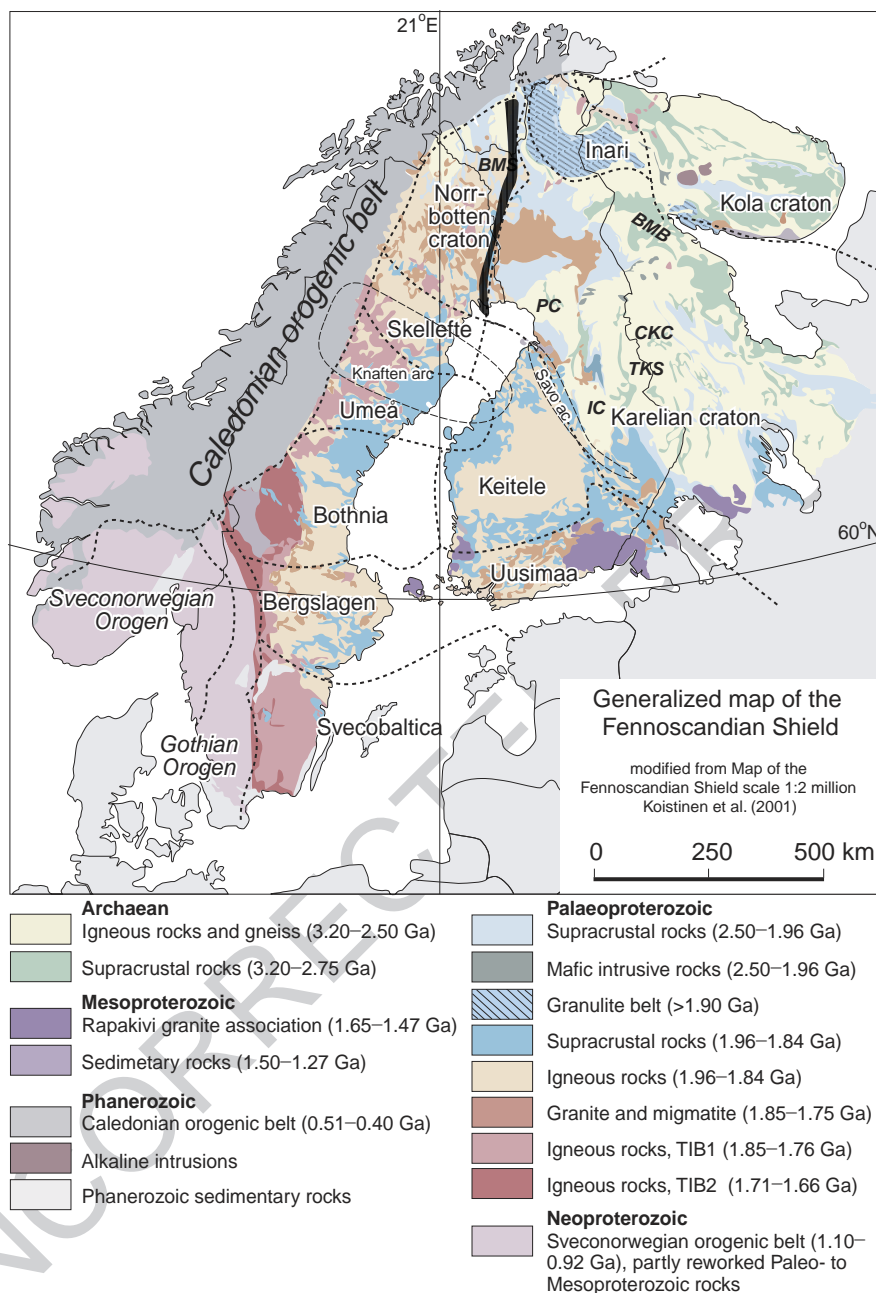


Fig. 1. Simplified geological map of the Fennoscandian Shield with major tectono-stratigraphic units discussed in text (after Lahtinen et al., 2005). Map adapted from Koistinen et al. (2001). BMB=Belomorian Mobile Belt, CKC=Central Karelian Complex, IC=Iisalmi Complex, PC=Pudasjärvi Complex, TKS=Tipasjärvi–Kuhmo–Suomussalmi greenschist complex. Shaded area, BMS=Bothnian Megashear.

107 terranes. However, in terms of their overall character-  
 108 istics, there is little to distinguish an Archaean or  
 109 Palaeoproterozoic VMS and an Archaean or Palaeo-

110 proterozoic orogenic gold deposit from their more  
 111 modern counterparts. At first sight, this is surprising  
 112 because physical and chemical conditions in the

113 Archaean (and Palaeoproterozoic?) mantle and crust  
114 should have been very different from those of today.  
115 Although we can expect the geodynamic processes to  
116 have remained constant through time, the conditions  
117 in which they have operated have changed. The man-  
118 tle was hotter and this would have led to more active  
119 and voluminous magmatism (Arndt et al., 1997). At  
120 spreading centres (Sleep and Windley, 1982), in man-  
121 tle plumes (Herzberg, 1992; Nisbet et al., 1993) and  
122 above subduction zones (Parman et al., 2001; Arndt,  
123 2003), the degree of mantle melting would have been  
124 greater and the magmas produced would have had  
125 more magnesian compositions. At spreading centres,  
126 the higher degree of mantle melting produced thicker  
127 oceanic crust. According to the estimates of Sleep and  
128 Windley (1982) and Vlaar (1986), Archaean oceanic  
129 crust was 20 to 30 km thick, compared with 6 to 8 km  
130 today. We are not sure how this crust subducted, but  
131 subduct it probably did, because rocks similar to those  
132 found in modern island arcs and convergent margins  
133 are recognized in most Archaean greenstone belts.  
134 Plate tectonics, though evolving under different con-  
135 ditions, appear to have been operating in the  
136 Archaean.

137 Thus, it is important when interpreting the forma-  
138 tion of Archaean and Palaeoproterozoic ore deposits  
139 that the likely conditions in the crust and upper  
140 mantle at the time, and the uncertainties about  
141 them, are taken into account. Inevitably, the evidence  
142 is speculative, but the following paragraphs offer a  
143 reasonable scenario.

144 At an Archaean oceanic ridge or back-arc basin  
145 spreading centre, with no significant sub-crustal litho-  
146 sphere, the geothermal gradient across a 30 km-thick  
147 Archaean oceanic crust, from  $<5^{\circ}\text{C}$  to at most  $50^{\circ}\text{C}$  on  
148 the ocean floor, to approximately  $1400^{\circ}\text{C}$  at the base of  
149 the crust, would have been  $45$  to  $46^{\circ}\text{C}/\text{km}$ , far less than  
150 the ca.  $200^{\circ}\text{C}/\text{km}$  gradient, from  $<5$  to  $1200^{\circ}\text{C}$ , across  
151 the 6 km thickness of modern oceanic crust. In a  
152 modern mid-ocean ridge or back-arc setting, magma  
153 chambers located at shallow levels at the spreading  
154 centre drive the fluid circulation. Although the geome-  
155 try of the magmatic plumbing system in the thicker  
156 oceanic crust of an Archaean spreading centre is  
157 unknown, the thicker crust, lower geothermal gradient  
158 and faster spreading rate would probably have com-  
159 bined to distribute magmatic heat sources both deeper  
160 and more dispersed. Only the uppermost few km of the

oceanic crust interact with seawater and become 161  
hydrated (de Wit et al., 1987). This interval represents 162  
a significant fraction of 6 km-thick modern oceanic 163  
crust but only a small fraction of thicker Archaean 164  
oceanic crust. Thus the temperature of fluid circulating 165  
in the crust at Archaean spreading centres would prob- 166  
ably have been lower than nowadays. 167

168 Just before subduction, the modern oceanic plate  
169 consists of a thin layer of sediments, thin, largely  
170 hydrated oceanic crust and a thick section of mantle  
171 lithosphere. Faster moving, hotter Archaean plates  
172 accumulated less sediment and contained a thinner  
173 section of mantle lithosphere (Sleep and Windley,  
174 1982). To initiate subduction, the basaltic section of  
175 the crust must convert, at least in part, to dense  
176 eclogite. It is not clear how this happens, even in  
177 the modern situation. If the lower parts of 30 km-  
178 thick Archaean crust were transformed to eclogite,  
179 this large volume of relatively cold, dense rock  
180 would have acted as a sinker, dragging down the  
181 rest of the slab, despite the thinner mantle portion of  
182 the lithosphere. The dips of Archaean subduction  
183 zones may have been high (Russell and Arndt,  
184 2005), not low, as is commonly proposed (e.g., Kar-  
185 sten et al., 1996; Foley et al., 2003). Hinge retreat or  
186 slab roll-back might have been common. In a subduc-  
187 tion zone, the relatively small proportion of hydrated  
188 crust would have become sandwiched between hot  
189 overlying mantle and the cold, thick lower part of  
190 the subducted crust. Perhaps Archaean oceanic crust  
191 was not always totally subducted. The partially  
192 hydrated, basalt-rich and less dense upper parts may  
193 have been obducted onto growing arcs or continents  
194 while the dense eclogitized lower parts plunged back  
195 into the mantle or, alternatively, the lower ultramafic  
196 cumulate part of a differentiated crust may have delam-  
197 inated and the upper section, composed of hydrated  
198 basaltic rocks, may have accreted to the growing  
199 island arc (Foley et al., 2003).

200 Fluids released by dehydration of subducting crust  
201 would have passed into a hot, overlying Archaean  
202 mantle wedge. These fluids contained little of the  
203 sedimentary component that dominates modern fluids  
204 and they interacted with peridotite in the mantle  
205 wedge that was highly depleted in the basaltic com-  
206 ponent because of the generally high degree of partial  
207 melting. This resulted in water-fluxed melting of a  
208 refractory mantle source. The magmas produced may

209 have been boninitic in character, rich in Mg, and poor  
210 in Fe and incompatible trace elements. These magmas  
211 would have ascended until they reached the crust of  
212 the underthrust plate. There they pooled, fractionated,  
213 degassed and perhaps provoked partial melting of the  
214 crustal rocks.

215 Some aspects of Archaean island arc successions  
216 are consistent with this scenario. Sequences in the  
217 Abitibi Belt of Canada (see [Thurston and Ayres,](#)  
218 [2004](#), for a recent review) contain both tholeiitic and  
219 calc-alkaline members, but the calc-alkaline rocks are  
220 poorer in alkalis than their modern counterparts. More  
221 significantly, Archaean arcs contain a bimodal volca-  
222 nic suite comprising basalts and dacite–rhyolites. True  
223 calc-alkaline andesites, and especially rocks contain-  
224 ing abundant, complexly zoned or eroded plagioclase  
225 phenocrysts like modern calc-alkaline andesites, are  
226 rare to absent. Boninites, though reported, also seem  
227 to be rare, perhaps because the crust formed an effec-  
228 tive filter that prevented the passage to the surface of  
229 dense, water-rich magmas.

230 The characteristics of hydrothermal systems on  
231 Archaean and Proterozoic island arcs and back-arc  
232 basins are a matter of speculation. Fluids may have  
233 been hotter or cooler than in modern subduction-  
234 related settings, depending on the geometry of the  
235 crust and the distribution of heat sources. Fluid fluxes  
236 may have been high, due to rapid dehydration of the  
237 upper part of the magnesian, serpentine-rich crust as it  
238 was dragged rapidly into hot Archaean or Proterozoic  
239 mantle. A clear difference would be a scarcity of  
240 sediment-hosted deposits like those in Japan and  
241 New Brunswick ([Allen et al., 2002](#)).

242 Continental crust formed episodically during the  
243 Archaean and Proterozoic. Compilations of reliable  
244 ages obtained on crustal rocks, and from detrital  
245 zircons in large rivers, produce age spectra character-  
246 ized by the presence of large peaks at 2.7, 2.5, 2.1 and  
247 about 1.9 to 1.8 Ga ([Goldstein et al., 1997](#); [Condie,](#)  
248 [2004](#); [Nelson, 2004](#)). Although some authors interpret  
249 these peaks as the times of supercontinent formation,  
250 arguments can be advanced that suggest that they  
251 represent periods of accelerated mantle convection  
252 and enhanced crustal growth, as could have been the  
253 case in the Fennoscandian Shield. In many regions,  
254 the peak of granitoid emplacement, the event that is  
255 recorded by U–Pb zircon ages, is preceded by about  
256 30 million years by the eruption of voluminous

257 mafic–ultramafic volcanic rocks ([Nelson, 2004](#)). In  
258 the southern Superior Province of Canada, in the  
259 Yilgarn of Australia, in Brazil, Zimbabwe and in  
260 parts of the Aldan Shield in Siberia, komatiites and  
261 basalts are dated from 2.73 to 2.70 Ga and the peak of  
262 granite emplacement at around 2.70 Ga. In the Bir-  
263 imian of West Africa, mafic volcanism is dated at 2.13  
264 Ga and the granites intruded mainly around 2.07 Ga.  
265 [Abouchami et al. \(1990\)](#) equate the Birimian mafic  
266 volcanism with the enormous oceanic plateaux  
267 emplaced in the Pacific in the Cretaceous and [Boher](#)  
268 [et al. \(1991\)](#) interpret the granites as accelerated sub-  
269 duction-related magmatism triggered by the period of  
270 enhanced plume activity. This idea has been taken  
271 further by [Stein and Hofmann \(1994\)](#) and [Condie](#)  
272 [\(2004\)](#) who have developed a model in which periods  
273 of enhanced plume-dominated mantle convection  
274 alternate with periods of plate tectonics.

275 The physical conditions in the crust and upper  
276 mantle when the Archaean and Palaeoproterozoic  
277 greenstone belts formed probably correlate with the  
278 types of ore deposits they contain. For example, the  
279 Abitibi belt in the Canadian Superior Province, which  
280 is believed to have formed through the accretion of  
281 oceanic crust, oceanic plateaux and island arcs ([Card,](#)  
282 [1990](#); [Kimura et al., 1993](#)), is the host of numerous  
283 large VMS and gold deposits but few Ni–PGE sul-  
284 phide deposits. In contrast, the greenstone belts of the  
285 Yilgarn craton in Western Australia apparently formed  
286 through flood volcanism on an older continental base-  
287 ment. This region contains few VMS deposits, abun-  
288 dant gold deposits and hosts, at Kambalda, the type  
289 examples of Ni–PGE sulphide deposits in komatiite  
290 lava flows ([Leshner, 1989](#)). The link between geody-  
291 namic context and Ni–PGE mineralization lies in the  
292 role that assimilation of continental crust played in the  
293 formation of the Kambalda deposits.

294 The formation of major Neoproterozoic VMS, oro-  
295 genic gold, and Ni–PGE mineralization seems to be  
296 restricted to the period ca. 2.74 to 2.69 Ga and appears  
297 to correspond to a period of intense intrabasinal mantle  
298 plumes and a subsequent global plume-breakout event  
299 ([Barley et al., 1998](#)). Apart from the low degree of  
300 exploration, especially in the eastern part, the obvious  
301 lack of major Neoproterozoic mineralization in the Fen-  
302 noscandian Shield could possibly be explained by the  
303 age of Neoproterozoic greenstone belts. Most of the  
304 Fennoscandian greenstone belts seem to be slightly

305 older than the global Neoarchaean peak in mineraliza-  
306 tion and mantle plume activity (e.g., Huhma et al.,  
307 1999) and, hence, magmatism and hydrothermal activ-  
308 ity might have been less intense and unable to form  
309 major metal deposits. This could also explain the lack  
310 of major lode gold deposits related to subsequent  
311 accretion during peak orogeny. It is also possible that  
312 the Fennoscandian Shield exhibits a smaller window  
313 into Archaean greenstone terrains, simply due to the  
314 local peculiarities of late orogenic evolution, when the  
315 thermal regime influences the extent of crustal remelt-  
316 ing and degree of exhumation (Peter Sorjonen-Ward,  
317 pers. comm. 2005). Hence, although there is evidence  
318 for Neoarchaean greenstone belts formed through the  
319 accretion of oceanic crust, oceanic plateaux and  
320 island arcs and those formed through flood volcanism  
321 on an older continental basement (see below), they  
322 apparently do not contain major ore deposits in the  
323 Fennoscandian Shield. This is in contrast to the  
324 Palaeoproterozoic period of ca. 1.95 to 1.80 Ga in  
325 the Fennoscandian Shield, which is intensely miner-  
326 alized and constitutes one of the major Palaeoproter-  
327 ozoic metallogenetic provinces on Earth. Most of the  
328 Fennoscandian ore deposits (i.e., VMS, IOCG, and  
329 orogenic gold) in the Palaeoproterozoic are related to  
330 the formation of island arcs, continental margin arcs,  
331 or subsequent accretion to the Archaean (Karelian)  
332 craton. This is discussed further below.

### 333 3. Tectonic evolution of the Fennoscandian Shield

#### 334 3.1. Archaean geology

335 The Archaean bedrock in the Fennoscandian  
336 Shield includes two cratonic nuclei, Karelia and  
337 Kola, that were fragmented and further reassembled  
338 during the Palaeoproterozoic (Fig. 1). The Karelian  
339 craton can be divided into the Belomorian mobile belt  
340 and three complexes: Central Karelian, Iisalmi, and  
341 Pudasjärvi (Fig. 1). The boundary zone between the  
342 Central Karelian Complex and the Belomorian mobile  
343 belt was formed by accretion of island arc and con-  
344 tinental fragments to the Karelian core in the Neoarch-  
345 aean (Mints et al., 2001). This boundary zone and the  
346 whole Belomorian mobile belt were strongly reactiv-  
347 ated in the Palaeoproterozoic (Gaál and Gorbatshev,  
348 1987; Bibikova et al., 2001).

Extensive areas of the granitoid and gneiss terrain  
of eastern Karelia are dated at 2.85 Ga, whereas rocks  
in the central part of the Karelian Province yield ages  
of ca. 3.05 Ga (Sm–Nd method, Slabunov and Bibi-  
kova, 2001). The Vodlozero terrane east of the Lake  
Onega and the central parts of the Pudasjärvi Com-  
plex, with ages up to 3.50 Ga, are the oldest parts of  
the Karelian Craton (Lobach-Zhuchenko et al., 1993;  
Huhma et al., 2004).

Geochronological studies in NW Russia indicate  
four generations of greenstones, with age groups of  
>3.20 to 3.10, 3.10 to 2.90, 2.90 to 2.80 and 2.80 to  
2.75 Ga (Slabunov and Bibikova, 2001). Based  
mainly on trace element and isotope geochemistry  
of the rocks, Svetov (2001) and Puchtel et al. (1999)  
inferred that the greenstones formed at a convergent  
ocean–continent boundary by tectonic accretion, and  
the final collision stages resulted in asymmetric struc-  
tures of the greenstone belts.

Detailed stratigraphic studies have been conducted  
in the Archaean Tipasjärvi–Kuhmo–Suomussalmi  
(TKS) greenstone complex (Fig. 1) in Finland,  
which therefore serves as a good example of the  
Archaean evolution (Piirainen, 1988; Papunen et al.,  
1998; Halkoaho et al., 2000). A bimodal volcanic  
sequence at the eastern margin of the Suomussalmi  
greenstone belt evidently belongs to an older supra-  
crustal formation. For example, Vaasjoki et al. (1999)  
reported a U–Pb age of  $2966 \pm 9$  Ma for the zircons of  
felsic volcanic rocks, and consider that there is a time  
gap of ca. 150 million years between the bimodal  
volcanic sequence and the lowermost felsic volcanism  
of the TKS greenstone belt. This time gap is also  
characterized by deformation, metamorphism, and  
resetting of U–Pb ages of the tonalite–trondhjemite–  
granitoid (TTG) complex at 2.83 Ga (Luukkonen,  
1992).

The lowermost stratigraphic unit of the TKS proper  
consists of 2.81 to 2.79 Ga, felsic to intermediate,  
subaerial to shallow water-deposited, calc-alkaline  
volcanic rocks. They occur at the margins of the  
belt and are geochemically similar to TTG rocks.  
The overlying volcanic formation is composed of  
pillowed and massive tholeiitic basalts with inter-  
layers of oxidic and sulphidic Algoma-type banded  
iron formations. A mafic sill, considered to be comag-  
matic with the tholeiitic basalts, has been dated at  
 $2790 \pm 18$  Ma and a gabbroic variety of a komatiitic

349  
350  
351  
352  
353  
354  
355  
356  
357  
358  
359  
360  
361  
362  
363  
364  
365  
366  
367  
368  
369  
370  
371  
372  
373  
374  
375  
376  
377  
378  
379  
380  
381  
382  
383  
384  
385  
386  
387  
388  
389  
390  
391  
392  
393  
394  
395  
396

397 cumulate yielded a zircon U–Pb age of  $2757 \pm 20$  Ma  
 398 that is so far the only direct age obtained from the  
 399 ultramafic sequence (Luukkonen, 1992; H. Huhma  
 400 pers. comm., 1998). A sequence of Al-depleted komati-  
 401 tiites and komatiitic basalts overlies the tholeiitic  
 402 basalts. The komatiite formation includes a thick  
 403 ultramafic olivine cumulate body and several ultra-  
 404 mafic lenses interpreted as channel facies olivine ad-  
 405 and meso-cumulates of komatiitic volcanic flows. The  
 406 cumulate body displays pyroxenitic marginal series  
 407 against the TTG wallrock and also contains enclaves  
 408 of tholeiitic basalt and felsic TTG gneisses. The  
 409 komatiites are overlain by basaltic volcanic rocks  
 410 and finally by detrital and lahar-like felsic to inter-  
 411 mediate volcanoclastic deposits, indicating rapid ero-  
 412 sion and infilling of basins. The volcanic sequence is  
 413 linked with a mantle hotspot activity in an intracra-  
 414 tonic basin. The continental crust partially melted in  
 415 the incipient phase to form the felsic volcanic rock  
 416 and subsequently contaminated the voluminous erup-  
 417 tions of komatiitic lavas.

418 The TKS greenstone belt was intruded by grano-  
 419 diorites and tonalites with zircon U–Pb ages ranging  
 420 from 2.75 to 2.69 Ga (Luukkonen, 1992) and was  
 421 isoclinally folded to form a wide synclinorium. Ductile  
 422 shear zones deformed the belt and acted as con-  
 423 ducts for ascending metamorphic fluids at ca. 2.75 to  
 424 2.67 Ga.

### 425 3.2. Palaeoproterozoic tectonic evolution from 2.5 to 426 1.9 Ga

427 Several periods of sedimentation and magmatism  
 428 characterize the Palaeoproterozoic evolution of the  
 429 shield before the Svecokarelian Orogeny. The  
 430 Archaean craton of Fennoscandia consolidated after  
 431 the last major phase of granitoid intrusions at 2.69  
 432 Ga. During the period 2.5 to 1.9 Ga, it underwent  
 433 several episodes of continental rifting and related,  
 434 dominantly mafic, magmatism, denudation and sedi-  
 435 mentation. These resulted in the formation of vol-  
 436 cano-sedimentary sequences, which were deformed  
 437 during the Svecokarelian Orogeny between 1.9 and  
 438 1.8 Ga. The lowermost stratigraphic units consist of  
 439 clastic sedimentary rocks and bimodal volcanism. An  
 440 unconformity characterized by polymict conglomer-  
 441 ates separates these groups from the overlying epi-  
 442 continental sediments and basalts and denotes a

period of weathering and quiescence in the tectonic  
 history.

#### 3.2.1. Incipient rifting, volcanism, and emplacement of layered igneous complexes and mafic dykes

The beginning of the rifting period between 2.51  
 and 2.43 Ga is indicated by intrusion of numerous  
 layered mafic igneous complexes (Alapieti and Lahti-  
 nen, 2002). Most of the intrusions are located along  
 the margin of the Archaean granitoid area, either at the  
 boundary against the Proterozoic supracrustal  
 sequence, totally enclosed by Archaean granitoid, or  
 enclosed by a Proterozoic supracrustal sequence.

Alapieti and Lahtinen (2002) divided the intrusions  
 into three types, (1) ultramafic–mafic, (2) mafic and  
 (3) intermediate megacyclic. They also interpret the  
 ultramafic–mafic and the lowermost part of the mega-  
 cyclic type to have crystallized from a similar, quite  
 primitive magma type, which is characterized by  
 slightly negative initial  $\epsilon_{\text{Nd}}^{\text{T}}$  values and relatively  
 high MgO and Cr, intermediate  $\text{SiO}_2$ , and low  $\text{TiO}_2$   
 concentrations, resembling the boninitic magma type.  
 The upper parts of megacyclic type intrusions and  
 most mafic intrusions crystallized from an evolved  
 Ti-poor, Al-rich basaltic magma.

Amelin et al. (1995) emphasize the existence of  
 two slightly different age groups of the intrusions, the  
 first with U–Pb ages between 2.505 and 2.501 Ga, and  
 the second of a slightly younger period, 2.449 to 2.430  
 Ga. The first includes intrusions along the Polmak–  
 Pechenga–Imandra–Varzuga greenstone belt, such as  
 Mt. Generalskaya in Pechenga and Imandra, Monche-  
 gorsk, Pana and Feodor Tundras in central Kola Penin-  
 sula and the second the intrusions in Karelia and the  
 Kola–Finnish Lapland areas (Fig. 2). However, the  
 timing of these intrusions is disputed, as contrasting  
 U–Pb ages of  $2496 \pm 10$  and  $2447 \pm 10$  Ma were  
 recently determined from two different stratigraphic  
 levels of the Mt. Generalskaya intrusion (Bayanova et  
 al., 1999) and similar results have been obtained from  
 the Panski Tundra intrusions (Mitrofanov and Baya-  
 nova, 1999).

Amelin et al. (1995) bracketed the U–Pb age of the  
 oldest basaltic volcanism between 2.443 and 2.440 Ga,  
 as the volcanic rocks are intruded by a  $2441.3 \pm 1.2$   
 Ma pluton but overlie a  $2442.1 \pm 1.4$  Ma pluton. Other  
 age determinations of volcanism in eastern Karelia  
 indicate ages between 2.45 and 2.43 Ga. Manninen

443  
444445  
446447  
448449  
450451  
452453  
454455  
456457  
458459  
460461  
462463  
464465  
466467  
468469  
470471  
472473  
474475  
476477  
478479  
480481  
482483  
484485  
486487  
488

489

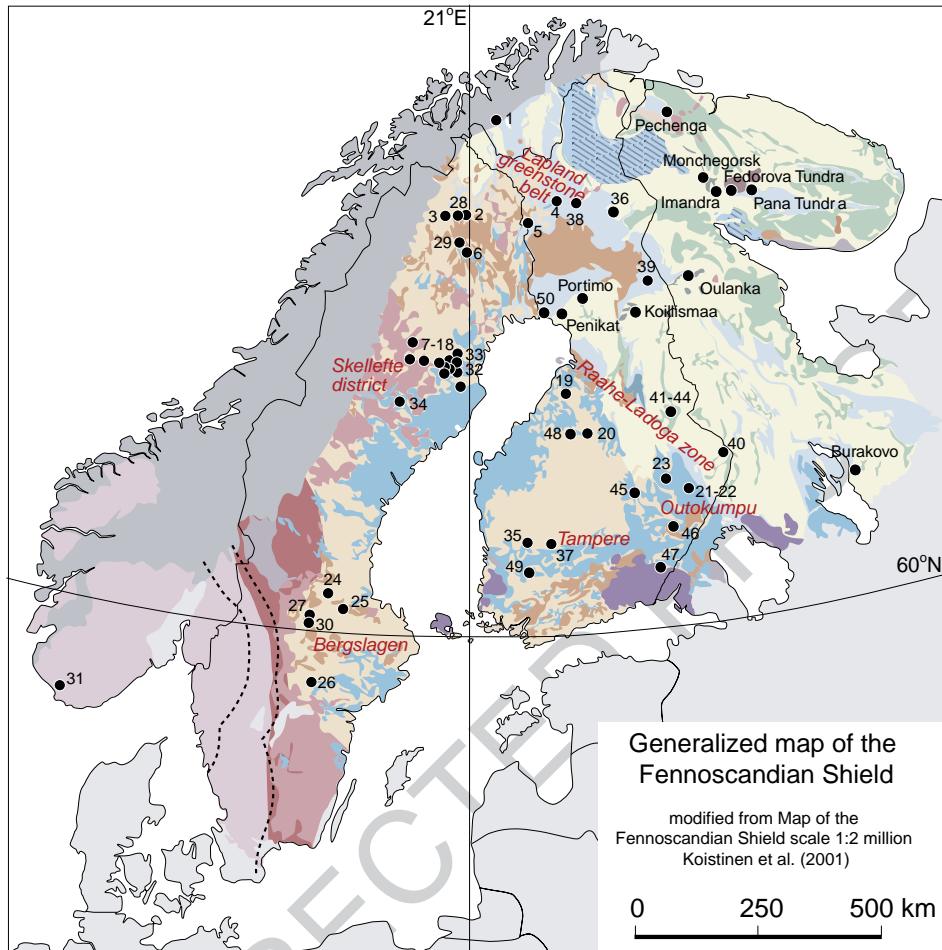


Fig. 2. Simplified geological map of the Fennoscandian Shield with major ore deposits discussed in text indicated. Map adapted from Koistinen et al. (2001). Numbers refer to deposits listed in Table 1. Deposits without numbers are discussed in the text but are not included in Table 1.

490 and Huhma (2001) reported similar ages from the  
 491 Central Lapland greenstone belt. Geochronological  
 492 data from Finland and from the Russian part of the  
 493 shield thus show that large volumes of continental  
 494 volcanic rocks were erupted contemporaneously with  
 495 the 2.44 to 2.45 Ga layered intrusions. A number of  
 496 coeval mafic dykes in the Karelian Craton have ages  
 497 around 2.44 Ga (Vuollo, 1994). Sm–Nd isotope stu-  
 498 dies indicate that boninitic dykes have negative  $\epsilon_{\text{Nd}}^{(T)}$   
 499 values from  $-1.2$  to  $-2.5$ , consistent with the values  
 500 obtained from the layered intrusions (Huhma et al.,  
 501 1990; Alapieti and Lahtinen, 2002).

502 Layered intrusions, mafic dyke swarms, and coeval  
 503 continental volcanism together suggest mantle plume

activity in an extensional setting (Amelin et al., 1995).  
 This model implies extension and crustal uplift before  
 volcanism and subsequent subsidence and formation  
 of graben structures during and after volcanism.  
 Poorly sorted sediments characteristic of graben infill  
 are recorded at this stratigraphic level (Gorbunov et  
 al., 1985). The intense faulting and displacement are  
 related to the late stages of rifting, probably to the  
 cooling and subsidence of the brittle layer of the  
 lithosphere after the buoyant rise of the base of the  
 lithosphere during the active rifting phase (see Ala-  
 pieti and Lahtinen, 2002). The intrusions were later  
 deformed and metamorphosed during the Svecokare-  
 lian Orogeny.

504  
 505  
 506  
 507  
 508  
 509  
 510  
 511  
 512  
 513  
 514  
 515  
 516  
 517



### 518 3.2.2. Evolution between 2.33 and 1.87 Ga

519 The Polmak–Pechenga greenstone belt extends for  
520 about 200 km from northern Finland to NW Russia.  
521 The area has been intensely studied since the discov-  
522 ery of the Pechenga Ni–Cu deposits in the 1920s, and  
523 the review here is mainly based on the work of [Hanski](#)  
524 (1992), [Melezhik](#) (1996), [Green and Melezhik](#) (1999)  
525 and [Barnes et al.](#) (2001). The 2.3 Ga, subaerially  
526 deposited, andesitic basalts of the lowermost volcanic  
527 unit of the Pechenga sequence represent the next  
528 episode of magmatic activity in the Fennoscandian  
529 Shield ([Melezhik](#), 1996). Conglomerate and a regolith  
530 on the Archaean crust underlie these basalts. The  
531 conglomerate contains clasts derived from the Mt.  
532 General'skaya layered complex ( $2505 \pm 1.6$  Ma U–  
533 Pb age of baddeleyite, [Amelin et al.](#), 1995), indicating  
534 that the crust had been deeply eroded to expose the  
535 intrusion before the onset of volcanism. The Pechenga  
536 sequence developed with cyclic sedimentation and  
537 volcanism in an intracratonic rift zone, but the volcan-  
538 ism at ca. 2.1 to 2.0 Ga represents a transition from an  
539 intracratonic to an intercontinental oceanic rift envir-  
540 onment that developed between 2.00 and 1.97 Ga into  
541 an oceanic rift with voluminous sedimentation and  
542 volcanism. The Pechenga sequence was subducted  
543 between 1.97 and 1.87 Ga and a continent–continent  
544 collision followed from 1.87 to 1.80 Ga in the region  
545 ([Melezhik](#), 1996). Ultramafic, ferropicritic volcanic  
546 rocks ([Hanski and Smolkin](#), 1989; [Hanski](#), 1992),  
547 dated at  $1,977 \pm 52$  Ma (Sm–Nd, Pb–Pb, [Hanski](#),  
548 1992) host the Pechenga Ni–Cu deposits. The ferro-  
549 picrites are enriched in LILE, LREE and HFSE and  
550 display similarities with the picritic volcanic rocks of  
551 the Central Lapland greenstone belt discussed below.  
552 Although the idea of a core signature has been sug-  
553 gested for the Fe-rich Archaean to Proterozoic ultra-  
554 mafic volcanic rocks ([Puchtel et al.](#), 1999), it has also  
555 been argued that the Archaean/Proterozoic picrites  
556 were 30% richer in Fe compared with modern OIB  
557 since the mantle was more Fe-rich at that time ([Fran-](#)  
558 [cis et al.](#), 1999; [Barnes et al.](#), 2001).

559 The Central Lapland greenstone belt (CLGB) is the  
560 most extensive belt of mafic volcanic rocks and  
561 related sedimentary units in Fennoscandia ([Fig. 2](#)).  
562 The CLGB is divided into seven lithostratigraphic  
563 groups ([Lehtonen et al.](#), 1998; [Hanski et al.](#), 2001a;  
564 [Vaasjoki](#), 2001), of which the oldest belong to the  
565 intracratonic hotspot-related rift evolution of 2.45 to

2.43 Ga discussed above. After this phase, epiclastic 566  
sedimentary rocks, quartzites, mica schists and minor 567  
carbonate rocks were deposited. [Räsänen and Huhma](#) 568  
(2001) reported ages between 2.45 and 2.22 Ga for 569  
mafic magmatism interlayered in the sedimentary 570  
sequence, but the extensive 2.2 Ga-old mafic sills 571  
represent the main phase of igneous activity, indicat- 572  
ing renewed rifting of the underlying craton. The 573  
depositional basin became deeper and fine-grained 574  
sediments, phyllites and carbonaceous sulphide-bear- 575  
ing black schists were deposited between 2.2 and 2.06 576  
Ga. These are characterized by isotopically heavy 577  
carbon with  $\delta^{13}\text{C}$  values up to +18‰, which correlate 578  
with the global heavy C-isotopes of carbonates of this 579  
time span ([Karhu](#), 1993; [Melezhik](#), 1996). The 580  
 $2058 \pm 4$  Ma Kevitsa mafic–ultramafic intrusion inter- 581  
sects the sequence and provides a minimum age for 582  
the sedimentary sequence. The sediments in the basin 583  
are overlain by a voluminous, 2.05 Ga, ultramafic 584  
komatiitic and picritic volcanic belt extending for 585  
350 km from central Lapland to northern Norway. 586  
The komatiites are exceptional in their chemical com- 587  
position with high Ti concentrations and flat LREE- 588  
depleted patterns ([Barnes and Often](#), 1990), whereas 589  
the picrites are LREE and HFSE enriched, which 590  
indicate mantle hotspot activity ([Hanski et al.](#), 2001b). 591

592 The overlying mafic submarine volcanic sequences 592  
of the CLGB display tectonic contacts against the 2.2 593  
to 2.05 Ga unit, with the contact zone being charac- 594  
terized by serpentinites interpreted as dismembered 595  
and overthrust pieces of ocean-floor ophiolites 596  
([Hanski](#), 1997). The submarine volcanic sequence is 597  
composed of tholeiitic mafic volcanic rocks and mafic 598  
to intermediate volcanoclastic rocks interlayered with 599  
fine-grained detrital and chemical sediments. This 600  
indicates the existence of oceanic crust, which was 601  
obducted to its present position before the intrusion of 602  
1.91 Ga granites. A U–Pb age of ca. 2.015 Ga has 603  
been obtained for the upper part of this unit ([Rastas et](#) 604  
[al.](#), 2001). 605

### 606 3.2.3. Summary of evolution between 2.5 and 1.87 Ga

607 Intracratonic basin evolution with intermittent vol- 607  
canism lasted for up to 500 million years with no 608  
indications of accretionary phases or formation of 609  
major new felsic crust. Recurrent mantle hotspot 610  
activity characterizes the period 2.5 to 2.05 Ga with 611  
numerous layered intrusions, komatiite and picrite 612

613 eruptions in Finnish Lapland at 2.05 Ga, and finally  
614 the extrusion/intrusion of the Pechenga ferropicrites at  
615 1.97 Ga. Oceanic crust only formed during the last  
616 phase of the extension and was finally obducted dur-  
617 ing accretion and continent–continent collision at ca.  
618 1.9 to 1.8 Ga.

619 Such a long period for the evolution of intracra-  
620 tonic, transient and oceanic basins deviates from the  
621 normal time span of Phanerozoic plate tectonic  
622 processes where a major intracratonic rifting is fol-  
623 lowed by opening of an ocean in a relatively short  
624 period of time. Also the time span of about 30  
625 million years that commonly separates the major  
626 mafic volcanic episodes from the intrusion of gran-  
627 itoids, as noted above, did not hold in the geotec-  
628 tonic evolution of the Fennoscandian Shield between  
629 2.5 and 2.0 Ga, as several phases of volcanism and  
630 mafic intrusions formed without related felsic mag-  
631 matism. This must have been the result of a profound  
632 change in mantle convection and interaction between  
633 asthenosphere and lithosphere at this time, but dis-  
634 cussion of these processes is beyond the scope of this  
635 paper.

### 636 3.3. The 1.9 to 1.8 Ga Svecokarelian Orogeny

637 The most intense crustal growth in the Palaeopro-  
638 tozoic took place during the Svecokarelian/Sveco-  
639 fennian Orogeny (both names occur in the literature)  
640 at ca. 1.9 to 1.8 Ga. [Hietanen \(1975\)](#) presented the  
641 first plate tectonic interpretation of the Svecofennian  
642 Orogeny based on the comparison between western  
643 North American Cordilleran and the Svecofennian.  
644 [Gaál \(1982\)](#) presented a plate tectonic model with a  
645 subduction towards ENE and collision at ca. 1.9 Ga.  
646 [Gaál and Gorbatshev \(1987\)](#) later extended this  
647 model. [Ward \(1987\)](#) argued that the scarcity of sub-  
648 duction-related magmatism in the Archaean craton  
649 margin and the easterly-directed tectonic transport  
650 implied westerly-directed subduction before collision.  
651 [Gaál \(1990\)](#) adopted this idea and included a subduc-  
652 tion reversal in his model to account for the volumi-  
653 nous magmatism in central Finland.

654 The ca. 1.95 Ga rocks in the Knaften area ([Was-  
655 ström, 1993](#)), south of the Skellefte District in Swe-  
656 den, and the 1.92 Ga primitive island arc rocks in the  
657 Savo Belt ([Korsman et al., 1997](#)), adjacent to the  
658 Archaean craton in Finland ([Fig. 1](#)), are the oldest

659 documented Svecofennian units in the shield, but  
660 older protoliths (~2.1 to 2.0 Ga) are inferred from  
661 Nd isotope geochemistry and detrital zircon studies  
662 ([Lahtinen and Huhma, 1997](#)). Island arc-type volca-  
663 nic rocks and coeval calc-alkaline granitoids aged  
664 1.90 to 1.87 Ga dominate in the central Fennoscandian  
665 Shield. Plutonic rocks in Sweden, aged 1.80 to  
666 1.78 Ga with mixed I- to A-type characteristics,  
667 represent the youngest major Palaeoproterozoic mag-  
668 matism in the central shield. Migmatites with tonalitic  
669 leucosome in Finland formed from immature  
670 psammites at 1.89 to 1.88 Ga, whereas younger  
671 migmatites with granite leucosome, and associated  
672 S-type granites, formed at 1.86 to 1.82 Ga in the  
673 Bothnian Basin and in the southern part of the  
674 Svecofennian domain ([Lundqvist et al., 1998](#); [Kors-  
675 man et al., 1999](#); [Rutland et al., 2001](#); [Weiher et al.,  
676 2002](#)). The southern Svecofennian domain includes  
677 the 1.90 to 1.89 Ga Bergslagen–Uusimaa belt ([Fig.  
678 1](#)), which formed, in part, in an intra-arc basin of a  
679 mature continental arc (e.g., [Kähkönen et al., 1994](#);  
680 [Allen et al., 1996a](#)). Metapelite-dominated sedimentary  
681 rocks, quartzites and carbonate rocks character-  
682 ize the southern part of the Svecofennian domain.  
683 Plutonism in that area occurred between 1.89 and  
684 1.85, 1.84 and 1.82, and 1.81 and 1.79 Ga. S-type  
685 granites and migmatites aged 1.84 to 1.82 Ga form a  
686 belt that extends from SE Finland to central Sweden  
687 (e.g., [Korsman et al., 1999](#)).

688 Reflection seismic studies in the 1980s indicated  
689 possible fossil subduction zones and remnant slabs  
690 from subduction immediately south of the Skellefte  
691 District in Sweden ([BABEL Working Group, 1990](#)).  
692 [Korja et al. \(1993\)](#) proposed a mantle underplating  
693 model to account for the thick crust in central Finland,  
694 whereas [Lahtinen \(1994\)](#) presented a model for the  
695 Svecofennian of Finland involving several accretionary  
696 units and three collisional stages at 1.91 to 1.90,  
697 1.89 to 1.88, and 1.86 to 1.84 Ga. [Korja \(1995\)](#)  
698 introduced the concept of orogenic collapse to account  
699 for the variation in crustal thickness in southern Fin-  
700 land, and [Nironen \(1997\)](#) presented a kinematic plate  
701 tectonic model for the Svecofennian Orogen starting  
702 with the opening of an ocean at 1.95 Ga, followed by  
703 progressive accretion of two arc complexes on to the  
704 Archaean craton between 1.91 and 1.87 Ga. The  
705 accretionary orogens are progressively younger  
706 towards the west, with the subsequent Gothian Oro-

707 geny between 1.75 and 1.55 Ga. Later reworking of  
708 the crust occurred during the Sveconorwegian/Gren-  
709 villian Orogeny at ca. 1.15 to 0.9 Ga (e.g., Gor-  
710 batschev and Bogdanova, 1993; Åhäll and Larson,  
711 2000).

712 According to Lahtinen et al. (2003, 2004, 2005)  
713 the ca. 2.00 to 1.92 Ga evolution of the shield  
714 involved the amalgamation of several microcontinents  
715 and island arcs. This included several pre-1.92 Ga  
716 cratons, >2.0 Ga microcontinents, and ca. 2.0 to  
717 1.95 Ga island arcs. Previous models have proposed  
718 a semi-continuous Svecokarelian/Svecofennian Oro-  
719 geny whereas Lahtinen et al. (2004, 2005) define five  
720 orogenies for the time period 1.92 to 1.79 Ga and  
721 divide this period into a microcontinent accretion  
722 stage (1.92 to 1.88 Ga), and a continent–continent  
723 collision stage (1.87 to 1.79 Ga).

724 The Palaeoproterozoic tectonic evolution of the  
725 Karelian craton, the Archaean nucleus of the shield,  
726 involved a long period of intracontinental extension  
727 between 2.5 and 2.1 Ga, finally leading to a conti-  
728 nental break-up at 2.06 Ga as described above. Sub-  
729 sequent convergence and microcontinent accretion  
730 (1.92 to 1.88 Ga) resulted in the collision of the  
731 Kola and Karelian cratons (cf. Fig. 1) that, according  
732 to Lahtinen et al. (2004, 2005), led to the Lapland–  
733 Kola Orogeny. The collision of the Karelian craton  
734 with the Norrbotten craton (the Archaean rocks west  
735 of the Bothnian megashear as defined by Berthelsen  
736 and Marker, 1986) and the Keitele microcontinent,  
737 and the docking of the Bothnia microcontinent (Fig.  
738 1), led to the Lapland–Savo Orogeny. The collision of  
739 the Bergslagen microcontinent with the newly formed  
740 Archaean–Palaeoproterozoic complex led to the Fen-  
741 nian Orogeny.

742 During subsequent continent–continent collision,  
743 two subduction zones, in the south and in the west,  
744 were active between 1.86 and 1.81 Ga. According to  
745 this model (Lahtinen et al., 2004, 2005), subduction  
746 was followed by oblique collision of Fennoscandia  
747 with Sarmatia between 1.84 and 1.80 Ga, defining the  
748 Svecobaltic Orogeny. A crustal-scale shear zone  
749 divided the Svecobaltic Orogen into two distinct com-  
750 pressional regimes; (1) a retreating subduction zone at  
751 an Andean-type margin in the SW, and (2) a trans-  
752 pressional regime in the SE. A collision between  
753 Amazonia and Fennoscandia affected the central and  
754 northern parts of the western edge of the Fennoscan-

dian Shield at 1.82 to 1.80 Ga and is defined as the  
Nordic Orogeny. Orogenic collapse and the stabiliza-  
tion of the Fennoscandian Shield essentially occurred  
between 1.79 and 1.77 Ga. This was followed by  
younger orogenies in the SW and a westward growth  
of the shield.

#### 4. Ore-forming processes—relationship between ore deposits and geodynamic setting

In the Fennoscandian Shield, the major deposit  
types are excellent guides to the geodynamic pro-  
cesses that operated in the Archaean and Proterozoic.  
Here we discuss five important deposit types and  
emphasize their relationship with the evolution of  
the shield. All deposit types contain ores that are or  
have been economic and that today are actively  
explored for in the shield. The five deposit types are  
(1) Ni–Cu–PGE deposits, (2) VMS (Zn–Cu–Pb ±  
Au ± Ag) deposits, (3) orogenic gold deposits, (4)  
iron oxide–copper–gold deposits (IOCG), including  
Kiruna-type Fe deposits and (5) Fe–Ti oxides in  
anorthosites. Major deposits in the Fennoscandian  
Shield are listed in Table 1 and their distribution is  
shown in Fig. 2.

##### 4.1. Ni–Cu–PGE deposits

Ni–Cu ± PGE deposits occur in several different  
settings within the shield. Mining of Ni as the main  
commodity has mainly occurred in NW Russia, (e.g.,  
Pechenga), in Finland (e.g., Kotalahti, Hitura and  
Vammala) and only to a lesser extent in Sweden  
(e.g., Lainejaur). It is possible to subdivide these  
deposits on the basis of their geodynamic setting  
into the following types: (1) deposits in Archaean  
greenstone belts (2.74 Ga), (2) deposits in mafic  
layered intrusions (2.49 to 2.45 Ga), (3) deposits in  
Palaeoproterozoic greenstone belts (2.2 to 2.05 Ga),  
(4) deposits in Palaeoproterozoic ophiolite complexes  
(1.97 Ga), (5) deposits associated with rift-related  
ultramafic volcanism (1.97 Ga), (6) deposits in Sve-  
cofennian orogenic mafic–ultramafic intrusions (1.88  
Ga) and (7) deposits in post-orogenic diabase dykes.  
Of these, type four is discussed in the VMS section  
and type seven is minor and will not be discussed  
further.

t1.1 Table 1  
t1.2 Grade and pre-mining tonnage of selected<sup>a</sup> ore deposits in the Fennoscandian Shield

t1.3	Type <sup>b</sup>	Ton. (Mt)	Cu %	Zn %	Pb %	Co %	Au ppm	Ag ppm	Fe %	Ni %	Cr %	TiO <sub>2</sub> %	Status	Reference <sup>c</sup>
t1.4	1) Bidjovagge	Cu–Au	2	1.2	–	–	3.6	–	–	–	–	–	Closed mine	Ettner et al. (1994)
t1.5	2) Viscaria	Strat. Cu	12.54	2.29	–	–	–	–	–	–	–	–	Closed mine	Martinsson et al. (1997)
t1.6	3) Pahtohavare	Cu–Au	1.7	1.9	–	–	0.9	–	–	–	–	–	Closed mine	Lindblom et al. (1996)
t1.7	4) Saattopora	Cu–Au	2.2	0.28	–	–	3.29	–	–	–	–	–	Closed mine	Grönholm (1999)
t1.8	5) Laurinoja	Cu–Au	4.6	0.88	–	–	0.95	–	–	–	–	–	Closed mine	Hiltunen (1982)
t1.9	6) Aitik	Porph.	1600	0.4	–	–	0.2	4	–	–	–	–	Active mine	Wanhainen et al. (2003)
	7) Boliden	VMS	8.3	1.4	0.9	0.3	15.5	50	–	–	–	–	Closed mine	Bergman Weihed et al. (1996)
t1.11	8) Långdal	VMS	4.4	0.1	5.8	1.7	1.9	149	–	–	–	–	Closed mine	Allen et al. (1996a)
t1.12	9) Långsele	VMS	12.0	0.6	3.9	0.3	0.9	25	–	–	–	–	Closed mine	Allen et al. (1996a)
t1.13	10) Renström	VMS	> 9	0.8	6.5	1.5	2.8	155	–	–	–	–	Active mine	Allen et al. (1996a)
t1.14	11) Petiknäs S	VMS	6.5	1.1	4.8	0.9	2.3	108	–	–	–	–	Active mine	Allen et al. (1996a)
t1.15	12) Udden	VMS	6.7	0.4	4.3	0.3	0.7	36	–	–	–	–	Closed mine	Allen et al. (1996a)
t1.16	13) Maurliden W.	VMS	6.9	0.2	3.4	0.4	0.9	49	–	–	–	–	Active mine	Allen et al. (1996a)
t1.17	14) Näsliden	VMS	4.6	1.1	3.0	0.3	1.3	35	–	–	–	–	Closed mine	Allen et al. (1996a)
t1.18	15) Rakkejaur	VMS	> 20	0.3	2.4	–	1.0	50	–	–	–	–	Closed mine	Allen et al. (1996a)
t1.19	16) Kristineberg	VMS	> 22	1.0	3.2	0.4	–	1.0	32	–	–	–	Active mine	Allen et al. (1996a)
t1.20	17) Rävliidmyran	VMS	7.5	1.0	3.9	0.6	–	0.8	51	–	–	–	Closed mine	Allen et al. (1996a)
t1.21	18) Rudtjebäcken	VMS	4.7	0.9	2.9	0.1	–	0.3	10	–	–	–	Closed mine	Allen et al. (1996a)
t1.22	19) Vihanti	VMS	28.1	0.48	5.12	0.36	–	0.49	25	–	–	–	Closed mine	Helovuori (1979)
t1.23	20) Pyhäsalmi	VMS	71	0.79	2.47	–	–	0.4	15	–	–	–	Active mine	Weihed (2001)
t1.24	21) Keretti	VMS	28.5	3.8	1.07	–	0.24	0.8	8.9	–	0.17	–	Closed mine	Gaál (1985)
t1.25	22) Vuonos	VMS	5.9	2.45	1.6	–	0.15	0.1	11	–	0.17	–	Closed mine	Gaál (1985)
t1.26	23) Luikonlahti	VMS	7.5	0.99	0.5	–	0.11	–	–	–	0.09	–	Closed mine	Gaál (1985)
t1.27	24) Falun	VMS	28.1	~3	4	1.5	–	~3 <sup>d</sup>	~20	–	–	–	Closed mine	Allen et al. (1996b)
t1.28	25) Garpenberg	VMS	21.5	0.3	5.3	3.3	–	0.65	98	–	–	–	Active mine	Allen et al. (1996b)
t1.29	26) Zinkgruvan	VMS	60?	–	10	2	–	–	50–100	–	–	–	Active mine	Allen et al. (1996b)
t1.30	27) Saxberget	VMS	6.8	0.9	7.1	2.2	–	0.4	42	–	–	–	Closed mine	Allen et al. (1996b)
t1.31	28) Kiirunavaara	FeOx	> 2000	–	–	–	–	–	> 60	–	–	–	Active mine	Martinsson (1997)

t1.32	29) Malmberget	FeOx	> 660	-	-	-	-	-	51-61	-	-	-	-	Active mine	Martinsson (1997)
t1.33	30) Grängesberg	FeOx	> 198	-	-	-	-	-	-	58-64	-	-	-	Closed mine	Allen et al. (1996b)
t1.34	31) Tellnes	Ti	> 300	-	-	-	-	-	-	-	-	-	18	Active mine	Charlier (this volume)
t1.35	32) Björkdal	Active mine	> 20	-	-	-	-	2.6	-	-	-	-	-	Active mine	Weihed et al. (2003)
t1.36	33) Åkerberg	Active mine	1.1	-	-	-	-	3	-	-	-	-	-	Closed mine	Sundblad (2003)
t1.37	34) Svartliden	Active mine	2.5	-	-	-	-	5.4	-	-	-	-	-	Active mine	Sundblad (2003)
t1.38	35) Haveri	VMS	1.5	0.37	-	-	-	2.8	-	-	-	-	-	Closed mine	Eilu et al. (2003)
t1.39	36) Pahtavaara	Active mine	> 3	-	-	-	-	3	-	-	-	-	-	Active mine	Eilu et al. (2003)
	37) Kutemajärvi	Epith. Au	2.0	-	-	-	-	9	-	-	-	-	-	Closed mine	Poutiainen and Grönholm (1996)
t1.41	38) Suurikuusikko	Active mine	17	-	-	-	-	5.2	-	-	-	-	-	Prospect	Eilu et al. (2003)
t1.42	39) Juomasuo	Active mine	1.8	-	-	-	0.2	3	-	-	-	-	-	Closed mine	Eilu et al. (2003)
t1.43	40) Pampalo	Active mine	1.2	-	-	-	-	8	-	-	-	-	-	Closed mine	Eilu et al. (2003)
t1.44	41) Peura-aho	Ni-Cu	0.26	0.24	-	-	-	-	-	-	-	0.58	-	Prospect	Kurki and Papunen (1985)
t1.45	42) Hietaharju	Ni-Cu	0.24	0.43	-	-	-	-	-	-	-	0.86	-	Prospect	Kurki and Papunen (1985)
t1.46	43) Arola	Ni-Cu	1.52	-	-	-	-	-	-	-	-	0.56	-	Prospect	Kurki and Papunen (1985)
t1.47	44) Sika-aho	Ni-Cu	0.18	-	-	-	-	-	-	-	-	0.66	-	Prospect	Kurki and Papunen (1985)
	45) Kotalahti	Ni-Cu	13	0.27	-	-	-	-	-	-	-	0.72	-	Closed mine	Papunen and Gorbunov (1985)
	46) Laukunkangas	Ni-Cu	6.7	0.22	-	-	-	-	-	-	-	0.76	-	Closed mine	Papunen and Gorbunov (1985)
t1.50	47) Telkkälä	Ni-Cu	0.6	0.35	-	-	-	-	-	-	-	1.41	-	Closed mine	Papunen and Vormaa (1985)
	48) Hitura	Ni-Cu	13	0.2	-	-	-	-	-	-	-	0.59	-	Closed mine	Papunen and Gorbunov (1985)
	49) Vammala	Ni-Cu	7.4	0.4	-	-	-	-	-	-	-	0.69	-	Closed mine	Papunen and Gorbunov (1985)
t1.53	50) Kemi	Cr	> 236	-	-	-	-	-	-	-	-	26	-	Active mine	Alapieti et al. (1989)

t1.54 The genesis of some deposits is still debated, this is discussed further in the text.

<sup>a</sup> This table lists all major deposits, or deposits discussed in the text, of each type in the Fennoscandian Shield where deposit data are available. Data for deposits 4, 5, 19, 20, 21, 22, 23, 35-50 from the Geological Survey of Finland deposit database, data for deposit 1, 2, 7-18 from Weihed (2001), data for deposit 6 from Boliden Mineral AB, data for deposits 24-27 from Allen et al. (1996b), data for deposits 28-30 from Geological Survey of Sweden mineral deposit database and data for deposit 31 from Charlier (2005).

<sup>b</sup> Abbreviations: Strat. Cu=Stratiform Cu deposits; Porph.=Porphyry type deposit; VMS=Volcanogenic massive sulphide deposit; FeOx=Fe-oxide deposit; Orog. Au=Orogenic gold deposit; Epith. Au=Epithermal Au deposit.

<sup>c</sup> There is only one reference for each deposit listed in the table. Where possible this is a recent reference containing more references to the deposit concerned.

t1.58 <sup>d</sup> Grade for epigenetic quartz vein hosted gold part of deposit.

#### 798 4.1.1. *Archaean greenstone belts*

799 Unlike many other Archaean areas, the greenstone  
800 belts of the Fennoscandian Shield include only minor  
801 occurrences of Ni–Cu sulphides of which the disse-  
802 minated Ni sulphide mineral deposits of Vaara and  
803 Kauniinlampi (Halkoaho and Pietikäinen, 1999) in a  
804 komatiitic cumulate of the Suomussalmi greenstone  
805 belt are the most notable. The Ni/S ratios are high and  
806 Cu tenors very low, similar to the Mt. Keith type of  
807 komatiitic sulphides (Naldrett, 1989). The prospects  
808 of Peura-aho and Hietaharju (Kurki and Papunen,  
809 1985; Table 1) are composed of massive and disse-  
810 minated Ni–Cu sulphides at the contact zone between  
811 a basal cumulate serpentinite lens of a komatiitic  
812 basalt flow and underlying sulphide-bearing felsic  
813 volcanic rock. The Arola and Sika-aho prospects  
814 (Table 1) are tectonically remobilized Ni-sulphides  
815 in shear zones, whereas the Tainiovaara deposit is  
816 located in a small, intensely metamorphosed and  
817 deformed ultramafic lens totally surrounded by  
818 Archaean granitoids.

819 The geological environment and stratigraphic  
820 sequences of the TKS greenstone complex (see  
821 above) are quite similar to those of the Norseman–  
822 Wiluna belt, Western Australia (Hill, 2001), although  
823 the dimensions of the TKS belt are much smaller.  
824 Thermal erosion of sulphidic substrates and channe-  
825 lized ultramafic volcanic flows are considered prere-  
826 quisites for the contamination and accumulation of  
827 Ni-bearing sulphides in komatiites (Huppert et al.,  
828 1984; Leshner et al., 1984; Hill, 2001; Naldrett,  
829 2001). In the Kuhmo belt, sulphide-bearing chert  
830 layers that locally underlie the komatiitic flows and  
831 cumulates in the lowermost komatiitic flow are  
832 depleted in Ni, indicating sulphide contamination  
833 and segregation somewhere in the passage of the  
834 flow (Papunen et al., 1998).

#### 835 4.1.2. *Mafic layered intrusions*

836 The 2.5 to 2.4 Ga period of igneous activity that  
837 resulted in the emplacement of numerous layered  
838 mafic–ultramafic intrusive complexes was important  
839 in terms of major chromitite and Ni–Cu–PGE deposits.  
840 According to Alapieti and Lahtinen (2002), approxi-  
841 mately two dozen layered mafic intrusions and intru-  
842 sion fragments are scattered within the Fennoscandian  
843 Shield. One belt extends along the Archaean–Proter-  
844 ozoic boundary and includes the Tornio–Kukkola

intrusion at the Finnish–Swedish border, the Kemi 845  
and Penikat intrusions and scattered remnants of the 846  
wide Portio and Koillismaa complexes. Another belt 847  
trends in a SE direction through Finnish Lapland into 848  
Russia, and includes the Kaamajoki–Tsohkkoaivi, 849  
Koitelainen and Akanvaara intrusions in Finland and 850  
the Oulanka complex in Russia. The largest layered 851  
intrusion in the shield, the Burakovo intrusion in Rus- 852  
sia, may be regarded as a continuation of this belt 853  
(Alapieti and Lahtinen, 2002). Several layered mafic 854  
intrusions also follow the margins of the Polmak– 855  
Pechenga–Imandra–Vazuga–Ust’Ponoy belt. 856

857 A number of the layered igneous complexes in 858  
Finland host Ni–Cu and PGE occurrences. In NW 859  
Russia the intrusions, such as Mt. Generalskaya, Mon- 860  
chegorsk, Imandra, Feodor Tundra and Pana Tundra, 861  
are extensive and display high potential for Ni–Cu 862  
and PGE deposits. Alapieti and Lahtinen (2002) clas- 863  
sified the PGE occurrences into six categories: (1) 864  
disseminated base-metal sulphide–PGE deposits, (2) 865  
PGE-bearing offset deposits, (3) base-metal sulphide- 866  
bearing PGE reefs, (4) sulphide-poor PGE reefs, (5) 867  
disseminated base-metal sulphide–PGE deposits asso- 868  
ciated with microgabbonorites and (6) PGE enrich- 869  
ments associated with “upper chromitites”. 870

871 Reef type PGE deposits characterize, for example, 872  
the Penikat complex, where the megacyclic units were 873  
interpreted to be the result of replenishment of the 874  
magma in the crystallizing magma chamber, and the 875  
lower contacts of the units correlate with both sul- 876  
phide-bearing and sulphide-poor PGE reefs. The dis- 877  
seminated base-metal sulphide–PGE deposits occupy 878  
the marginal part of the intrusion where the crystal- 879  
lization sequence is inverted and the rock is hetero- 880  
geneous with abundant wall-rock fragments and 881  
breccia structures. The Kemi intrusion hosts a 882  
world-class chromite deposit (see Table 1). The de- 883  
posit consists of stratiform, massive or semi-massive 884  
chromitite in the ultramafic basal cumulate of a 885  
layered igneous complex. The ore deposit is anoma- 886  
lously thick, up to 90 m, and it extends subvertically 887  
to at least a depth of 500 m. According to Alapieti et 888  
al. (1989), contamination of parental magma caused 889  
the crystallizing evolved melt to move to the primary 890  
liquidus field of chromite, and the dynamic conditions 891  
and tectonically-shaped form of the magma chamber 892  
accumulated chromite into a thick pile around the 893  
magma vent. 894

893 4.1.3. Ni–Cu deposits in Palaeoproterozoic  
894 greenstone belts associated with rift-related  
895 ultramafic volcanism

896 Rift-related subaerial to submarine volcanism, ranging in composition from ultramafic to mafic and  
897 intermediate, characterizes the Palaeoproterozoic  
898 greenstone belts within the Karelian Craton. The  
899 majority of the associated mineral deposits are iron  
900 formations, but there is also a notable low-grade Ni–  
901 Cu and PGE deposit related to the intrusion of the  
902 2.06 Ga Kevitsa layered igneous complex (cf. Fig. 2)  
903 in Central Lapland (Mutanen, 1997). The best sections  
904 of the disseminated mineralization are related to tec-  
905 tonic remobilization, which upgraded the primary  
906 igneous sulphides.

907 The Pechenga Ni–Cu deposits (Fig. 2) in NW  
908 Russia are hosted by both ultramafic, weakly differ-  
909 entiated ferropicritic flows and differentiated gabbro–  
910 wehrlite intrusions within the 600 to 1000 m thickness  
911 of the Pilgijärvi volcano-sedimentary formation  
912 (Hanski, 1992; Melezhik, 1996). The mineralized  
913 ultramafic bodies are structurally controlled by the  
914 West Rift Graben and related palaeotectonic setting.  
915 Two eruptive centres, Kaula and Kierdzhpori, have  
916 been identified in the Pilgijärvi formation on the  
917 western and eastern sides of the graben, respectively  
918 (Melezhik et al., 1994). The ultramafic bodies are  
919 further divided into the western, located higher up in  
920 the stratigraphy, and eastern group. Green and Melezhik  
921 (1999) suggested that the western group is com-  
922 posed of several flows, or portions of one flow,  
923 interlayered with sediments, ferropicritic flows, and  
924 tuffs, whereas the eastern group is composed of frac-  
925 tionated gabbro–wehrlite sills emplaced close to the  
926 base of the sedimentary sequence. According to Green  
927 and Melezhik (1999), 226 differentiated ultramafic–  
928 mafic bodies can be distinguished: 25 contain Ni–Cu  
929 deposits of economic interest, 68 are classified as  
930 “Ni–Cu-bearing”, and the remaining 113 are described  
931 as “barren”. There are four Ni–Cu sulphide ore types:  
932 massive ultramafic-hosted, brecciated, disseminated,  
933 and “black shale”-hosted, and predominantly Cu-rich  
934 stringer ores (Gorbunov et al., 1985). The ores, which  
935 extend up to 400 m away from the gabbro–wehrlite  
936 intrusions, are Cu-rich, containing 2% Ni and up to  
937 10% Cu. The ultramafic bodies of Souker, Raisoavi,  
938 Mirona, Kierdzhpori, Pilgijärvi and Onki in the  
939 eastern group host disseminated and massive Ni–Cu  
940

deposits in differentiated gabbro–wehrlite intrusions, 941  
and the Pilgijärvi intrusion is particularly voluminous 942  
(500 m thick, 6 km strike length) and well differen- 943  
tiated. The ultramafic mineralized ferropicritic flows 944  
of Semiletka, Kammikivi, Kotselvaara and Kaula of 945  
the western ore group are thin (<100 m) and contain 946  
all ore types (Green and Melezhik, 1999). Hanski 947  
(1992) and Melezhik (1996) consider that the host 948  
rocks of all the Ni–Cu sulphide mineral deposits 949  
originated from the same ferropicritic parental 950  
magma (Fig. 3). This magma was derived from the 951  
stem of a mantle plume and erupted along a graben 952  
structure in the western ultramafic group as a flow on 953  
top of the sediments, whereas in the eastern group the 954  
magma intruded within a sedimentary pile where the 955  
magma cooled slowly and fractionated. Based on the 956  
sulphide textures and geochemistry, sulphur isotope 957  
studies (Hanski, 1992; Melezhik et al., 1994, 1998; 958  
Abzalov and Both, 1997), Re–Os isotope data 959  
(Walker et al., 1997) and PGE data (Abzalov and 960  
Both, 1997), Barnes et al. (2001) modelled the for- 961  
mation of ores and concluded that the ferropicritic 962  
magma reached sulphide saturation prior to ore for- 963  
mation. Sulphur was derived from the unconsolidated 964  
sediments and reacted with the ultramafic flow, col- 965  
lected metals and accumulated sulphide melt in struc- 966  
tural traps where sulphides were fractionated and 967  
separated Mss-rich crystals from Cu-rich residual 968  
melt. Finally the breccia sulphides formed during 969  
deformation. 970

4.1.4. Ni–Cu deposits in Svecofennian orogenic 971  
mafic–ultramafic intrusions 972

A number of mafic–ultramafic intrusions were 973  
emplaced during the Svecofennian Orogeny at 1.89 974  
to 1.87 Ga. Peltonen (2005) divides them into three 975  
Groups (I, II and III), of which the Group I intrusions, 976  
derived from hydrous arc-type tholeiitic basalts, were 977  
emplaced close to the peak of the Svecofennian Oro- 978  
geny (at ~1.89 Ga). Group II intrusions are large 979  
synvolcanic layered gabbro complexes in the southern 980  
Finland arc complex and represent low-pressure crys- 981  
tallization products of relatively juvenile subalkalic 982  
tholeiitic basalts, within an oceanic arc. These intru- 983  
sions have low potential for Ni deposits. Group III 984  
intrusions include Ti–Fe–P-rich anorogenic gabbros 985  
within the central Finland granitoid region, and host 986  
a few Ti–P deposits. 987

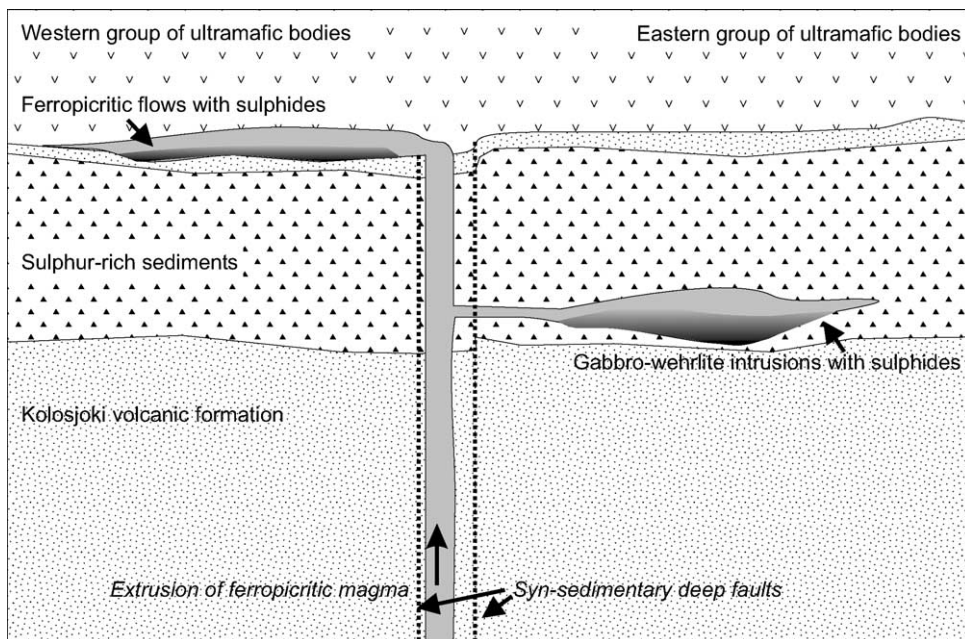


Fig. 3. Depositional model of the formation of the Pechenga Ni–Cu deposits after Melezhik (1996) and Barnes et al. (2001).

988 The Group I intrusions host several magmatic Ni–  
 989 Cu sulphide occurrences, and nine of them have been  
 990 mined in central Finland since the 1960s, producing a  
 991 total of 0.28 Mt of contained nickel metal and 0.1 Mt  
 992 copper (Papunen, 1989, 2003; Puustinen et al., 1995).  
 993 This group is described below in more detail.

994 There are three main nickel ore belts in the Sveco-  
 995 fennian area (Papunen and Gorbunov, 1985), which  
 996 can be further divided into several subzones (Puusti-  
 997 nen et al., 1995). Two of the belts, the Kotalahti belt  
 998 and the Vammala belt, are located in central Finland,  
 999 whereas the Lappvattnet belt is located in northern  
 1000 Sweden. The Kotalahti belt roughly parallels the  
 1001 Archaean–Proterozoic boundary and is hosted by  
 1002 sedimentary–volcanic formations between the Keitele  
 1003 microcontinent and the Archaean craton, whereas the  
 1004 Vammala belt parallels the Tampere schist belt along  
 1005 the southern margin of the Keitele microcontinent  
 1006 against the Bergslagen microcontinent (see Section 5  
 1007 below). The Lappvattnet belt is situated along the  
 1008 southern margin of the Knafthen area against the Both-  
 1009 nia microcontinent in Sweden (Fig. 1). Intensely  
 1010 deformed metasediments with black schist interlayers  
 1011 characterize the environment of the intrusions and the  
 1012 wall-rocks are commonly migmatized to neosome-

rich schollen migmatites. The neosome intersects the  
 intrusions as random granitic vein networks. The  
 felsic veins metasomatized the ultramafic olivine-  
 bearing parts of the intrusions, forming zoned margins  
 composed of talc, tremolite, and chlorite against the  
 phlogopite-bearing vein fill (Papunen, 1971; Marshall  
 et al., 1995; see also Menard et al., 1999). The zoned  
 margins were not developed around the veins in pyroxenitic  
 and gabbroic parts of the intrusions. Structural analysis  
 implies that the intrusion of mafic magma took place  
 before or at the peak of D<sub>2</sub> deformation and the intrusions  
 were deformed and brecciated during late F<sub>2</sub> folding  
 (Kilpeläinen, 1998). The contact zones against felsic  
 migmatites experienced metasomatic alteration and  
 peridotites were altered to serpentinites and pyroxenites  
 to amphibole–chlorite rocks. In the Vammala belt the  
 metamorphic conditions reached upper amphibolite to  
 lower granulite facies (i.e., 600 to 700 °C and 5 to 6  
 kbar; Peltonen, 1990) and the cooling from peak conditions  
 was slow, as evident from the subsolidus re-equilibration  
 of olivine and chromite spinel and redistribution of Ca  
 between pyroxenes (Peltonen, 1995b).

Two main types of Group I mafic–ultramafic intrusions  
 host Ni–Cu sulphides: a) differentiated perido-

1013  
 1014  
 1015  
 1016  
 1017  
 1018  
 1019  
 1020  
 1021  
 1022  
 1023  
 1024  
 1025  
 1026  
 1027  
 1028  
 1029  
 1030  
 1031  
 1032  
 1033  
 1034  
 1035  
 1036  
 1037



1038 tite–gabbro ± diorite bodies (e.g., Kotalahti, Laukun-  
 1039 kangas and Telkkälä) and b) weakly differentiated  
 1040 ultramafic olivine-dominated cumulate bodies (e.g.,  
 1041 Vammala; Fig. 4, Kylmäkoski, and Hitura; Mäkinen,  
 1042 1987). The Group Ia intrusions are situated at the  
 1043 craton margin in the eastern part of the Kotalahti  
 1044 belt. Ni–Cu deposits hosted by differentiated intru-  
 1045 sions have been mined in Kotalahti, Laukunkangas,  
 1046 Hälvälä, and Tekkälä in SE Finland (Fig. 5; Papunen  
 1047 and Vorma, 1985), of which Kotalahti is the largest  
 1048 deposit that has been mined so far (see Table 1). The  
 1049 host intrusions vary in shape, size and composition,  
 1050 and the rock suite ranges from peridotites to diorites  
 1051 (Makkonen, 1996; Papunen, 2003). In Kotalahti (Fig.  
 1052 5) and Telkkälä the most ultramafic members are  
 1053 located in the central parts of the intrusive bodies,  
 1054 but in Laukunkangas the ultramafic rock is located at  
 1055 the base of the predominantly mafic body. Locally,  
 1056 gabbroic and dioritic members of the differentiation  
 1057 series display anomalously low Ni content of mafic  
 1058 silicates.

1059 Olivine is the earliest cumulus mineral in all miner-  
 1060 alized Group Ia intrusions, followed by orthopyroxene  
 1061 and plagioclase. Chromite is rare or totally absent, but  
 1062 primary magmatic amphiboles are common intercu-  
 1063 mulus minerals. In gabbroic intrusions orthopyroxene  
 1064 is the dominant cumulus phase, followed by plagioc-  
 1065 clase. Sulphides are of disseminated and breccia type,  
 1066 partly outside the intrusion as offset orebodies. The  
 1067 parental magmas of the Ia intrusions were tholeiitic  
 1068 basalts, with MgO contents ranging from 8% to 11%  
 1069 and an Al<sub>2</sub>O<sub>3</sub>/TiO<sub>2</sub> ratio of around 10 (Makkonen,  
 1070 1996). Their concentrations of compatible elements,  
 1071 notably Ni, are relatively high, but the PGE contents  
 1072 are low (Papunen, 1989). Evidence for contamination  
 1073 includes elevated LREE and Zr and low average  
 1074  $\epsilon_{\text{Nd}}^{(1.9 \text{ Ga})}$  value, +0.7 (Makkonen, 1996).

1075 The Group Ib intrusions and related Ni–Cu depos-  
 1076 its are situated in the Vammala belt, although the  
 1077 Group Ia intrusions also occur in the western exten-  
 1078 sion of the belt (e.g., Hyvelä). Group Ib intrusions  
 1079 also characterize the Lappvattnet belt and the Hitura  
 1080 area. The rock types range from dunites to wehrlites  
 1081 and early-crystallized chromian spinel is a common  
 1082 accessory mineral. Early crystallization of clinopyrox-  
 1083 ene and lack of cumulus plagioclase in Group Ib are  
 1084 the main distinctive features. The sulphides are mainly  
 1085 of disseminated type and accumulated at the basal

1086 contact zones of primary olivine ± clinopyroxene  
 1087 cumulates (Fig. 4). The average  $\epsilon_{\text{Nd}}^{(1.9 \text{ Ga})}$  value of the  
 1088 type Ib intrusions in the Vammala belt is +1.7, which  
 1089 is lower than the corresponding value of +2.7  
 1090 obtained from the mafic intrusions and extrusions of  
 1091 the Group II intrusions south of the Vammala belt  
 1092 (Peltonen, 2005).

1093 The geodynamic setting of orogenic Ni–Cu depos-  
 1094 its at convergent boundaries of microplates is greatly  
 1095 obscured by severe tectonic deformation, metamorph-  
 1096 ism and metasomatic overprints. Gaál (1972, 1985)  
 1097 and Puustinen et al. (1995) inferred that the Group Ia  
 1098 intrusions were emplaced into a subvertical D<sub>3</sub>  
 1099 wrench lineament, which is clearly visible along the  
 1100 Kotalahti belt in tectonic and geophysical maps. How-  
 1101 ever, in detail most of the intrusions occur outside the  
 1102 shear zone and a genetic relationship is ambiguous.  
 1103 According to Peltonen (2005), the plutonism occurred  
 1104 over a wide zone due to westward subduction during  
 1105 the final stages of the closure of the basin between the  
 1106 primitive arc complex and the Archaean craton. Syn-  
 1107 chronous transtensional shear systems, developed at  
 1108 the continental margin, facilitated the ascent of melts  
 1109 locally along subvertical shear zones. During D<sub>3</sub> the  
 1110 zones were reactivated and the intrusions were  
 1111 deformed and brecciated. Early assimilation of felsic  
 1112 sedimentary material and related increase of silica in  
 1113 the ascending magma resulted in the crystallization  
 1114 sequence olivine–orthopyroxene–plagioclase typical  
 1115 of type Ia intrusions (Haughton et al., 1974). Accord-  
 1116 ingly, low  $\epsilon_{\text{Nd}}^{(T)}$  values and elevated LREE and Zr  
 1117 abundances indicate contamination (Makkonen,  
 1118 1996). The primary parental magma was sulphide  
 1119 unsaturated and the concentrations of chalcophile ele-  
 1120 ments, notably Ni, were high. Contamination with  
 1121 sulphide-bearing sediments turned the magma to sul-  
 1122 phide saturation and accumulation of sulphides took  
 1123 place. Mutually intrusive breccias between the mem-  
 1124 bers of the differentiation series, lack of compositional  
 1125 layering, breccia type sulphides also as offset orebod-  
 1126 ies outside the intrusion proper, and complicated  
 1127 shapes of the intrusive complexes are all evidence of  
 1128 polyphase intrusion, where the melt fractionated inter-  
 1129 mittently in a magma chamber before final emplace-  
 1130 ment (Papunen, 2003). Syn-magmatic deformation  
 1131 squeezed the melt and early-crystallized silicates  
 1132 from high stress to low stress areas. At this stage  
 1133 the evolved, depleted and barren melt from the

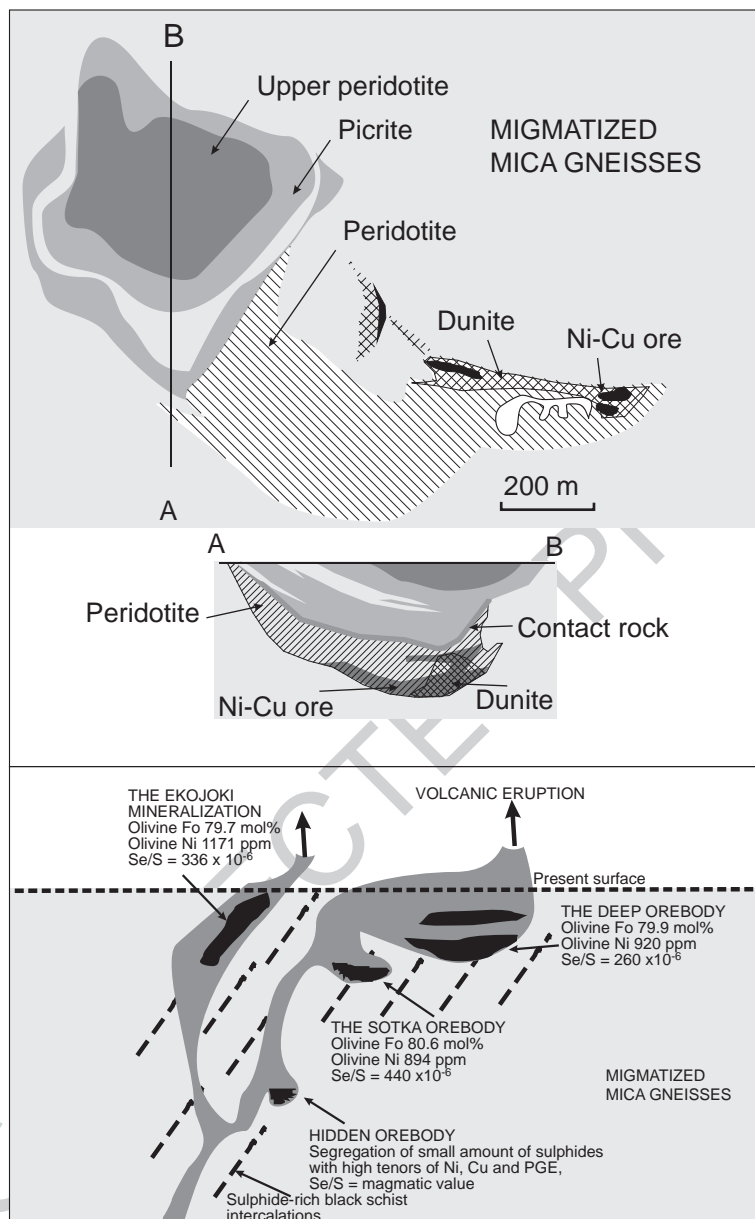


Fig. 4. The Vammala Ni–Cu deposit: the host rock of the Vammala Ni–Cu deposit is the Stormi ultramafic intrusion, which has the shape of a shallow bowl with mineralized dunitic portions at the base. Upper part of the intrusion consists of picrite and “upper peridotite”, which are barren and geochemically different from the mineralized lower dunite–peridotite intrusion. The picritic portion represents an ultramafic volcanic formation, which belongs to the supracrustal sequence and pre-dates the intrusion of the fertile dunite–peridotite body. The wall-rocks are migmatized mica gneisses, which also exist as inclusions and tongues inside the picritic layer and locally also between the lower peridotite and picrite. The whole ultramafic body is metamorphosed and intersected by felsic pegmatite dykes. The deposit was mined between 1973 and 1995 and produced 7.4 Mt ore at 0.69% Ni and 0.4% Cu. The Vammala genetic model: according to [Peltonen \(1995a\)](#) the Vammala-type intrusions are feeder channels of basaltic lava flows. The magma became contaminated by wall-rock sulphides and accumulated disseminated and semi-massive sulphides together with early crystallized olivine, spinel and pyroxenes in suitable parts of the intrusion channel. Composition of olivine can be used to follow the evolution of magma in the feeder channel.

1134 upper part of the magma chamber separated and  
 1135 formed Ni-depleted regions of the intrusive complex.  
 1136 In the final phase, the sulphide-bearing ultramafic  
 1137 cumulates and magma from the lower part of chamber  
 1138 intruded to form mineralized ultramafic bodies.  
 1139 Finally the accumulated massive sulphides were  
 1140 squeezed out from the deeper parts of the magma  
 1141 chamber and deposited breccia offset orebodies in a  
 1142 zone of tectonic weakness.

1143 [Peltonen \(2005\)](#) considers that the Group Ib ultra-  
 1144 mafic cumulate bodies represent former feeder chan-  
 1145 nels for mafic shallow intrusions, sills or volcanic  
 1146 eruptions ([Fig. 4](#)). Calculations based on the composi-  
 1147 tion of the most magnesian olivine in the intrusions  
 1148 and Fe/Mg distribution between olivine and melt  
 1149 indicate that the MgO contents of the parental mag-  
 1150 mas ranged from 8% up to 12% MgO. Common  
 1151 magmatic intercumulus amphibole suggests a hydrous  
 1152 parental magma indicative of arc-type basalt. Accord-  
 1153 ingly, the mass calculations based on the high Mg  
 1154 content of cumulates compared to the composition of  
 1155 parental magma suggest that the ultramafic cumulates  
 1156 visible at the present erosion level represent only a  
 1157 minor portion of the total igneous complex from  
 1158 which the upper part was eroded away ([Peltonen,](#)  
 1159 [1995a](#)). Trace element composition, low Se/S in sul-  
 1160 phides, lower than mantle  $\epsilon_{\text{Nd}}^{(1.9 \text{ Ga})}$  values, and com-  
 1161 mon graphite in ultramafic cumulates show that the  
 1162 trace element composition of the parental magma for  
 1163 the Group Ib intrusions was strongly modified during  
 1164 emplacement through the crust. The mantle-derived  
 1165 magma was sulphide unsaturated, but became satu-  
 1166 rated at the level of crust due to interaction with  
 1167 sulphur derived from the black schists ([Peltonen,](#)  
 1168 [1995a](#)). The sulphides accumulated at suitable traps  
 1169 in feeder channels together with early crystallizing  
 1170 olivine and spinel.

1171 The differences between Group Ia and Ib intrusions  
 1172 are due to the more profound contamination of Group  
 1173 Ia intrusions, their fractionation in an intermittent  
 1174 magma chamber, and intrusion as fractionated batches  
 1175 to their present positions in the crust. The Group Ib  
 1176 intrusions represent feeder channels of a more open  
 1177 intrusive–volcanic system, and probably also a more  
 1178 voluminous intrusion of magma into an environment  
 1179 where the crustal contaminant was slightly different  
 1180 and the tectonic evolution more tranquil than for  
 1181 Group Ia intrusions.

#### 4.2. VMS deposits

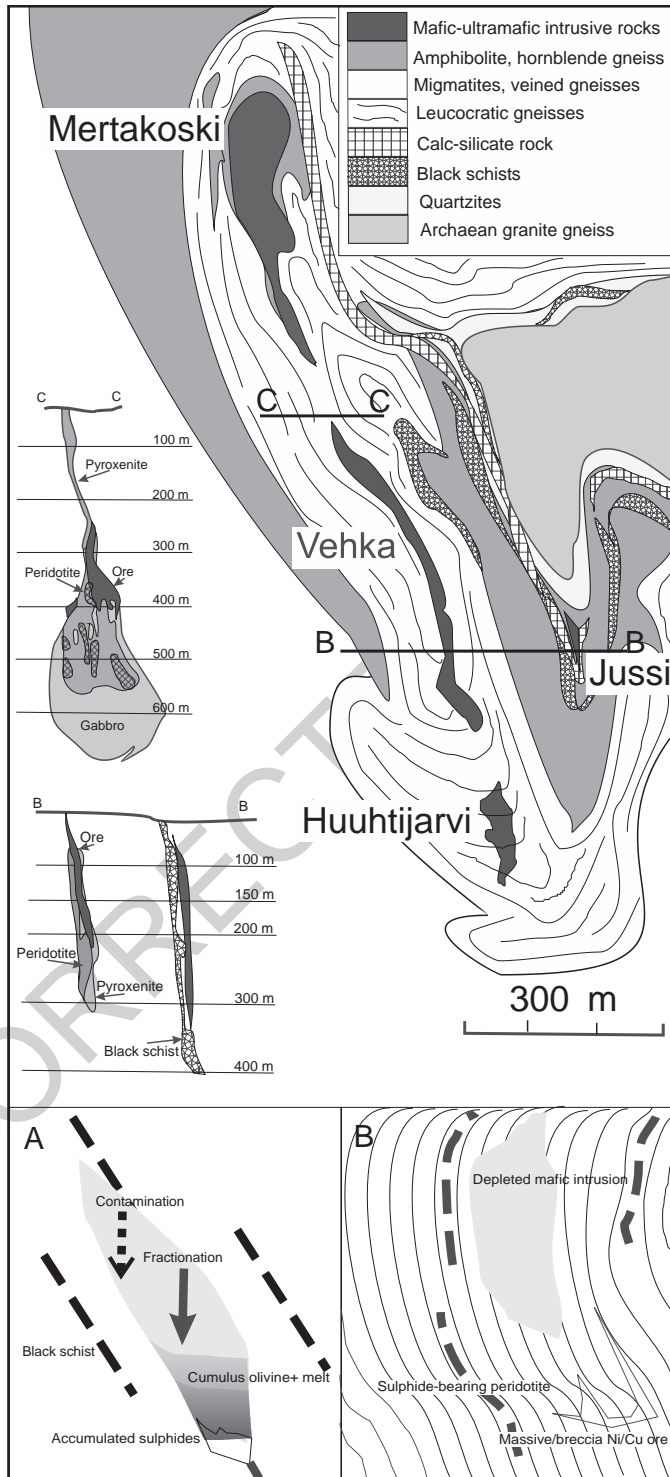
1182  
 1183 Volcanogenic massive sulphide (VMS) deposits are  
 1184 the ore type that is currently the most exploited in the  
 1185 Fennoscandian Shield. Five deposits are currently  
 1186 mined in the Skellefte district in northern Sweden,  
 1187 one deposit in the Pyhäsalmi area in central Finland  
 1188 and two deposits in the Bergslagen region of south-  
 1189 central Sweden. However, it is unclear whether or not  
 1190 some of the major deposits in the Bergslagen region  
 1191 should be classified as VMS deposits (e.g., [Garpen-](#)  
 1192 [berg and Zinkgruvan](#)), see below. Also an open ques-  
 1193 tion is whether or not the Outokumpu deposits  
 1194 ([Kontinen, 1998; Sorjonen-Ward et al., 2004](#)),  
 1195 although discussed in this section, really are VMS  
 1196 deposits *sensu stricto*.

##### 4.2.1. Geodynamic setting

1197  
 1198 Significant VMS deposits ([Table 1](#)) are associated  
 1199 exclusively with Palaeoproterozoic volcanic arc ter-  
 1200 ranes in the Fennoscandian Shield (Box 8-1, [Weihed](#)  
 1201 [and Eilu, 2005](#), this volume). With recent improve-  
 1202 ments in radiogenic dating techniques it has been  
 1203 shown that the host volcanic arcs have different ages  
 1204 and were accreted to the old Karelian craton at differ-  
 1205 ent stages during the evolution of the Svecokarelian  
 1206 orogen, between ca. 1.95 and 1.85 Ga. The earliest  
 1207 expressions of Svecokarelian accretionary processes  
 1208 are the Jormua, Outokumpu, and possibly Nuttio  
 1209 ophiolitic sequences, which formed at ca. 1.97 Ga  
 1210 and were emplaced onto the Karelian Craton between  
 1211 1.94 and 1.89 Ga.

1212 The 1.93 to 1.92 Ga Pyhäsalmi arc was the next to  
 1213 be accreted and contains Kuroko-style VMS deposits,  
 1214 as does the Skellefte volcanic arc that formed 20 to 30  
 1215 million years later than the Pyhäsalmi arc. The Berg-  
 1216 slagen–Uusimaa belt in south-central Sweden and  
 1217 southern Finland contains VMS deposits of a more  
 1218 continental arc affinity that formed roughly at the  
 1219 same time as the Skellefte deposits.

1220 The Palaeoproterozoic arc assemblages also seem  
 1221 in detail to represent slightly different tectonic set-  
 1222 tings, apart from their age differences ([Fig. 6](#)). The  
 1223 Pyhäsalmi bimodal volcanic rocks formed during rift-  
 1224 ing of a Palaeoproterozoic oceanic island arc, whereas  
 1225 the younger Skellefte volcanic rocks were formed  
 1226 during extension of an immature continental volcanic  
 1227 arc. The Bergslagen province formed by volcanism in



1228 a continental margin setting and is fundamentally  
 1229 different in the composition of its host rocks and  
 1230 associated metallogeny compared to the Pyhäsalmi  
 1231 and Skellefte provinces. The Vihanti–Pyhäsalmi and  
 1232 Skellefte deposits show many similarities with Kur-  
 1233 oko-type deposits, whereas the Outokumpu deposits  
 1234 have been described as “Cyprus-type” deposits (Helo-  
 1235 vuori, 1979; Ekdahl, 1993; Allen et al., 1996a).  
 1236 Recently, however, the idea of exhalative ore forma-  
 1237 tion for the Outokumpu deposits has been questioned,  
 1238 as the chemical composition of the host rocks indi-  
 1239 cates that they are subcontinental lithospheric mantle  
 1240 rocks (Kontinen, 1998; Sorjonen-Ward et al., 2004).  
 1241 Sorjonen-Ward et al. (2004) propose that mineraliza-  
 1242 tion instead may represent deep levels of subseafloor  
 1243 hydrothermal convection.

1244 The apparent restriction of Palaeoproterozoic VMS  
 1245 mineralization to the Fennoscandian Shield is some-  
 1246 what enigmatic. The deposits of the Fennoscandian  
 1247 Shield have ages that are similar, within error, to those  
 1248 of the Trans-Hudson and Penokean orogenies in North  
 1249 America (e.g., in the Flin-Flon and Snow Lake areas)  
 1250 and share many other features with these deposits (see  
 1251 Syme et al., 1982). The scarcity of known VMS  
 1252 mineralization in the Archaean of the Fennoscandian  
 1253 Shield can be attributed to two factors: (1) the lack of  
 1254 suitable host sequences of the appropriate age, as  
 1255 explained above, and (2) the unexplored nature of  
 1256 the Archaean areas, especially in Russia.

#### 1257 4.2.2. Timing and relation to regional tectonic 1258 evolution of the shield

1259 The *Pyhäsalmi area* is characterized by bimodal  
 1260 volcanic sequences. The mafic volcanic rocks are low-  
 1261 K, island-arc tholeiite metabasalts and basaltic meta-  
 1262 andesites, whereas the felsic volcanic rocks include  
 1263 low-K, transitional to calc-alkaline rhyodacites, rhyo-

1264 lites, and high-silica rhyolites (Rasilainen, 1991; 1264  
 1265 Koussa et al., 1994; Lahtinen, 1994). The local base- 1265  
 1266 ment to the bimodal volcanic sequence is suggested to 1266  
 1267 comprise a collage of ca. 2.0 to 1.94 Ga volcanic 1267  
 1268 rocks (Lahtinen, 1994). Within the bimodal volcanic 1268  
 1269 sequence, massive sulphide deposits occur either at 1269  
 1270 the transition from mafic to felsic volcanic rocks, or 1270  
 1271 are entirely hosted by felsic pyroclastic rocks (Huh- 1271  
 1272 tala, 1979; Mäki, 1986; Rasilainen, 1991). Deformed 1272  
 1273 1.93 to 1.91 Ga tonalites and trondhjemites are spa- 1273  
 1274 tially associated with ore-associated bimodal volcanic 1274  
 1275 sequences (Lahtinen, 1994). Isotope and trace element 1275  
 1276 data from these rocks show that they were produced 1276  
 1277 by partial melting of ca. 2.0 Ga primitive island-arc 1277  
 1278 tholeiite basalts (Lahtinen, 1994; Lahtinen and 1278  
 1279 Huhma, 1997). The intrusive rocks are geochemically 1279  
 1280 similar to and of the same age as the ore-associated 1280  
 1281 metarhyolites, and are therefore considered to repre- 1281  
 1282 sent subvolcanic equivalents of the latter (Koussa et al., 1282  
 1283 1994; Lahtinen, 1994).

1284 In places, the bimodal volcanic sequence is over- 1284  
 1285 lain by migmatitic metasedimentary rocks with inter- 1285  
 1286 calated calc-silicate and graphite-bearing interlayers. 1286  
 1287 In turn, this sequence is succeeded by a younger 1287  
 1288 (~1.88 Ga) calc-alkaline volcanic suite formed in a 1288  
 1289 mature arc setting (Koussa et al., 1994).

1290 According to Lahtinen (1994), the 1.93 to 1.91 Ga 1290  
 1291 volcanic rocks that host Zn–Cu deposits in the 1291  
 1292 Vihanti–Pyhäsalmi district formed within a rifted pri- 1292  
 1293 mitive island arc. Intra-arc rifting in a juvenile setting 1293  
 1294 is implied by the occurrence of bimodal volcanism, 1294  
 1295 low-K tholeiitic basalts, and minimal hornblende frac- 1295  
 1296 tionation in the generation of rhyolites. The felsic 1296  
 1297 subvolcanic intrusions have juvenile  $\epsilon_{\text{Nd}}$  values, indi- 1297  
 1298 cating an origin by partial melting of a primitive low- 1298  
 1299 K island-arc basalt source (Koussa et al., 1994; Lahti- 1299  
 1300 nen, 1994).

Fig. 5. Kotalahti: this is an example of fractionated intrusions, which host Ni–Cu deposits in the Svecofennian area of Finland. The main rock types are peridotite and pyroxenite in the upper part of the subvertical, plate-shaped intrusion and in the southern Huuhtijärvi vertical pipe-shaped body, but gabbros abound in the deep part of the Vehka body. Contacts between different rock types are commonly sharp or gradual over a short distance. The disseminated and breccia ores occur mainly in peridotites and pyroxenites, and gabbros in the deeper part of the intrusion, in particular, are barren and even depleted in nickel. The intrusion is metamorphosed and intersected by felsic dykes. The massive Jussi orebody with high-grade Ni–Cu sulphides exists about 150 m east of the intrusion as a vertical slab in black schist and calc-silicate rock environment. The mine produced 13 Mt of ore at 0.7% Ni and 0.27% Cu. The Kotalahti model: the model of the Kotalahti-type deposits is based on early contamination of mantle-derived melt by sedimentary sulphides and felsic country rocks, which caused sulphide immiscibility and fractionation in a magma chamber where the upper part became depleted in chalcophile elements and sulphides and mafic crystals accumulated at the lower part of the chamber (A). In subsequent orogenic deformation the different parts of the fractionated chamber remobilized and intruded separately to form depleted mafic and intermediate intrusions and sulphide-bearing peridotite and pyroxenite bodies. Sulphides remobilized with the ultramafic portion and could also be intruded as offset ores outside the intrusion proper (B).

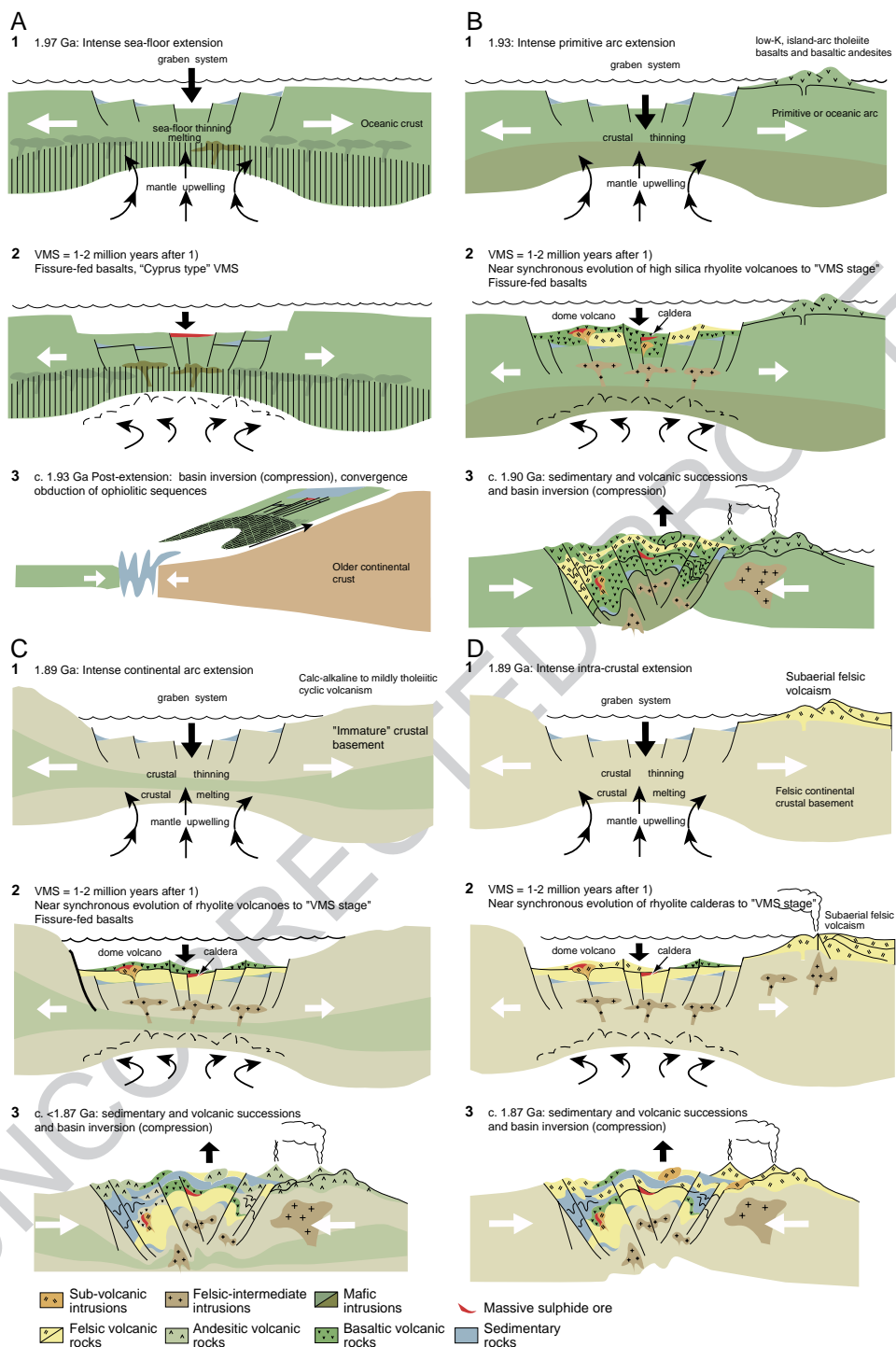


Fig. 6. Key geodynamic features of VMS deposits. Model adapted from Allen et al. (2002). Tectonic setting during formation of (A) ophiolitic VMS deposits (Outokumpu type), (B) primitive arc VMS deposits (Vihanti-Pyhäsalmi type), (C) mature arc or continental margin VMS deposits (Skellefte type) and (D) intracrustal VMS deposits (Bergslagen type).

1301 Roberts (2002) suggested that the basalts and rhyo-  
 1302 lites in the immediate host sequence to these deposits  
 1303 did not form in a proto-arc setting. Instead, Roberts  
 1304 (2002) interprets the district as a rifted primitive vol-  
 1305 canic arc. Roberts (2002) also suggests that an asso-  
 1306 ciation with tholeiitic basalts and transitional to calc-  
 1307 alkalic rhyolites, including high-silica varieties,  
 1308 broadly fits within the “bimodal mafic type” classifi-  
 1309 cation of Barrie and Hannington (1999) and argues  
 1310 that the association of Zn–Cu mineralization within a  
 1311 relatively mature arc assemblage is analogous to the  
 1312 observations of Bailes and Galley (1999) in the Flin-  
 1313 Flon Belt, Canada, where Zn-dominant deposits occur  
 1314 within mature arc assemblages, and most Cu-domi-  
 1315 nant deposits occur within primitive arc assemblages.  
 1316 The Skellefte district is a 120 × 30 km Palaeopro-  
 1317 toerozoic volcanic-dominated belt that contains over 80  
 1318 massive sulphide deposits (Rickard, 1986; Weihed et  
 1319 al., 1992; Allen et al., 1996b). The volcanic stratigra-  
 1320 phy is composed of calc-alkaline basalt–andesite–  
 1321 dacite–rhyolite, tholeiitic basalt–andesite–dacite,  
 1322 high-Mg (komatiitic) basalt and subordinate sedimen-  
 1323 tary rocks, and is intruded by syn- and post-volcanic  
 1324 granitoids (Vivallo and Claesson, 1987; Allen et al.,  
 1325 1996b, 2002). About half the volcanic rocks are rhyo-  
 1326 lites. Primitive isotopic signatures suggest that mag-  
 1327 mas were mainly mantle-derived (Billström and  
 1328 Weihed, 1996). The stratigraphy is very complex,  
 1329 laterally variable, and diachronous, and marker hori-  
 1330 zons are rare. On a regional scale, however, a lower  
 1331 >3 km thick, ore bearing, marine volcanic complex  
 1332 (~1.90 to 1.88 Ga) is overlain by a >4 km thick,  
 1333 mixed sedimentary and volcanic sequence. According  
 1334 to Allen et al. (2002), the dominance of marine  
 1335 depositional environments throughout the lower vol-  
 1336 canic complex indicates strong extension and subsi-  
 1337 dence. The overlying mixed sedimentary and volcanic  
 1338 sequence records rapid uplift, erosion and renewed  
 1339 rifting, and includes medial–distal facies of volumi-  
 1340 nous, ca. 1.88 to 1.87 Ga, subaerial felsic magmatism.  
 1341 Allen et al. (2002) point out that the stratigraphic  
 1342 architecture, range of volcanic compositions and  
 1343 abundance of rhyolites indicate that the district is a  
 1344 remnant of a strongly extensional intra-arc region that  
 1345 developed on continental or mature arc crust in con-  
 1346 trast to the primitive volcanic arc setting for the  
 1347 Vihanti–Pyhäsalmi belt. Most VMS ores occur in  
 1348 near-vent facies associations at the top of local volca-

1349 nic cycles, especially rhyolitic dome–tuff cone volca-  
 1350 noes (Allen et al., 1996b). Regionally, these VMS  
 1351 ores occur on at least two stratigraphic levels, most  
 1352 commonly near the upper contact of the lower volca-  
 1353 nic complex.

1354 The Bergslagen district, located in south-central  
 1355 Sweden, and the extension into SW Finland, the  
 1356 Uusimaa belt, are 1.90 to 1.87 Ga in age and char-  
 1357 acterized as a felsic magmatic region. The volcanic  
 1358 succession is 1.5 km thick and overlies turbiditic  
 1359 metasediments in the east, and is over 7 km thick  
 1360 with no exposed base in the west (Lundström, 1987;  
 1361 Allen et al., 1996a). The basement is interpreted to be  
 1362 older, unexposed, continental crust.

1363 In contrast to the Vihanti–Pyhäsalmi and Skellefte  
 1364 districts, Bergslagen contains a diverse range of ore  
 1365 deposits, including banded iron formations, magnetite  
 1366 skarns, manganiferous skarns and marble-hosted iron  
 1367 ores, apatite–magnetite iron ores, stratiform and stra-  
 1368 tabound Zn–Pb–Ag–(Cu–Au) sulphide ores, and W  
 1369 skarns (Hedström et al., 1989; Sundblad, 1994; Allen  
 1370 et al., 1996b).

1371 Although traditionally described as massive sul-  
 1372 phide ores divided into the Ämmeberg and Falun  
 1373 types (Sundblad, 1994), and historically among the  
 1374 first ore deposits in Sweden described as exhalative  
 1375 (Koark, 1962), their classification as typical VMS  
 1376 deposits can be questioned. The ore deposits conform,  
 1377 with some exceptions, to a regional ore stratigraphy.  
 1378 Based on physical characteristics, the main base-metal  
 1379 deposits span a range between two end-member types  
 1380 (Allen et al., 1996b). The first type comprises sheet-  
 1381 like, bedded, stratiform Zn–Pb–Ag–rich, Fe and Cu  
 1382 sulphide-poor deposits such as Zinkgruvan. These  
 1383 deposits are hosted by rhyolitic ash–siltstones with  
 1384 marble, skarn, and siliceous chemical sediment beds,  
 1385 and have intense footwall potassic alteration, silicifi-  
 1386 cation, and subordinate Mg-rich alteration (Hedström  
 1387 et al., 1989). Allen et al. (1996b) named these deposit  
 1388 “stratiform ash siltstone”-hosted Zn–Pb–Ag sulphide  
 1389 deposits (SAS type) and included some deposits of the  
 1390 Ämmeberg type (see Sundblad, 1994 and references  
 1391 therein). The second end-member type according to  
 1392 Allen et al. (1996b) includes irregular multi-lens and  
 1393 pod-like, strata-bound, massive and disseminated Zn–  
 1394 Pb–Ag–Cu mineralization such as Garpenberg, and  
 1395 more massive pyritic Cu–Zn–Pb–Ag–Au mineraliza-  
 1396 tion such as Falun. These deposits straddle marble

1397 beds within felsic metavolcanic rocks, are closely  
1398 associated with Mg-rich tremolite–diopside skarn  
1399 and dolomite zones within the marbles, and have  
1400 intense footwall Mg-rich alteration (phlogopite–  
1401 biotite–talc–almandine–cordierite–amphibole–quartz  
1402 schists). These deposits are designated “strata-bound”,  
1403 volcanic-associated, limestone–skarn Zn–Pb–Ag–Cu–  
1404 Au sulphide deposits, SVALS type, by Allen et al.  
1405 (1996b) and correspond approximately to the Falun  
1406 type (see Sundblad, 1994 and references therein).

1407 Allen et al. (1996b) suggested that most of the  
1408 sulphide ores at Garpenberg and Stollberg formed as  
1409 synvolcanic stratabound subsea-floor replacements  
1410 and that the thin sheet-like superficially stratiform  
1411 massive sulphide layers are tectonically mechanically  
1412 remobilized ore. They also suggested that much of the  
1413 ore deposition occurred by reaction of the ascending  
1414 hydrothermal solutions with limestones below the sea  
1415 floor. This distinguishes them from VMS deposits  
1416 sensu stricto. Also the Zinkgruvan type stratiform  
1417 Zn–Pb–Ag sulphide deposits are difficult to classify  
1418 as VMS deposits sensu stricto (Allen et al., 1996b).  
1419 They have some similarities to VMS deposits and to  
1420 some stratiform sediment-hosted Pb–Zn deposits.  
1421 However, they appear most similar to the Broken  
1422 Hill-type deposits; sheetlike ore lenses, Zn–Pb–Ag-  
1423 rich and Cu-poor, mainly pyrite-poor composition,  
1424 stratigraphic succession grading from coarse-grained  
1425 metavolcanic and metasedimentary rocks below the  
1426 ores to pelites above, proximity to banded iron-for-  
1427 mations, association with limestone, calc-silicate  
1428 rocks, mafic sills (amphibolites) and unusual chemical  
1429 sedimentary rocks such as garnet quartzite.

1430 The volcanic succession in this district is domi-  
1431 nated by calc-alkaline rhyolites with minor calc-alka-  
1432 line dacite and andesite, and chemically unrelated,  
1433 probably tholeiitic basalts (Allen et al., 1996a,  
1434 2002). The stratigraphy is composed of: (1) a lower,  
1435 1 to 5 km thick, poorly stratified felsic complex  
1436 dominated by a proximal–medial facies of interfinger-  
1437 ing and overlapping large caldera volcanoes, and  
1438 minor interbedded marble, (2) a middle, 0.5 to 2.5  
1439 km thick, well-stratified interval dominated by med-  
1440 ial–distal juvenile volcanoclastic facies and marble  
1441 sheets, and (3) an upper, >3 km thick, post-volcanic  
1442 meta-argillite–turbidite sequence (Allen et al., 1996a).  
1443 Depositional environments fluctuated mainly between  
1444 shallow and moderately deep subaqueous throughout

the lower and middle stratigraphic intervals, and  
became consistently deep subaqueous in the upper  
interval (Allen et al., 1996a).

The supracrustal succession has been intruded by  
syn- and post-volcanic granitoids. The stratigraphy  
reflects an evolution from intense magmatism, thermal  
doming, and crustal extension, followed by waning  
extension, waning volcanism, and thermal subsidence,  
then reversal from extension to compressional deforma-  
tion and metamorphism (Allen et al., 2002). The  
region is interpreted as an extensional intra-continental  
or continental margin back-arc, region (Allen et al.,  
1996a).

#### 4.3. Orogenic gold

Orogenic gold deposits, following the terminology  
of Groves et al. (1998), are present in both Archaean  
and Proterozoic units of the Fennoscandian Shield  
(Fig. 2). Some gold-only deposits have been described  
with alternative genetic models; for example, the  
Enåsen (Hallberg, 1994) and Kutemajärvi (Poutiainen  
and Grönholm, 1996) have been interpreted as meta-  
morphosed epithermal deposits. The largest gold  
deposit in the Fennoscandian Shield, the Boliden  
deposit, has also been described as a hybrid epither-  
mal VMS deposit (Bergman Weihed et al., 1996). In  
the northernmost part of the Fennoscandian Shield  
Cu–Au deposits such as Bidjovagge (Ettner et al.,  
1994), Pahtohavare (Lindblom et al., 1996) and Saat-  
topora (Grönholm, 1999) have been described as oro-  
genic gold deposits, but the high content of Cu makes  
these deposit more akin to IOCG deposits (see  
Weihed, 2001).

Although the currently economic deposits are  
strongly concentrated in the Palaeoproterozoic  
domains (cf. Sundblad, 2003), tens of occurrences  
have also been identified in Archaean areas that  
have been explored for gold by modern methods  
(Eilu et al., 2003). The apparent scarcity of Archaean  
economic deposits is probably due to the fact that little  
exploration for gold has been performed in the Rus-  
sian part of the shield and that exploration in the  
Finnish part is relatively recent.

Age data on orogenic gold mineralizing events are  
scarce, but it is possible to constrain three major  
periods of mineralization; 2.72 to 2.67, 1.90 to 1.86  
and 1.85 to 1.79 Ga (Box 8-2, Eilu and Weihed, 2005,

1445  
1446  
14471448  
1449  
1450  
1451  
1452  
1453  
1454  
1455  
1456  
1457

1458

1459  
1460  
1461  
1462  
1463  
1464  
1465  
1466  
1467  
1468  
1469  
1470  
1471  
1472  
1473  
1474  
1475  
14761477  
1478  
1479  
1480  
1481  
1482  
1483  
1484  
1485  
14861487  
1488  
1489  
1490



1491 this volume), excluding a few minor younger events  
 1492 (Luukkonen, 1992; Sorjonen-Ward, 1993; Mänttari,  
 1493 1995; Bark and Weihed, 2003; Eilu et al., 2003;  
 1494 Weihed et al., 2003). The age data appear to define  
 1495 a rough zonation from NE to SW, which seems to be  
 1496 related to the south-westward growth of the Fennos-  
 1497 candian Shield with time.

#### 1498 4.3.1. Geodynamic setting

1499 The periods of orogenic mineralization in the Fen-  
 1500 noscandian Shield fit into two of the main global  
 1501 periods of orogenic gold mineralization during the  
 1502 Precambrian, at ca. 2.7 to 2.6 and ca. 1.9 to 1.8 Ga,  
 1503 which correlate with the major episodes of juvenile  
 1504 continental growth discussed above (Stein and Hof-  
 1505 mann, 1994; Goldfarb et al., 2001). More specifically,  
 1506 the periods of orogenic gold mineralization can be  
 1507 correlated with the main compressional to transpres-  
 1508 sional events, with peak regional metamorphism and  
 1509 the latest main stage of deformation during major  
 1510 orogenies in the shield (Luukkonen, 1992; Sorjonen-  
 1511 Ward, 1993; Lahtinen et al., 2003; Eilu et al., 2003;  
 1512 Sundblad, 2003; Weihed et al., 2003):

1513

- 1514 (i) The 2.72 to 2.67 Ga stage coincides with the  
 1515 global period of accelerated crustal growth near  
 1516 the end of the Archaean.
- 1517 (ii) The 1.90 to 1.86 Ga stage relates to microcon-  
 1518 tinent accretion (see Section 5) that formed part  
 1519 of a second peak of crustal growth. For the  
 1520 Archaean units, this includes the collision of  
 1521 the Karelian craton with the Kola craton in the  
 1522 north and Norrbotten craton in the west, as  
 1523 discussed below. Simultaneously, to the SW of  
 1524 the Archaean units, the Palaeoproterozoic Kei-  
 1525 tele microcontinent collided with the Karelian  
 1526 craton (Lapland–Savo Orogeny), eastward sub-  
 1527 duction under the Norrbotten craton started at  
 1528 1.89 to 1.88 Ga, the Bergslagen microcontinent  
 1529 started to accrete (Fennian Orogeny), and  
 1530 finally, in the south, the Bothnia and Bergslagen  
 1531 microcontinents amalgamated at 1.87 to 1.86  
 1532 Ga. The stage resulted in the formation of a  
 1533 large continental plate, the Fennoscandia Plate.
- 1534 (iii) The 1.85 to 1.79 Ga stage involved collision of  
 1535 the Fennoscandia continental plate with Sarmat-  
 1536 ia in the SE and Amazonia in the west (Sveco-  
 1537 baltic and Nordic orogenies, respectively).

#### 4.3.2. Timing and relation to regional tectonic evolution of the shield

Most of the greenstone belts in the Archaean Kar-  
 elian craton formed after the earliest well-recorded  
 magmatic and metamorphic event at 2.84 Ga and  
 were deformed and intruded by tonalitic to granitic  
 magmas between 2.76 and 2.70 Ga (O'Brien et al.,  
 1993; Vaasjoki et al., 1993, 1999). In the Ilomantsi  
 greenstone belt in the easternmost part of Finland,  
 there is textural and structural evidence that gold  
 mineralization slightly preceded the peak of the regio-  
 nal metamorphism (Sorjonen-Ward, 1993; Sorjonen-  
 Ward and Luukkonen, 2005). Large areas of the  
 Archaean domain were reheated by burial beneath a  
 sequence of nappes in the foreland of the Palaeopro-  
 terozoic orogenies around 1.9 Ga. Despite also indi-  
 cations of Proterozoic fluid activity in the region (e.g.,  
 Poutiainen and Partamies, 2003), there is no evidence  
 for a distinct Proterozoic gold mineralization event in  
 the area (Kontinen et al., 1992; O'Brien et al., 1993).  
 The lack of Proterozoic gold in the Archaean areas  
 could simply be due to the style of the Proterozoic  
 tectonic processes in the area: a system of subhori-  
 zontal nappes typically does not contain deep, trans-  
 crustal structures necessary to tap the fluid and metal  
 sources and focus enough mineralizing fluids for oro-  
 genic gold deposits to form (Goldfarb et al., 2001).

For the Palaeoproterozoic greenstone belts in  
 northern Finland, most of the radiometric age dating  
 and structural evidence suggest mineralization  
 between ca. 1.85 and 1.79 Ga (Sorjonen-Ward et al.,  
 1992; Mänttari, 1995). On the other hand, structural  
 evidence and a few radiometric ages of the wall-rocks  
 from some of the gold occurrences point towards  
 mineralization between ca. 1.90 and 1.88 Ga (Män-  
 ttäri, 1995). In any case, most of the available evi-  
 dence supports the occurrence of orogenic  
 mineralization in northern Finland during the peak  
 deformation stage of the collisional epoch at 1.85 to  
 1.79 Ga. Two different styles of epigenetic gold  
 occurrence in the region are displayed in Figs. 5 and  
 6, respectively. The Suurikuusikko deposit (Fig. 7)  
 exhibits features that are typical of shear zone-hosted  
 orogenic gold deposits, whereas the Saattopora Cu–  
 Au deposit (Fig. 8) exhibits many features that are  
 typical of orogenic gold lode deposits, but also  
 includes some features characteristic of IOCG depos-  
 its (see Box 8-2, Eilu and Weihed, 2005, this volume).

1538

1540

1541

1542

1543

1544

1545

1546

1547

1548

1549

1550

1551

1552

1553

1554

1555

1556

1557

1558

1559

1560

1561

1562

1563

1564

1565

1566

1567

1568

1569

1570

1571

1572

1573

1574

1575

1576

1577

1578

1579

1580

1581

1582

1583

1584

1585

1586

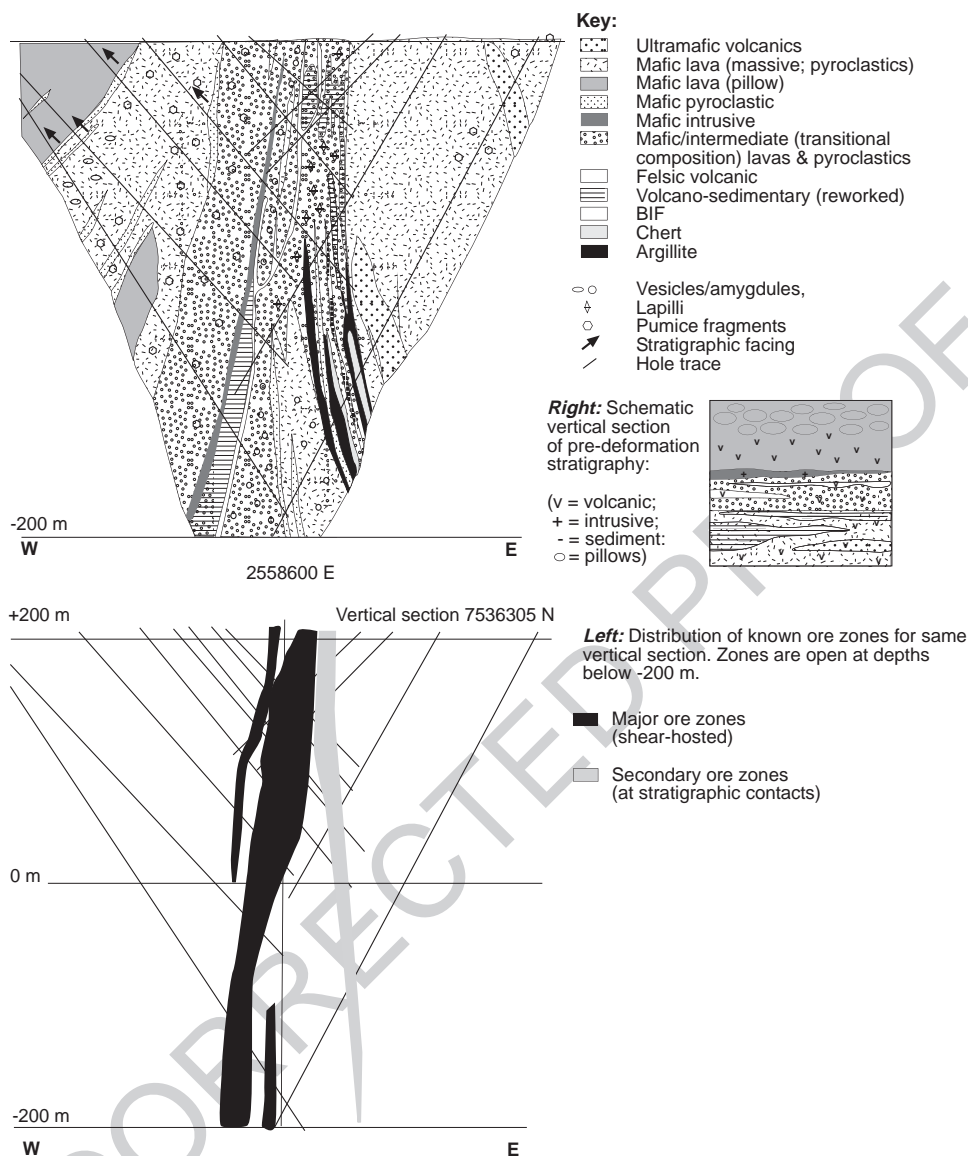


Fig. 7. Simplified vertical cross-section showing the host rocks of the Suurikuusikko gold deposit. Major ore zones typically occur within the central part of the host stratigraphy (Mafic/intermediate (transitional composition) lavas and pyroclastics). These volcanic to volcanogenic sedimentary rocks have a geochemical composition transitional between mafic and intermediate. Primary volcanoclastic textures and thin felsic volcanic layers are also more abundant in this part of the local stratigraphy. Secondary ore zones occur on stratigraphic contacts throughout the entire host rock package. All parts of the local stratigraphy appear to have a geochemical affinity with the 2.012 Ga Vesmajärvi Formation (as defined in Lehtonen et al., 1998). In the structure hosting Suurikuusikko (Kiistala Shear Zone, not shown), the most intense shearing associated (spatially and temporally) with mineralization was focused within the central units of the local stratigraphy.

1587 In the Svecofennian domain of Finland, orogenic  
1588 mineralization post-dates the earliest deformation.  
1589 However, some of the occurrences were recrystal-  
1590 lized and deformed to varying degrees after miner-

1591 alization between 1.84 and 1.80 Ga (e.g., 1591  
1592 Kontoniemi, 1998). This indicates that the timing of 1592  
1593 mineralization was either ca. 1.90 to 1.86 or 1.84 to 1593  
1594 1.80 Ga. 1594

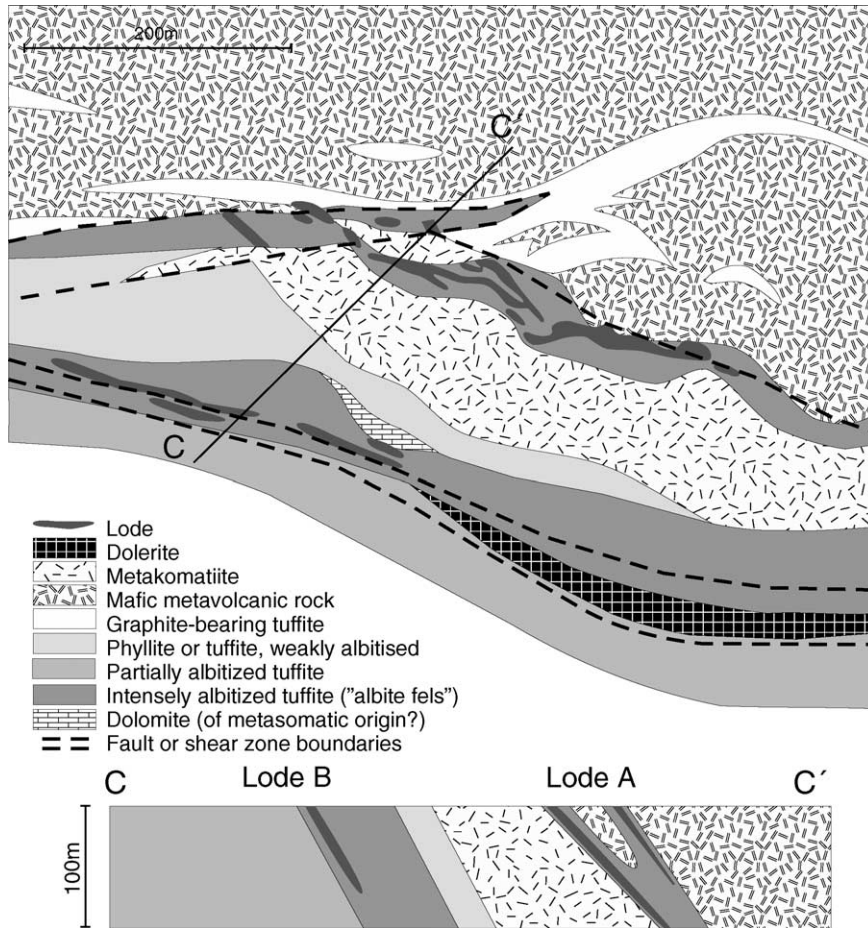


Fig. 8. Plan view and cross-section of the Saattopora deposit. Geology is based on Korvuo (1997); stratigraphy on Lehtonen et al. (1998).

1595 Recent age data on orogenic gold deposits in the  
 1596 western part of the shield indicate that many of the  
 1597 deposits, at least in part, formed slightly after peak  
 1598 metamorphism, as late as ca. 1.79 to 1.77 Ga (Bark  
 1599 and Weihed, 2003; Weihed et al., 2003). Later remo-  
 1600 bilization may also have occurred and there is abun-  
 1601 dant evidence for young, post-1.78 Ga, hydrothermal  
 1602 activity in northernmost Sweden (see Section 4.4).

#### 1603 4.3.3. Controls on mineralization

1604 Orogenic gold deposits in the Fennoscandian  
 1605 Shield are structurally controlled. All occurrences  
 1606 are in second- to lower-order shear or fault zones, at  
 1607 their intersections, or at the intersections between  
 1608 antiforms and crosscutting fault and shear zones, all  
 1609 indicative of a compressional to transpressional

1610 regime at the time of mineralization, as exemplified  
 1611 in the Palaeoproterozoic Central Lapland and Kuu-  
 1612 samo greenstone belts. In Central Lapland, the W- to  
 1613 NW-trending Sirkka Shear Zone, a major crustal-scale  
 1614 structure, is located close to most of the gold occur-  
 1615 rences, which in many cases are in lower-order shear  
 1616 or fault zones branching from the main structure and  
 1617 at localities where younger faults cut across the latter  
 1618 (Eilu et al., 2003). In the Kuusamo greenstone belt,  
 1619 nearly all occurrences are located within two NE- to  
 1620 NW-trending antiforms located in the central part of  
 1621 the greenstone belt, at or near intersections between  
 1622 antiforms and crosscutting faults (Pankka, 1992; Van-  
 1623 hanen, 2001). Similarly, deposits in central and south-  
 1624 ern Finland display a close association with major  
 1625 faults, but are hosted by second- and third-order

1626 structures branching from the large faults. In the  
1627 Björkdal deposit in the Skellefte district in Sweden,  
1628 the gold is related to third-order structures. There, the  
1629 gold precipitated in or adjacent to conjugate quartz  
1630 veins in the footwall of a major duplex structure that  
1631 formed during roughly E–W crustal shortening at ca.  
1632 1.80 Ga (Weihed et al., 2003).

1633 On a local scale, favoured sites for gold minerali-  
1634 zation are (1) pre-gold albitized units, (2) competent  
1635 units enveloped by softer rocks, and (3) contact zones  
1636 between chemically-reactive rocks with a significant  
1637 competency difference. There are examples of each of  
1638 these in Lapland: in the Saattopora mine (Fig. 8), the  
1639 pre-gold albitization significantly increased the com-  
1640 petency of the host tuffites and phyllites, providing  
1641 pathways for the mineralizing fluids where these units  
1642 were brecciated (Grönholm, 1999). Grönholm (1999)  
1643 further suggests that precipitation of gold at Saatto-  
1644 pora was induced by reduction–oxidation reactions  
1645 between the mineralizing fluid and graphite in the  
1646 albitized wallrock. Increased competency due to pre-  
1647 gold albitization has also been suggested for most of  
1648 the Kuusamo deposits (Pankka, 1992; Vanhanen,  
1649 2001). A large number of occurrences in Central  
1650 Lapland are located in contact zones between chemi-  
1651 cally reactive rocks with a significant competency  
1652 difference, for example between intensely carbonated  
1653 and more competent metakomatiites and more plastic  
1654 graphitic tuffite or phyllite (Eilu et al., 2003). At  
1655 Björkdal, the gold mineralization appears to be related  
1656 to the competency contrast between the host inter-  
1657 mediate intrusion and the surrounding supracrustal

rocks, including a mylonitized marble unit (Weihed  
et al., 2003). In the Fäbodliden deposit, south of the  
Skellefte district in Sweden, the gold is spatially  
related to graphite-bearing pelitic metasedimentary  
rocks, possibly implying a strong redox control on  
gold precipitation.

#### 4.4. IOCG deposits

The northern region of the Fennoscandian Shield,  
including parts of Finland, Norway and Sweden, is an  
economically important metallogenic province domi-  
nated by Fe-oxide and Cu ± Au ores. Based on the  
style of Fe and Au–Cu mineralization and the exten-  
sive albite and scapolite alteration, the region has been  
regarded as a typical IOCG province (e.g., Martins-  
son, 2001; Williams et al., 2003). These deposits are  
quite variable in character and include four major  
types: stratiform Cu ± Zn deposits, skarn-rich iron  
deposits, Kiruna type Fe-oxide deposits (apatite iron  
ores), and epigenetic and porphyry style Cu ± Au and  
Au deposits. In strictly genetic terms only some of  
these deposits may be classified as typical IOCG  
deposits whereas others only share a few characteristic  
features with this rather loosely defined ore type (see  
Hitzman et al., 1992; Hitzman, 2000). In addition,  
orogenic gold deposits and subeconomic banded  
iron formations (BIF) also occur in the region. Some  
examples of potential IOCG occurrences and their  
characteristic features are listed in Table 2.

Economically, the most important deposit type for  
the region has been the apatite–iron ores, presently

t2.1 Table 2

t2.2 Examples of deposits potentially belonging to the IOCG category in northern Finland and Sweden

Ore type	Occurrence	Character	Main ore minerals	Alteration	Hosting sequence	Approx dep. age (Ga)
t2.3 Fe-oxide–Fe-sulphide–Cu	Laurinoja, Kuervitikko	Massive lenses	Mt, Py, Po, Cp	Di, Bi, Ab, Am	SG	1.86 to 1.76
t2.5 Fe-oxide ± Co–Cu–Au	Vähäjoki	Breccia	Mt, Py, Cp, Co	Am, Bi	TF	1.9 to 1.8?
t2.6 Fe-oxide	Mertainen	Breccia	Mt, (Ht)	Ab, Am, Sc	KiG	1.88
t2.7 Fe-oxide–apatite ± REE	Kiirunavaara, Rektorn	Massive lenses	Mt, Ht	Am, Ab, Bi, Kf	KiG KiG	1.88
t2.8 Fe-oxide–apatite–Cu ± Au	Tjärrojäkka Nautanen	Disseminated, veins	Mt, Cp, Py, Bo	Kf, Sc, Bi, To	PoG PoG	1.77?
t2.9 Fe-oxide–Cu ± Co ± Au	Kiskamavaara	Disseminated, breccia	Mt, (Ht), Py, Cp	Kf, Bi, Sc	PoG PoG	1.86?
Cu ± Au ± Fe-oxide	Aitik, Pikkujärvi	Disseminated, veins	Cp, Py, Po,	Ab, Sc, Bi, Kf,	KiG KiG	1.89 1.88
	Pahtohavare		Bo, Cc, Mt	To	KGG	1.88 to 1.86?
t2.11 Cu–Au	Lieteksavo Ferrum	Vein, disseminated	Bo, Cp	Sc, To, Bi	KiG	1.76

Mineral abbreviations: Ab=albite, Am=amphibole, Bi=biotite, Bo=bornite, Cc=chalcocite, Co=cobaltite, Cp=chalcopyrite, Di=diopside,

t2.12 Ht=hematite, Kf=K feldspar, Mt=magnetite, Po=pyrrhotite, Py=pyrite, Sc=scapolite, SG=Savukoski Group, To=tourmaline.

t2.13 Host sequence abbreviations: KiG=Kiirunavaara Group, KGG=Kiruna Greenstone Group, PoG=Porphyrite Group, TF=Tikanmaa Formation.

1688 with an annual production of about 31 Mt of ore from  
 1689 the Kiirunavaara and Malmberget mines and a total  
 1690 production of about 1600 Mt from 10 mines during  
 1691 the last 100 years. Copper and gold have been mined  
 1692 on a large scale in Sweden (Aitik, Viscaria, Pahtoha-  
 1693 vare), Finland (Saattopora, Pahtavaara) and Norway  
 1694 (Bidjovagge). All of the sulphide deposits are hosted  
 1695 by Palaeoproterozoic greenstones and are small to  
 1696 medium sized except for Aitik, which occurs in Sve-  
 1697 cofennian volcanoclastic rocks and is a world-class  
 1698 deposit with a total tonnage >1000 Mt and an annual  
 1699 production of 18 Mt.

#### 1700 4.4.1. Geodynamic setting

1701 Fe-oxide and Cu ± Au ores in Norrbotten in north-  
 1702 ernmost Sweden formed during the evolution of a  
 1703 Palaeoproterozoic continental margin arc from ca.  
 1704 1.89 to 1.75 Ga (e.g., Juhlin et al., 2002). The deposits  
 1705 occur where the margin developed above Archaean  
 1706 continental crust and are hosted both by juvenile rocks  
 1707 and by older Palaeoproterozoic volcano-sedimentary  
 1708 sequences formed during rifting of the Archaean cra-  
 1709 ton (Martinsson and Weihed, 1999). The rift-related,  
 1710 2.2 to 2.0 Ga Karelian greenstones comprise mafic  
 1711 and ultramafic volcanic rocks, graphitic schists and  
 1712 sedimentary carbonate rocks. The lower part of the  
 1713 sequence contains clastic sedimentary and inferred,  
 1714 evaporitic units (Martinsson, 1997; Vanhanen,  
 1715 2001). At ca. 1.9 Ga, subduction of oceanic crust at  
 1716 the SW margin of the Karelian craton involved both  
 1717 strong reworking of older crust and the formation of  
 1718 juvenile crust by accretion of several volcanic arc  
 1719 complexes with the cratonic nucleus (see Section  
 1720 4.2). This ca. 1.90 to 1.88 Ga magmatism is repre-  
 1721 sented by the calc-alkaline and andesite-dominated  
 1722 volcanic successions and the co-magmatic, intrusive  
 1723 Haparanda Suite within the NW part of the craton. In  
 1724 the Kiruna area, these rocks are succeeded by the  
 1725 bimodal Kiirunavaara Group volcanic rocks and the  
 1726 coeval and chemically similar Perthite Monzonite  
 1727 Suite (Bergman et al., 2001). This 1.88 to 1.86 Ga  
 1728 magmatic activity has a more alkaline character that  
 1729 suggests an extensional intraplate setting.

1730 The magmatism related to the Svecokarelian oro-  
 1731 gen after ca. 1.86 Ga is mainly of S-type (1.81 to 1.78  
 1732 Ga Lina suite intrusions) derived from anatexic melts  
 1733 in the middle crust. In the western part of the shield,  
 1734 extensive I- to A-type magmatism formed a roughly

1735 N–S-trending belt of batholiths (the Trans-scandina-  
 1736 vian Igneous Belt) coeval with the S-type magmatism,  
 1737 possibly as a result of eastward subduction (Weihed et  
 1738 al., 2002), followed by collision between Fennoscan-  
 1739 dia and Amazonia (see Section 5). Although the  
 1740 metamorphic history of the northern part of the shield  
 1741 is not well-constrained, in time or in space, it appears  
 1742 that metamorphic peaks more or less overlap with the  
 1743 main magmatic events at about 1.88 and 1.80 Ga. A  
 1744 model for the tectonic setting of the IOCG deposits is  
 1745 presented in Fig. 9.

#### 1746 4.4.2. General features and controls on mineralization

1747 Skarn-rich and lens- to irregularly-shaped Fe-oxide  
 1748 occurrences consisting of magnetite, and Mg and Ca–  
 1749 Mg silicates are common within the greenstones of  
 1750 northern Sweden and the westernmost part of northern  
 1751 Finland. Some of the deposits are spatially associated  
 1752 with oxide- and silicate-facies BIF. These skarn or  
 1753 skarn-like iron deposits occur in association with  
 1754 tuffite, graphitic schist, and dolomitic to calcitic mar-  
 1755 ble, and are located mainly in the upper parts of the  
 1756 greenstone sequences. These occurrences have pre-  
 1757 viously been suggested to be metamorphic expres-  
 1758 sions of originally syngenetic exhalative deposits  
 1759 (Frietsch, 1977; Bergman et al., 2001) or intrusion-  
 1760 related skarn deposits (Hiltunen, 1982). Several skarn-  
 1761 rich iron deposits have been mined in the Kolari area  
 1762 in NW Finland and in the Misi region in southern  
 1763 Finnish Lapland (Nuutilainen, 1968; Hiltunen, 1982;  
 1764 Niiranen et al., 2003). In addition, significant amounts  
 1765 of Cu and Au have been recovered from the Laurinoja  
 1766 orebody in the Kolari area (Hiltunen, 1982; Geologi-  
 1767 cal Survey of Finland, 2004).

1768 Kiruna is the type area for apatite–iron ores (Kir-  
 1769 una type Fe-oxide ores) with the Kiirunavaara deposit  
 1770 as the largest and best known example (Table 1). In  
 1771 all, about 40 apatite–iron deposits are known from the  
 1772 northern Norrbotten ore province in northernmost  
 1773 Sweden. This type of deposits is mainly spatially  
 1774 restricted to areas occupied by the Kiirunavaara  
 1775 Group and very few occurrences exist outside the  
 1776 Kiruna–Gällivare area. The apatite–iron ores exhibit  
 1777 a considerable variation in host rock composition and  
 1778 relationship, alteration, P content, and associated  
 1779 minor components. It is possible to distinguish two  
 1780 subgroups: breccia deposits and stratiform–strata-  
 1781 bound deposits. A third and less distinct group has

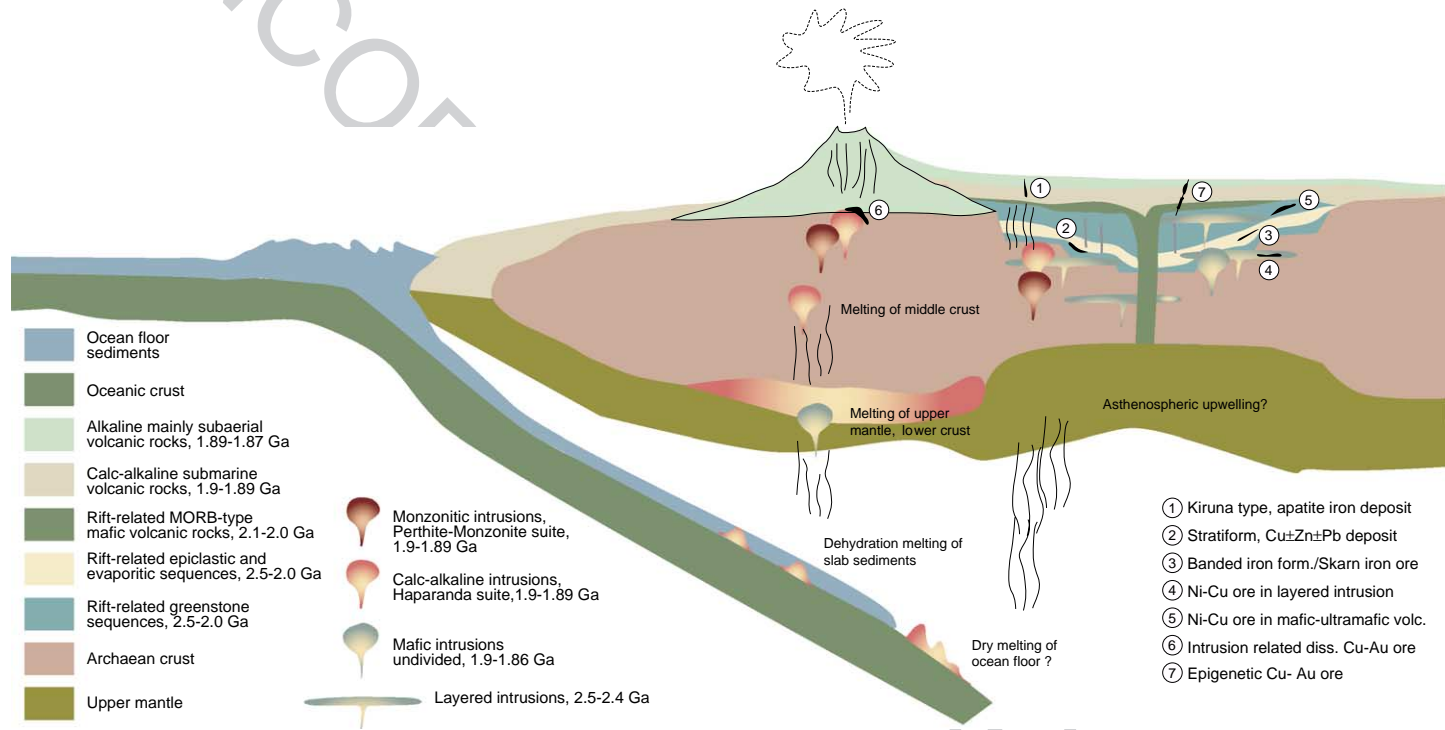


Fig. 9. Key geodynamic features of IOCG deposits. The generalized tectonic section illustrates the relationship between host rocks, tectonic setting and IOCG deposits and other greenstone-related ore types. The section is not meant to illustrate specific temporal relationships, but is a generalization over 500 million years of basically intracontinental to continental margin evolution of the rifted Karelian craton between 2.45 and 1.85 Ga.

1782 features similar to both of the other two groups (Berg-  
1783 man et al., 2001). Breccia-type apatite–iron ores (e.g.,  
1784 Mertainen) are mainly associated with intermediate to  
1785 mafic volcanic rocks, in a stratigraphically low posi-  
1786 tion of the Svecofennian Kiirunavaara Group or  
1787 within the underlying Porphyrite Group. The strati-  
1788 form–stratabound type (e.g., Nukutus, Henry,  
1789 Rektorn, Lappmalmen and Ekströmsberg) comprises  
1790 hematite-dominated lenses at stratigraphically high  
1791 positions within the Kiirunavaara Group. The inter-  
1792 mediate types of apatite–iron ore (e.g., Kiirunavaara  
1793 and Tjärrojåkka) are dominantly stratabound in char-  
1794 acter, but have breccia ores developed along the wall-  
1795 rock contacts (Box 8-3, Edfelt and Martinsson, 2005,  
1796 this volume). Magnetite is the dominant, or the sole  
1797 Fe-oxide.

1798 Apatite–iron ores have been suggested to represent  
1799 an iron-dominated and sulphide-poor end member of  
1800 the Fe-oxide–Cu–Au class of metallic ore deposits  
1801 (Hitzman et al., 1992), which makes them important  
1802 not only as sources of iron, but also for the metallo-  
1803 genetic understanding of the northern Norrbotten Fe–  
1804 Cu–Au province. Suggested genetic models include  
1805 sedimentary, hydrothermal or magmatic processes  
1806 (Parák, 1975; Hitzman et al., 1992; Nyström and  
1807 Henriquez, 1994). Most features of the ores are com-  
1808 patible with either a magmatic intrusive origin or a  
1809 hydrothermal origin. Probably both magmatic and  
1810 hydrothermal processes were involved, explaining  
1811 the large variation in mineralization style recognized  
1812 within and between individual deposits. Most of the  
1813 massive deposits are suggested to have a mainly  
1814 magmatic origin with minor overprinting hydrother-  
1815 mal phases altering the wall-rocks and forming the  
1816 veins. Some deposits (e.g., Tjärrojåkka) may represent  
1817 transitional forms between a magmatic and hydrother-  
1818 mal origin similar to that at Lightning Creek in the  
1819 Cloncurry area, Queensland, Australia (Perring et al.,  
1820 2000).

1821 Sulphides are mostly rare constituents in the apa-  
1822 tite–iron ores and occur disseminated or in veinlets.  
1823 Significant Cu mineralization spatially associated with  
1824 apatite ores occurs only in a few places (e.g., Tjärro-  
1825 jåkka and Gruvberget). A genetic relationship  
1826 between Cu and Fe-oxide mineralization has not  
1827 been proved, but is probable at Tjärrojåkka (Edfelt  
1828 and Martinsson, 2004). At Gruvberget, the relation-  
1829 ship might be more of a coincidence with the Cu

1830 occurrence representing a later separate event and  
1831 the iron ore only acting as a chemical–structural trap  
1832 (Lindskog, 2001). U–Pb titanite ages indicate that Cu  
1833 mineralization at Tjärrojåkka and Gruvberget is ca.  
1834 1.8 Ga in age (Billström and Martinsson, 2000),  
1835 which is significantly younger than the suggested  
1836 ca. 1.9 Ga emplacement age for apatite–iron ores in  
1837 the Kiruna area.

1838 Epigenetic Cu ± Au deposits form a heterogeneous  
1839 group with extensive variation in the style of miner-  
1840 alization, metal association and host rock. Most  
1841 deposits are hosted by tuffitic units of the Karelian  
1842 greenstones (e.g., in Central Lapland and Kuusamo in  
1843 Finland) and mafic to intermediate volcanic rocks  
1844 within the Svecofennian porphyries (e.g., in Porphyri-  
1845 te and Kiirunavaara Groups in Sweden). Some of  
1846 them display close genetic links (e.g., Aitik), sup-  
1847 ported by stable isotope and fluid inclusion evidence  
1848 (Yngström et al., 1986; Wanhainen et al., 2003), and/  
1849 or spatial relation to intrusive rocks of the Haparanda  
1850 and Perthite Monzonite suites, varying in composition  
1851 from monzodiorite to granite. The deposits with a  
1852 close genetic link to intrusive rocks are regarded by  
1853 many authors as porphyry style deposits (see Weihed,  
1854 2001; Wanhainen et al., 2003). Magnetite is a com-  
1855 mon minor component in many occurrences and  
1856 locally they occur adjacent to major magnetite depos-  
1857 its. A close spatial relationship with regional shear  
1858 zones is common, with second- to fourth-order struc-  
1859 tures controlling the location of an occurrence (Eilu et  
1860 al., in press). In addition to structural traps, chemical  
1861 traps may also be important with redox reactions  
1862 involving an originally high graphite or magnetite  
1863 content of the host rock to trigger sulphide precipita-  
1864 tion. In addition to Cu, several occurrences also con-  
1865 tain Co and/or Au in economic to subeconomic  
1866 amounts. Other elements that may be significantly  
1867 enriched include LREE, Ba, U, and Mo (e.g., Mar-  
1868 tinsson, 2001; Vanhanen, 2001).

1869 Highly saline fluid inclusions with 30 to 45 eq.  
1870 wt.% NaCl and depositional temperatures of 500 to  
1871 300 °C are recorded for the epigenetic Cu ± Au  
1872 deposits in the region (Ettner et al., 1993; Lindblom  
1873 et al., 1996; Broman and Martinsson, 2000; Wanhai-  
1874 nen et al., 2003; Williams et al., 2003; Edfelt et al.,  
1875 2004; Niiranen pers. comm. 2004).

1876 Extensive hydrothermal alteration systems produ-  
1877 cing, for example, scapolite, albite, K-feldspar, bio-

1878 tite, amphibole and tourmaline characterize the north-  
 1879 ern part of the Fennoscandian Shield, indicating  
 1880 extensive interaction between hydrothermal fluids  
 1881 and the crust. These systems occur both on a regio-  
 1882 nal scale and directly coupled with different kinds of  
 1883 mineralization (Frietsch et al., 1997; Bergman et al.,  
 1884 2001). The importance of evaporites in the genesis of  
 1885 Fe-oxide–Cu–Au deposits has been argued by Barton  
 1886 and Johnson (1996) and evaporitic units are sug-  
 1887 gested to have been present in the Karelian green-  
 1888 stones based on the abundance of albite and scapolite  
 1889 in certain stratigraphic units (Tuisku, 1985; Martins-  
 1890 son, 1997; Vanhanen, 2001; Eilu et al., in press) and  
 1891 the Br/Cl ratio of the ore bearing fluids (Wanhainen  
 1892 et al., 2003; Williams et al., 2003). On a broad scale,  
 1893 most of the Kiruna-type Fe-oxide and epigenetic  
 1894 Cu ± Au deposits are located in areas where both  
 1895 strong Na–Cl alteration and calc-alkaline to alkali-  
 1896 calcic, monzonitic magmatism occur (Fig. 9). In  
 1897 areas where either regional scapolitization or monzo-  
 1898 nitic magmatism is lacking, only minor deposits are  
 1899 found. Thus, it seems that continental margin mag-  
 1900 matism interacting with evaporitic sequences is a  
 1901 metallogenetically important feature in the Fennos-  
 1902 candian Shield (cf. Fig. 9).

1903 A fairly comprehensive U–Pb age data set exists  
 1904 for titanite from Kiruna-type Fe-oxide and epigenetic  
 1905 Cu ± Au occurrences, but it should be noted that in  
 1906 more complex systems with overprinting alteration  
 1907 assemblages, different titanite age determinations  
 1908 may occasionally yield disparate ages. Age data dis-  
 1909 played in Fig. 10 from epigenetic Cu ± Au deposits  
 1910 and related hydrothermal alteration systems in the  
 1911 northern Norrbotten ore province in Sweden indicate

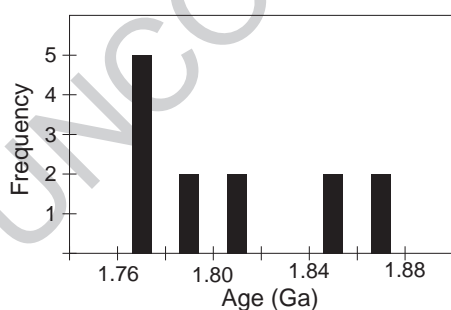


Fig. 10. Histogram showing U–Pb titanite ages for epigenetic Fe–Cu–Au occurrences from northern Sweden. Data from Billström and Martinsson (2000) and Billström (unpublished).

two major events of ore formation at ca. 1.81 to 1.76  
 and 1.88 to 1.85 Ga (Billström and Martinsson, 2000).  
 Deposits in the northern parts of Norway and Finland  
 exhibit the same two events plus a third probable  
 stage of mineralization at ca. 1.84 to 1.81 Ga (Bjør-  
 lykke et al., 1990; Mänttari, 1995). Ages for Kiruna-  
 type Fe-oxide ores are only published from the Kiruna  
 area and suggest that these ores were formed between  
 1.89 and 1.88 Ga (Romer et al., 1994; Cliff et al.,  
 1990). Thus, there is both a strong spatial and tem-  
 poral correlation with the Kiirunavaara Group and a  
 temporal correlation with the older intrusions of the  
 Perthite–Monzonite Suite, co-magmatic with the Kiir-  
 unavaara Group rocks.

Fe-oxide–Cu–Au style mineralization in the Fen-  
 noscandian Shield seems to be a product of multistage  
 magmatic, metamorphic and tectonic processes,  
 invariably involving saline hydrothermal fluids. Sev-  
 eral different age groups of mineralization, 1.89 to  
 1.88 (Kiruna-type Fe-oxide), 1.89 to 1.85, 1.84 to  
 1.82, and 1.81 to 1.76 Ga (epigenetic Cu ± Au),  
 imply that mineralization took place in different tec-  
 tonic settings. The older Kiruna type Fe-oxide occur-  
 rences formed in a continental margin arc, possibly  
 from Fe-oxide magmas genetically related to monzo-  
 nitic intrusions. High-salinity fluids formed as a result  
 of magma–crust interaction and were responsible for  
 epigenetic Cu ± Au mineralization. The younger  
 deposits formed largely during or slightly after the  
 peak of the orogeny, during convergence, and at least  
 partly by remobilization of older mineralization. The  
 hydrothermal fluids responsible for the younger  
 deposits were focused along crustal-scale shear  
 zones with mineralization in second to fourth order  
 structures.

#### 4.5. Fe–Ti oxides in anorthosites

Magmatic ilmenite deposits are typically hosted by  
 massif-type anorthosites. The largest deposit in the  
 world is the Lac Tio ilmenite body in the Havre St  
 Pierre anorthosite complex in Quebec. The second  
 largest, the Tellnes ilmenite norite deposit, sits in the  
 Åna-Sira anorthosite (Fig. 11) in Rogaland, southern  
 Norway. Understanding of the formation of ilmenite  
 deposits thus relies on the nature of the anorthosites,  
 the nature of their parent magma, and the tectonic  
 setting in which they were emplaced.



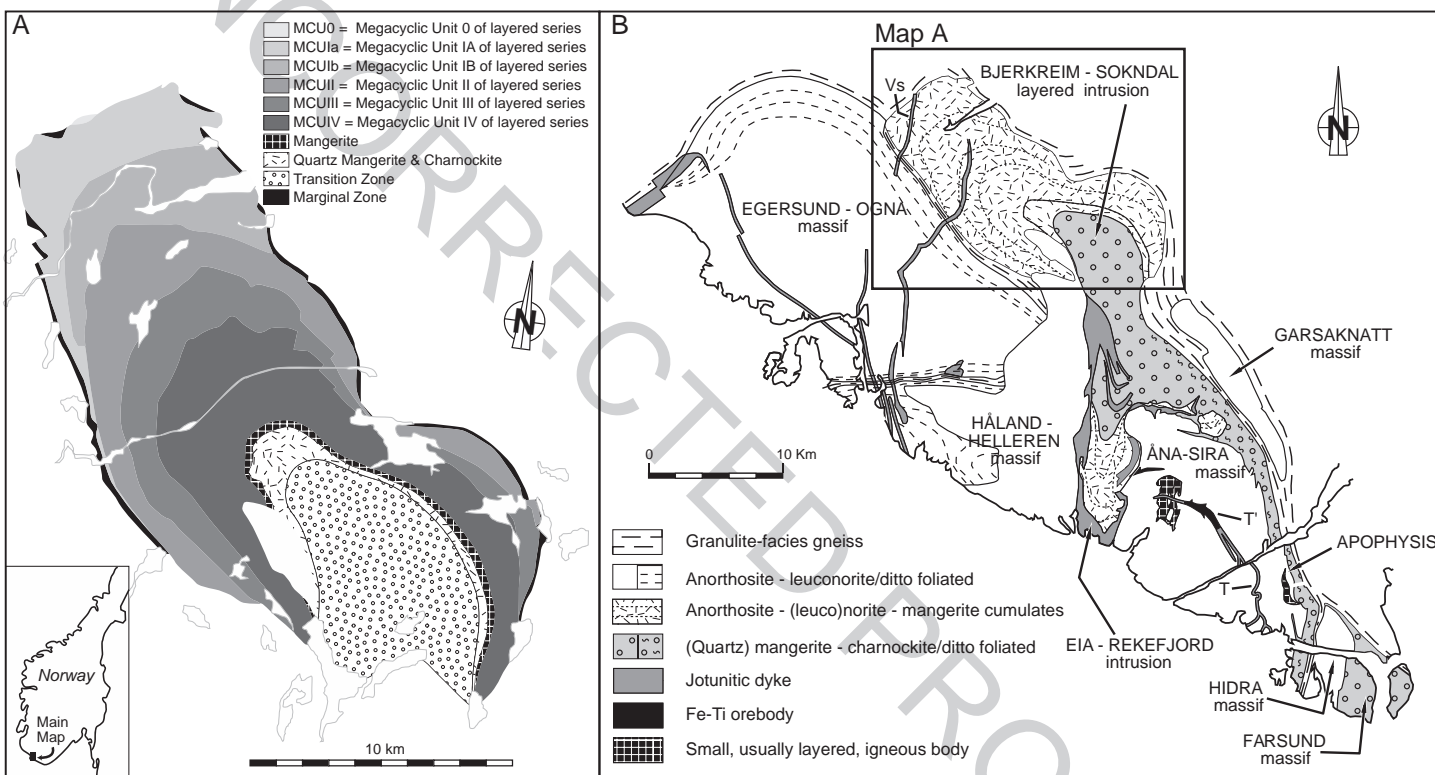


Fig. 11. The geology of the Bjerkreim–Sokndal intrusion, SW Norway, after [Robins and Wilson \(2001\)](#), illustration A; and [Duchesne and Bingen \(2001\)](#), illustration B. T=Tellnes “main dyke”; T’=Tellnes ilmenite deposit.

1958 The consensus model for anorthosite petrogenesis,  
1959 summarized by Ashwal (1993), involves a deep-  
1960 seated magma chamber in which a mantle-derived  
1961 mafic magma ponds at the crust–mantle interface.  
1962 Differentiation produces a lower density plagioclase  
1963 cumulate at the roof of the chamber, from which, due  
1964 to gravity instabilities, blobs of plagioclase mush  
1965 detach and rise diapirically through the lower crust  
1966 to be emplaced at mid-crustal levels, where they  
1967 coalesce to form anorthosite plutons.

1968 In the last decade, this model has been improved  
1969 and partly modified to account for new field, experi-  
1970 mental and geochemical constraints. The typical high-  
1971 alumina orthopyroxene megacrysts (with plagioclase  
1972 exsolutions) that form subophitic aggregates with pla-  
1973 gioclase megacrysts is stable at 10 to 13 kbar in  
1974 contrast to the <5 kbar pressure of final emplacement  
1975 (Fram and Longhi, 1992; Longhi et al., 1993), con-  
1976 firming the polybaric character of the crystallization.  
1977 The diapirism mechanism was verified by finite ele-  
1978 ment modelling, taking into account the thermo-  
1979 mechanical properties of anorthosite and mid- and  
1980 lower crustal rocks (Barnichon et al., 1999).

1981 Experimental data for dry basaltic systems (Longhi  
1982 et al., 1999) show that the parent magma compositions  
1983 of anorthosite massifs (high-alumina basalt at Harp  
1984 Lake, Nain; hypersthene monzodiorite or jotunite in  
1985 Rogaland) occur on a thermal maximum of the plagi-  
1986 oclase+orthopyroxene+clinopyroxene cotectic, in the  
1987 pressure range (10 to 13 kbar) typical of the high-  
1988 alumina orthopyroxene megacrysts. Consequently,  
1989 the parent magmas cannot be generated by fractiona-  
1990 tion of a mantle-derived basaltic magma, but result  
1991 from the melting of a mafic rock (containing plagioc-  
1992 lase and two pyroxenes) between 40 and 50 km  
1993 depth. Re–Os isotope data strongly support a mafic  
1994 lower crust origin (Stein et al., 1998; Wiszniewska  
1995 et al., 2002), particularly in Rogaland where high Os  
1996 isotopic ratios can only be accounted for by a mafic  
1997 source, because there is no significantly older crust in  
1998 SW Scandinavia (Schillerup et al., 2000).

1999 Detailed field studies in several anorthosite com-  
2000 plexes have shown that anorthosites are frequently  
2001 associated with zones of weakness in the crust that  
2002 may have favoured their emplacement at mid-crust  
2003 levels (Emslie et al., 1994; Scoates and Chamberlain,  
2004 1997). In SW Scandinavia, terrane boundaries have  
2005 been traced in deep seismic profiles to Moho offsets

or to tongues of lower crustal material (the so-called  
Telemark Craton Tongue) underthrust to depths  
greater than 40 to 50 km (Andersson et al., 1996).  
In Poland the Suwalki anorthosite was emplaced in  
the Svecofennian platform along the E–W-trending  
Mazury lineament (Wiszniewska et al., 2002). In  
Ukraine, the Korosten pluton occurs at the intersection  
of two lithospheric-scale faults, imaged by geophys-  
ical methods (Bogdanova et al., 2004). It has been  
suggested that such tongues of underthrust, mafic  
lower crust can reach sufficiently high temperatures  
to melt and produce the parent magma of massive  
anorthosites, if accompanied by delamination along  
the weakness zone and asthenospheric uprise (Duch-  
esne et al., 1999). This hypothesis seems superior to  
the classical hot-spot hypothesis, which is unable to  
explain how several generations of anorthosites, sepa-  
rated by hundreds of millions of years, can occur in  
the same province (Scoates and Chamberlain, 1997;  
Hamilton et al., 1998). An alternative crustal tongue  
melting model (Duchesne et al., 1999) links anortho-  
site production to a local geochemical property of the  
lower crust, which permits melting each time heat is  
added.

In the light of these new developments, the concept  
of an intraplate setting, typical of the consensus model  
of anorthosite formation, has also been reconsidered.  
Emplacement along weakness zones can be favoured  
by relative movements between terranes either in a  
post-collisional setting or, if a local source of extra  
heat is provided, during tectonic rejuvenation (Duch-  
esne et al., 1999), possibly due to distant collisions at  
the margins of the craton.

Ilmenite deposits are hosted in andesine anortho-  
sites (Anderson and Morin, 1969; Ashwal, 1993) and  
their genesis has been interpreted to reflect complex  
diapiric evolution of the host anorthosite and frac-  
tional crystallization of the parent magma (Duchesne,  
1999; Duchesne and Schillerup, 2001). The diapiric  
mechanism has been verified by finite element mod-  
elling, taking into account the thermo-mechanical  
properties of anorthosite and mid- and lower-crustal  
rocks (Barnichon et al., 1999). There are multiple  
lines of evidence to indicate that the parental magmas  
of andesine anorthosites are enriched in Fe and Ti,  
whichever model is invoked for their genesis. In the  
underplating model, crystallization of olivine and high  
alumina orthopyroxene megacrysts in the deep-seated

2006  
2007  
2008  
2009  
2010  
2011  
2012  
2013  
2014  
2015  
2016  
2017  
2018  
2019  
2020  
2021  
2022  
2023  
2024  
2025  
2026  
2027  
2028  
2029  
2030  
2031  
2032  
2033  
2034  
2035  
2036  
2037  
2038  
2039  
2040  
2041  
2042  
2043  
2044  
2045  
2046  
2047  
2048  
2049  
2050  
2051  
2052  
2053

2054 magma chamber enriches the residual melts in Fe, Ti  
2055 and P to produce ferrodiorite (Ashwal, 1993). In the  
2056 crustal tongue melting model, a Fe–Ti–P rich melt,  
2057 hypersthene monzodiorite (jotunite), is directly pro-  
2058 duced by dry melting of gabbonorite in the lower  
2059 crust (Longhi et al., 1999). In the deep-seated magma  
2060 chamber, this melt can generate andesine anorthosite  
2061 mushes liable to rise diapirically. The melt can also  
2062 rise through dykes to shallower magma chambers  
2063 where it can differentiate at lower pressure conditions.  
2064 The Bjerkreim–Sokndal layered intrusion in Rogaland  
2065 (Duchesne and Hertogen, 1988; Vander Auwera and  
2066 Longhi, 1994; Wilson et al., 1996) is an example of  
2067 such a hypersthene monzodiorite (jotunite) magma  
2068 chamber (Fig. 11).

2069 These Ti-rich magmas are, however, unable to  
2070 produce ilmenite concentrations of economic value  
2071 under normal conditions. Norite layers rarely contain  
2072 more than 8% TiO<sub>2</sub> (Charlier and Duchesne, 2003).  
2073 Ilmenite must therefore be concentrated to generate  
2074 an orebody. Ilmenite–silicate liquid immiscibility has  
2075 long been invoked (Philpotts, 1967) because it seems  
2076 to account for field observations of ilmenite dykes  
2077 with sharp contacts, suggesting a liquid behaviour of  
2078 pure ilmenite (Duchesne, 1996). Although this  
2079 mechanism is appealing it has not been confirmed  
2080 experimentally (Lindsley, 2003), because of the high  
2081 temperature (1400 °C) required to produce pure  
2082 ilmenite melt. The apparent liquid behaviour of ilme-  
2083 nite therefore probably results from its ability to  
2084 creep in the solid state in response to stress (Paludan  
2085 et al., 1994; Duchesne, 1996). Fractional crystalliza-  
2086 tion of hypersthene monzodiorite (jotunite), illustrated  
2087 by the succession of cumulates in the Bjerkreim–  
2088 Sokndal intrusion (Wilson et al., 1996) and well con-  
2089 strained experimentally (Vander Auwera and Longhi,  
2090 1994), shows that ilmenite is the second mineral to  
2091 appear on the liquidus, after plagioclase but before  
2092 orthopyroxene. Provided that an adequate mechanism  
2093 (crystal sorting, delayed nucleation, oscillation of the  
2094 cotectic with pressure, or some other more enigmatic  
2095 mechanism) was involved, ilmenite might be sepa-  
2096 rated from plagioclase to form monomineralic layers.  
2097 In this respect, the debate is similar to that on the  
2098 origin of the chromitite layers of the Bushveld Com-  
2099 plex (Wager and Brown, 1968; Cawthorn, 1996).  
2100 Cotectic crystallization of ilmenite and plagioclase,  
2101 however, raises another problem. In layered bodies

2102 such as the Bjerkreim–Sokndal intrusion, the amount  
2103 of plagioclase–ilmenite cumulates is small relative to  
2104 plagioclase–ilmenite–orthopyroxene cumulates and  
2105 plagioclase–ilmenite–magnetite–orthopyroxene–clin-  
2106 opyroxene–apatite cumulates. In a large deposit such  
2107 as Lac Tio, the inverse situation is observed; the mass  
2108 of ilmenite is much greater than the mass of norite and  
2109 gabbonorites. Selective erosion of the ilmenite-poor  
2110 rocks is possible, but not completely convincing.  
2111 Flushing of a magma through an unconsolidated crys-  
2112 tal mush in a conduit can account for the large quan-  
2113 tity of primitive cumulates, but also begs the question  
2114 of the norite and gabbonorite counterparts. Finally,  
2115 solid-state creep can also be invoked to explain the  
2116 ilmenite enrichment by separating it from the more  
2117 competent plagioclase (Duchesne, 1999). The diapiric  
2118 environment of anorthosite in which crystallization  
2119 and deformation occur at high temperature is suitable  
2120 for such a mechanism in massif anorthosite-hosted  
2121 deposits (Duchesne, 1999).

2122 The trace element contents of ilmenite and accom-  
2123 panying magnetite are an important issue because they  
2124 drastically constrain the economic value of a deposit;  
2125 Cr and Mg are deleterious in ilmenite and V is ben-  
2126 efiticial in magnetite. Cr and V occur in the magma  
2127 with different valence states, essentially 3+, 4+, and  
2128 5+. Only the trivalent species can substitute in ilme-  
2129 nite and magnetite. It can thus be anticipated that the  
2130 oxygen fugacity will be a controlling factor of the  
2131 trace element contents (Toplis and Corgne, 2002). The  
2132 other factors controlling the partitioning of Cr and V  
2133 into oxides are the contents in the parental magma, the  
2134 degree of fractional crystallization, and the intensity of  
2135 subsolidus readjustment between oxide minerals  
2136 (Duchesne, 1999). The mineral/melt partition coeffi-  
2137 cient for Mg in ilmenite does not vary with pressure  
2138 (Vander Auwera et al., 2003) and thus the most critical  
2139 factor remains the composition of the magma. The  
2140 content of Cr and V in magnetite drastically depends  
2141 on the degree of evolution of the magma when mag-  
2142 netite appears at the liquidus. Toplis and Corgne  
2143 (2002) have calculated that in ilmenite-free systems  
2144 a decrease of oxygen fugacity by two orders of mag-  
2145 nitude (e.g., from NNO+1 to NNO-1) will increase  
2146 the V content of magnetite by a factor of 3 (e.g., from  
2147 1% V<sub>2</sub>O<sub>5</sub> to 3% V<sub>2</sub>O<sub>5</sub>). Clearly, in ilmenite-bearing  
2148 systems, the ilmenite content will also be indirectly  
2149 influenced by such behaviour.

2150 **5. Discussion**

2151 The formation of Precambrian ore deposits has  
 2152 been studied extensively in most shields around the  
 2153 world. Genetic models of these deposits have devel-  
 2154 oped largely in parallel with the evolving concepts of  
 2155 Precambrian plate tectonics. Today there is little argu-  
 2156 ment about the existence of subduction processes in  
 2157 the Proterozoic and the late Archaean, but there is a  
 2158 debate about the rate of subduction, how efficient the  
 2159 subduction processes were, and the effects of subduc-  
 2160 tion on magmatism. As discussed above, geodynamic  
 2161 processes must have operated very differently from  
 2162 those of the modern Earth since the mantle was hotter,  
 2163 leading to more active and voluminous magmatism,  
 2164 and the degree of mantle melting was probably  
 2165 greater, leading to more Mg-rich magmas. Faster  
 2166 moving, hotter Archaean (and Palaeoproterozoic)  
 2167 plates also probably accumulated less sediment and  
 2168 contained a thinner section of lithospheric mantle  
 2169 (Sleep and Windley, 1982).

2170 Precambrian continental crust formed episodically  
 2171 around ca. 2.7, 2.5, 2.1 and 1.9 to 1.8 Ga (Goldstein  
 2172 et al., 1997; Condie, 1999). As noted above, these  
 2173 peaks are interpreted by some authors as the times of  
 2174 supercontinent formation: for Fennoscandia, the data  
 2175 simply suggest that they represent periods of  
 2176 enhanced crustal growth and possibly accelerated  
 2177 mantle convection. However, economic mineral  
 2178 deposits in the Fennoscandian Shield are mainly  
 2179 hosted in Palaeoproterozoic rocks. Only a few sig-  
 2180 nificant examples of Archaean orogenic gold and Ni–  
 2181 Cu deposits are known. In Ilomantsi, the gold miner-  
 2182 alization slightly preceded or was synchronous with  
 2183 the peak of the regional metamorphism (Sorjonen-  
 2184 Ward, 1993). There is no really good understanding  
 2185 as to why the Archaean seems to be less prospective  
 2186 in the Fennoscandian Shield compared with most  
 2187 other shield areas. One possible reason is that large  
 2188 parts of the Archaean greenstone belts are located in  
 2189 Russia and are under-explored by modern standards.  
 2190 Also parts of the Archaean in Finland, especially  
 2191 under thick overburden, are under-explored. Large  
 2192 areas of the Archaean have also experienced a sub-  
 2193 stantial Palaeoproterozoic thickening, which might  
 2194 have produced an erosional level devoid of green-  
 2195 stone belts. The period from ca. 2.74 to 2.69 Ga  
 2196 corresponds to a period of intense intrabasinal mantle

plumes and a subsequent global plume-breakout event  
 (Barley et al., 1998). The greenstone belts in the  
 Fennoscandian Shield seem to be slightly older than  
 the global Neoarchaean peak in mineralization and  
 mantle plume activity (e.g., Huhma et al., 1999) and,  
 hence, magmatism and hydrothermal activity might  
 have been less intense and unable to form major Ni–  
 PGE and VMS deposits. This could also explain the  
 lack of large orogenic gold deposits related to sub-  
 sequent accretion during peak orogeny.

In contrast to the Archaean, the Palaeoproterozoic  
 sequences are intensely mineralized and contain a  
 wealth of economic mineral deposits. It is therefore  
 suitable here to discuss the Palaeoproterozoic geody-  
 namic evolution and metallogeny in more detail,  
 especially for the time period from ca. 2.1 to 1.8  
 Ga when the vast majority of known economic  
 deposits formed. We will utilize a slightly modified  
 version of the recent geodynamic model for this  
 period by Lahtinen et al. (2005), which is displayed  
 in Fig. 12 as twelve generalized cartoons (a–l), show-  
 ing the plate tectonic geometry at different stages  
 between 2.06 and 1.78 Ga. The ore deposit types  
 discussed in this paper are also indicated for those  
 stages during which they are suggested to have  
 formed. The cartoons are accompanied by schematic  
 cross-sections (Fig. 13, adapted from Lahtinen et al.,  
 2005), displaying the tectonic environments of ore  
 formation. The geodynamic settings of ore deposits  
 are discussed below within the framework of (1)  
 Palaeoproterozoic rifting of the Archaean continent  
 at 2.5 to 2.06 Ga, (2) microcontinent accretion at 1.96  
 to 1.88 Ga, (3) continent–continent collision at 1.87 to  
 1.79 Ga and (4) oblique continent–continent collision  
 at 1.84 to 1.78 Ga.

### 5.1. Palaeoproterozoic rifting of the Archaean continent at 2.5 to 2.06 Ga

The Archaean cratonic nucleus of the Fennoscan-  
 dian Shield rifted in several stages during the Early  
 Proterozoic. The hot spot-related rifting event at 2.4  
 Ga is manifested in layered igneous complexes, mafic  
 dyke swarms, intracontinental and continental margin  
 volcanism, and epicontinental sedimentation. Erosion  
 of the Archaean craton is indicated by numerous  
 coarse clastic units deposited within rift basins during  
 the time interval between 2.5 and 2.06 Ga.

2197  
 2198  
 2199  
 2200  
 2201  
 2202  
 2203  
 2204  
 2205  
 2206  
 2207  
 2208  
 2209  
 2210  
 2211  
 2212  
 2213  
 2214  
 2215  
 2216  
 2217  
 2218  
 2219  
 2220  
 2221  
 2222  
 2223  
 2224  
 2225  
 2226  
 2227  
 2228  
 2229  
 2230  
 2231  
 2232  
 2233  
 2234  
 2235  
 2236  
 2237  
 2238  
 2239  
 2240  
 2241  
 2242

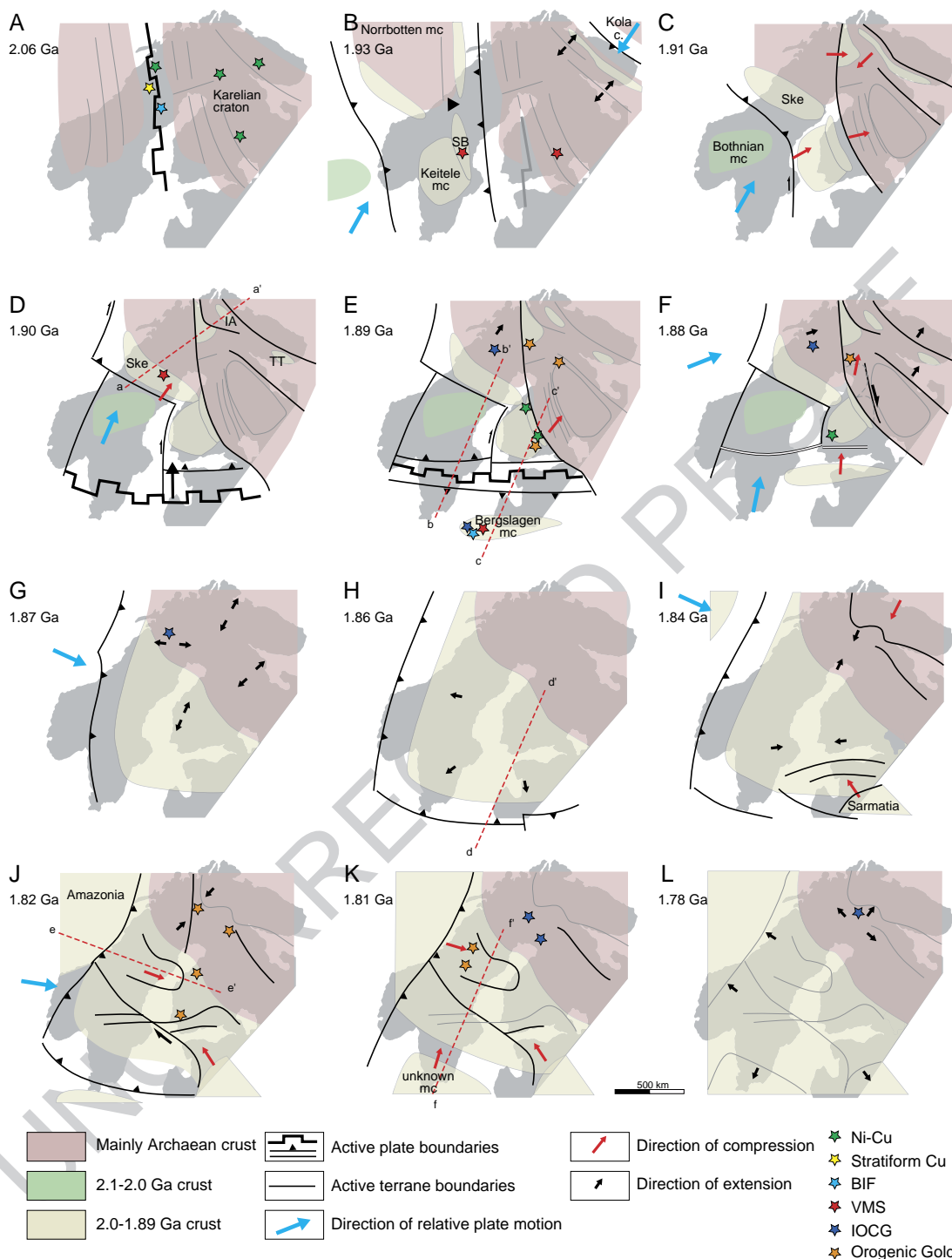


Fig. 12. The geodynamic evolution of the Fennoscandian Shield between 2.06 and 1.78 Ga after Lahtinen et al. (2005). The temporal and spatial relationship between tectonic setting and ore types is indicated and discussed in the text. Generalized cross-sections a–a' to f–f' are shown in Fig. 13.

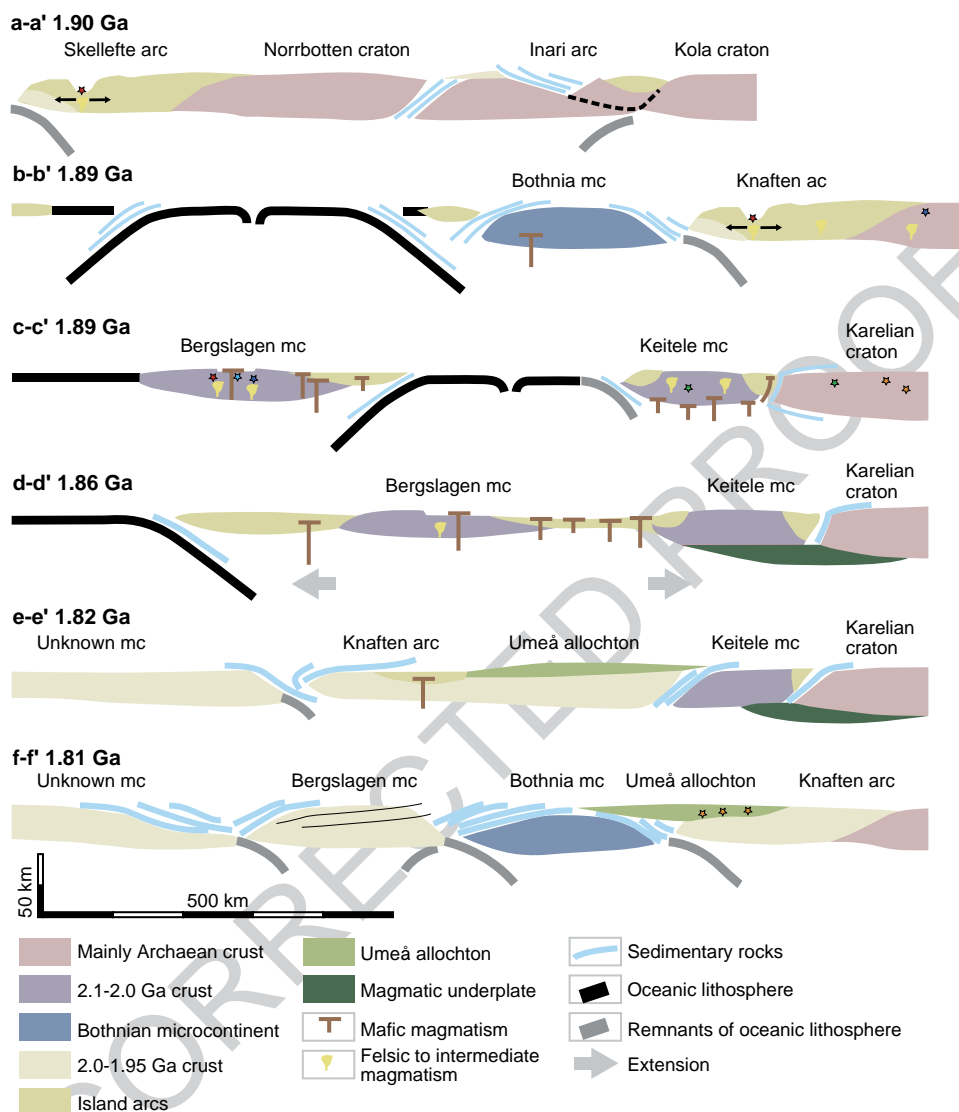


Fig. 13. Generalized cross-sections indicated in Fig. 12 after Lahtinen et al. (2005). Stars denote mineralization styles as in Fig. 12. mc=microcontinent. According to Lahtinen et al. (2005) lithologic, geochemical, isotopic and geophysical data suggest the following pre-1.92 Ga components in the Fennoscandian Shield, illustrated in the cross-sections:

- The Karelian, Kola and Norrbotten Archaean cratons
- The Keitele, Bergslagen and Bothnia >2.0 Ga age microcontinents
- The Kittilä ~2.0 Ga island arc and oceanic crust
- The Savo, Knaften, Inari and Tersk ~1.95 Ga island arcs

The Karelian and Kola cratons are well exposed, whereas the Norrbotten craton is not exposed. The Paleoproterozoic microcontinents Keitele, Bergslagen and Bothnia have no identified surface expressions. The Kittilä and Savo arcs are partly exposed and only small slivers of the Knaften arc are found at surface. The relationship of the Inari and Tersk arcs with the Archaean crust is not well known. The Umeå allochthon consists of a pre 1.9 Ga rock sequence, which is overlain by younger rocks in the Bothnian basin.

2243 In this environment, the mafic layered intrusions  
2244 that were emplaced during the early phases of the  
2245 rifting of the craton contain major chromitite and Ni–  
2246 Cu sulphide–PGE deposits. In the rift basins, conti-  
2247 nental to submarine volcanism, ranging in composition  
2248 from ultramafic to mafic and intermediate, is asso-  
2249 ciated with iron formations, but also with 2.2 to 2.05  
2250 Ga, low-grade, Ni–Cu and PGE deposits within  
2251 layered igneous complexes (e.g., Keivitsa) and high-  
2252 grade Ni–Cu deposits in ultramafic volcanic rocks and  
2253 fractionated mafic–ultramafic intrusions (e.g., Pe-  
2254 chenga). In some of the rift basins, stratiform  
2255 Cu ± Fe-oxide deposits formed within volcanoclastic  
2256 units of the greenstone belts (Inkinen, 1979; Martins-  
2257 son, 1997). The largest and sole economic deposit of  
2258 this category is the Viscaria Cu deposit in Kiruna.  
2259 The tectonic situation at the end of extension and the  
2260 onset of convergence, leading to basin inversion, and  
2261 the Svecofennian orogen (below subdivided into  
2262 several discrete tectonic events) are illustrated in  
2263 Fig. 12.

#### 2264 5.2. Microcontinent accretion at 1.96 to 1.88 Ga

2265 The first prominent evidence of convergence is the  
2266 obduction of ca. 1.97 to 1.96 Ga ophiolitic sequences  
2267 at Jormua and Outokumpu in Finland. These ophi-  
2268 olitic slices contain VMS-like deposits. However, as  
2269 they have recently been described as hosted by mantle  
2270 rocks (Kontinen, 1998; Sorjonen-Ward et al., 2004),  
2271 an exhalative or shallow seafloor replacement ori-  
2272 gin is excluded and they cannot be classified into the  
2273 VMS category *sensu stricto*. The tectonic situation  
2274 after the obduction of these ophiolites is illustrated  
2275 in Fig. 13 where subduction and back-arc rifting in the  
2276 Lapland–Kola area, westward subduction under the  
2277 Keitele microcontinent (Savo Belt) and Norrbotten  
2278 microcontinent (Kittilä), and NE subduction under  
2279 the Norrbotten microcontinent are the main tectonic  
2280 features at ca. 1.93 Ga. A rifted primitive island arc  
2281 complex (the Savo belt), formed by north-eastward  
2282 subduction west of the craton, contains the VMS  
2283 deposits formed in the Pyhäsalmi area in Finland  
2284 (Lahtinen, 1994).

2285 The Savo belt was accreted to the craton at ca. 1.91  
2286 to 1.90 Ga during the peak of the Lapland–Kola and  
2287 Lapland–Savo orogenies (Fig. 12C, D). The initial  
2288 stage of collision of the Bothnian microcontinent

with the Norrbotten and Keitele microcontinents  
2289 also occurred at this stage. Large areas of the  
2290 Archaean domain were reheated by burial beneath a  
2291 sequence of nappes in the foreland of the Palaeopro-  
2292 toerozoic orogens around 1.9 Ga, but there is no evi-  
2293 dence for a distinct Proterozoic gold mineralization  
2294 event in the area at this stage. The Skellefte arc  
2295 formed during the collision of the Bothnian micro-  
2296 continent with the Norrbotten and Keitele microcon-  
2297 tinents (Fig. 12D), either as a continental margin arc  
2298 or possibly as an accreted island arc. There is evi-  
2299 dence that this extensively mineralized arc was under  
2300 extension during the formation of the VMS ores  
2301 (Allen et al., 2002). Extension in the Skellefte district  
2302 was followed by basin inversion and rapid uplift and  
2303 erosion of the arc. Porphyry copper deposits were  
2304 formed at this stage, and also on the continent side  
2305 of the arc (Weihed et al., 1992). Docking of the  
2306 Bothnian microcontinent with the Norrbotten and  
2307 Keitele microcontinents and differences in relative  
2308 plate motions resulted in a transform fault between  
2309 the Keitele and Bothnian microcontinents (Fig. 12D).  
2310 Polarity reversal of subduction, and the onset of sub-  
2311 duction towards the north under the Keitele micro-  
2312 continent, was also initiated at ca. 1.90 Ga (Fig. 12D).  
2313

2314 During subduction switchover and the onset of  
2315 subduction towards the north under the Bothnian  
2316 microcontinent, magmatism was intense along the  
2317 craton margin. During crustal shortening, orogenic  
2318 gold mineralization occurred in the thickened crust  
2319 within accreted terranes at ca. 1.89 to 1.88 Ga, during  
2320 which period metamorphism peaked within the cra-  
2321 ton. Subduction under the Keitele microcontinent  
2322 locked up and the ocean basin was consumed by  
2323 subduction towards the south under the combined  
2324 Uusimaa island arc and the Bergslagen microconti-  
2325 nent (Fig. 12E, F). Magmatism along the craton mar-  
2326 gin produced mafic intrusion-hosted Ni–Cu deposits.  
2327 Magmatic hydrothermal fluids and fluids derived  
2328 from heating of evaporitic sequences in the rift-related  
2329 greenstone sequences within the craton, possibly  
2330 related to extension of the continental crust, formed  
2331 iron-oxide and IOCG deposits in areas underlain by  
2332 older Palaeoproterozoic cratonized crust. The Bergsla-  
2333 gen microcontinent started to accrete from the south  
2334 due to consumption of the ocean by subduction at ca.  
2335 1.88 Ga. In extensional settings within continental  
2336 margin arcs within the Bergslagen continent, VMS,  
2337

2337 iron-oxide and banded iron formations formed, clo-  
2338 sely related in space and time.

2339 The peak of the Svecokarelian Orogeny at ca. 1.88  
2340 to 1.87 Ga in the eastern part of the shield involved a  
2341 strong compressional stage. The Keitele–Bergslagen  
2342 collision resulted in substantial shortening within the  
2343 collision zone, overthrusting at the western margin of  
2344 the Karelian craton, basin inversion in Lapland, and  
2345 reactivation of the Lapland–Savo suture zone. Sub-  
2346 duction beneath the Bothnian microcontinent was still  
2347 active. Subduction towards the east under the Norr-  
2348 botten microcontinent commenced and local exten-  
2349 sional domains in the Kola and Belomorian areas  
2350 were initiated (Fig. 12F, G). The continued crustal  
2351 shortening within the craton resulted in orogenic  
2352 gold mineralization, especially in the eastern part of  
2353 the shield.

2354 *5.3. Continent–continent collision between 1.87 and*  
2355 *1.79 Ga, and possible orogenic collapse*

2356 The period between 1.87 and 1.83 Ga is still rather  
2357 poorly understood in terms of tectonic evolution.  
2358 There is evidence of scattered magmatism within the  
2359 craton as well as deformation and metamorphism that  
2360 may have peaked later in the western part of the  
2361 shield. Lahtinen et al. (2005) propose an attempted  
2362 orogenic collapse of the Svecokarelian orogen at ca.  
2363 1.87 to 1.85 Ga, whilst at the western margin the  
2364 subduction zone migrated southwards (Fig. 12G, H).  
2365 There is, however, little hard evidence for orogenic  
2366 collapse and, in fact, many orogenic gold occurrences,  
2367 notably in Finland, possibly formed within this time-  
2368 frame (Eilu et al., 2003). At the southern margin of the  
2369 craton, subduction towards the SE and the NE was  
2370 initiated (c.f., sections d–d' and f–f' in Fig. 13) and,  
2371 according to Lahtinen et al. (2005), large-scale exten-  
2372 sion took place in the hinterland. After ca. 1.87 Ga  
2373 there is little evidence of any other major ore forma-  
2374 tion until crustal shortening related to E–W subduc-  
2375 tion and subsequent continent–continent collision at  
2376 ca. 1.84 to 1.78 Ga.

2377 *5.4. Oblique continent–continent collision at 1.84 to*  
2378 *1.78 Ga*

2379 The Sarmatian crustal segment collided with the  
2380 SE margin of Fennoscandia at ca. 1.84 Ga (Fig. 12I).

This initiated what Lahtinen et al. (2005) refer to as  
the Svecobaltic Orogeny, expressed as basin inversion  
and thrusting. Subduction in the W and SW was still  
active and docking of Laurentia to Fennoscandia in  
the NE led to the final emplacement of the Lapland  
Granulite Belt and reactivation of the Belomorian  
mobile zone. The peak of the Svecobaltic Orogeny  
and the onset of the Nordic Orogeny occurred at ca.  
1.82 Ga (Lahtinen et al., 2005). The oblique collision  
of Fennoscandia with Sarmatia resulted in the migra-  
tion of a transform fault within the continent. This  
crustal-scale shear zone divided the Svecobaltic oro-  
gen into two different compressional regimes, a  
retreating subduction zone active in the SW, whilst a  
transpressional regime prevailed in the SE. The Nor-  
dic Orogeny started with collision of Amazonia and  
Fennoscandia in the NW with crustal-scale thrusting  
occurring in the hinterland (Fig. 12J). This collision  
caused crustal shortening in the hinterland and fluids  
circulating in the middle to upper crust formed oro-  
genic gold deposits in, at least, the western part of the  
shield. Far-field effects of this collision may also have  
caused reactivation of shear zones further east and  
orogenic gold mineralization may also have occurred  
in the eastern part of the craton in Finland. The crustal  
shortening caused extensive deformation and meta-  
morphism as well as partial melting of the middle  
continental crust. These processes also led to late-  
stage remobilization and formation of Cu–Au occur-  
rences within the NW part of the shield in the hinter-  
land to the active collision. Subsequent amalgamation  
of Laurentia, Fennoscandia, Amazonia, Sarmatia and  
an unknown continent in the SW came to an end at ca.  
1.81 to 1.79 Ga, forming the Palaeoproterozoic super-  
continent (Fig. 12J, K). The westward growth of the  
Fennoscandian Shield was initiated and the Fennos-  
candian Shield was stabilized between 1.79 and 1.77  
Ga (Fig. 12L).

The Anorthosite-hosted Ti-deposits in the SW part  
of the shield are related to continued westward growth  
and orogenic stacking in the craton. The Tellnes Ti-  
deposit occurs in part of the 930 to 920 Ma (Schärer et  
al., 1996) Rogaland Anorthosite Province, (Charlier,  
2005, Box 8–4). This magmatic province was formed  
in the SW part of the Sveconorwegian orogen during  
granulite facies metamorphism, post-dating the last  
regional deformation by ca. 40 million years (Box  
8–4, Charlier, 2005, this volume).



2429 **6. Conclusions**

2430 The Palaeoproterozoic, not the Archaean, hosts  
 2431 most of the economic mineral deposits in the Fen-  
 2432 noscandian Shield. Although the reason for this is not  
 2433 fully understood, the fact that a major part of the  
 2434 Archaean located in Russia is under-explored by  
 2435 modern standards may be one reason why not many  
 2436 major deposits have been found in the Archaean  
 2437 units. Another reason might be that most of the  
 2438 Archaean greenstone belts seem to be slightly older  
 2439 than the global Neoproterozoic peak in mineralization  
 2440 and mantle plume activity (e.g., Huhma et al., 1999)  
 2441 and, hence, magmatism and hydrothermal activity  
 2442 might have been less intense and unable to form  
 2443 major deposits.

2444 In contrast, the Palaeoproterozoic is well endowed  
 2445 with metallic resources. It appears that Precambrian  
 2446 geodynamics involved faster moving, hotter plates  
 2447 that accumulated less sediment and contained a thin-  
 2448 ner section of lithosphere mantle than the present  
 2449 plate-tectonic processes. This scenario also fits with  
 2450 the complex evolution of the Fennoscandian Shield  
 2451 between 2.06 and 1.78 Ga, when rapid accretion of  
 2452 island arcs and several microcontinent–continent col-  
 2453 lisions in a complex array of orogens was manifested  
 2454 in short-lived but intense orogenies. Most of the major  
 2455 ore deposits in the area also formed during this evolu-  
 2456 tionary stage and thus a strong geodynamic control on  
 2457 ore deposit formation is suggested.

2458 Throughout the evolution of the Fennoscandian  
 2459 Shield the orogenic gold deposits, where direct or  
 2460 indirect constraints on age are available, also reflect  
 2461 the orogenic younging of the shield towards the SW  
 2462 and west. Most orogenic gold deposits formed during  
 2463 periods of crustal shortening and mineralization pro-  
 2464 cesses peaked at 2.72 to 2.67, 1.90 to 1.86, and 1.85 to  
 2465 1.79 Ga.

2466 At ca. 2.5 to 2.4 Ga the Archaean craton rifted for  
 2467 the first time, facilitating the emplacement of exten-  
 2468 sive layered intrusions and mafic dyke swarms. At his  
 2469 stage and, to some extent, also during the later rifting  
 2470 stages at 2.2 to 2.05 Ga, Ni–Cu ± PGE deposits  
 2471 formed both as part of layered igneous complexes  
 2472 and associated with mafic volcanism in the rift basins.  
 2473 Synorogenic mafic–ultramafic intrusions formed dur-  
 2474 ing the peak of the Svecokarelian orogen at ca. 1.89 to  
 2475 1.88 Ga. These host numerous Ni–Cu deposits and are

2476 confined to linear belts that slightly post-date arc  
 2477 volcanism.

2478 Nearly all VMS-style deposits in the Fennoscandian  
 2479 Shield formed during the time span between 1.97  
 2480 and 1.88 Ga in extensional settings during basin  
 2481 inversion and accretion. The oldest, the Outokumpu-  
 2482 type ophiolitic Cu–Co–Au deposits were apparently  
 2483 formed at ca. 1.97 Ga in mantle rocks and were  
 2484 obducted on to the Archaean continent during onset  
 2485 of convergence. The next, more typical VMS deposits  
 2486 formed at 1.93 to 1.91 Ga in an accreted, primitive,  
 2487 bimodal arc setting formed during extension of only  
 2488 slightly older volcanic crust in the Pyhäsalmi area in  
 2489 central Finland. Their host rocks are tholeiitic basalts  
 2490 and transitional to calc-alkaline rhyolites, including  
 2491 high-silica varieties, and the deposits broadly fit  
 2492 within the “bimodal mafic type” classification of Bar-  
 2493 rie and Hannington (1999). The Skellefte VMS de-  
 2494 posits are 20 to 30 million years younger and Allen et al.  
 2495 (2002) suggest that, in contrast to the VMS deposits of  
 2496 the Pyhäsalmi area, the district is a remnant of a  
 2497 strongly extensional intra-arc region that developed  
 2498 on continental or mature arc crust where the basement  
 2499 was only slightly older. The Bergslagen–Uusimaa  
 2500 belt, with a much more diverse metallogeny compared  
 2501 to the Skellefte and Pyhäsalmi areas, is coeval with  
 2502 the Skellefte area, but was formed within or at the  
 2503 margin of a microcontinent that collided with Fennos-  
 2504 candia at ca. 1.88 to 1.87 Ga. The Bergslagen region  
 2505 is interpreted as an intra-continental extensional or  
 2506 continental margin back-arc region developed on  
 2507 older continental crust.

2508 IOCG occurrences in the Fennoscandian Shield are  
 2509 diverse in style. At least the oldest mineralizing stages  
 2510 at ca. 1.88 Ga are coeval with magmatism having a  
 2511 monzonitic fractionation trend and calc-alkaline to  
 2512 alkaline subaerial volcanism more akin to continental  
 2513 arc or magmatism inboard of an active arc. There is also  
 2514 evidence for multiple metal introduction or remobiliza-  
 2515 tion between ca. 1.80 and 1.77 Ga related to late- to  
 2516 post-orogenic magmatism distal to the active N–S sub-  
 2517 duction zone in the west. Models have also been sug-  
 2518 gested where the interaction of magmas with evaporitic  
 2519 sequences in the older Palaeoproterozoic rift sequences  
 2520 is important for forming fluids that have the right  
 2521 composition to carry large amounts of Fe, Cu and Au.

2522 Large volumes of anorthositic magmas characterize  
 2523 the Sveconorwegian Orogeny, in the SW part of the

2524 Fennoscandian Shield. The best example of a major  
2525 concentration of Ti associated with these anorthosites is  
2526 the Tellnes deposit. The Tellnes ilmenite deposit  
2527 belongs to the Mesoproterozoic (930 to 920 Ma) Rogal-  
2528 land Anorthosite Province in SW Norway. The rocks of  
2529 this province were emplaced in the SW part of the  
2530 Sveconorwegian orogenic belt under granulite facies  
2531 conditions, ca. 40 million years after the last regional  
2532 deformation of the Sveconorwegian Orogeny.

2533 This paper has demonstrated the intimate interplay  
2534 between Precambrian geodynamics and metal concen-  
2535 trations. All ore types discussed in this paper ultimately  
2536 have their genesis determined by their tectonic setting  
2537 and therefore the understanding of geodynamic pro-  
2538 cesses in the Precambrian will be a critical part in future  
2539 sustainable exploration and exploitation of metal  
2540 resources in shield areas around the world.

#### 2541 Acknowledgements

2542 We would like to thank Nicole Patison of Riddar-  
2543 hyttan Resources AB for providing the cross-section  
2544 of the Suurikuusikko deposit. Discussions with Tero  
2545 Niiranen and Juhani Ojala were valuable during the  
2546 process of producing this paper. We would also like to  
2547 express our sincere gratitude to Derek Blundell for  
2548 continuous encouragement while writing this manu-  
2549 script and also for his skills and enthusiasm that made  
2550 the GEODE project a success. The reviewers Mark  
2551 Barley and Michael Lesher are warmly thanked for  
2552 thoughtful comments and suggestions that improved  
2553 the manuscript substantially.

#### 2554 References

2555

2556 Abouchami, W., Boher, M., Michard, A., Albarède, F., 1990. A  
2557 major 2.1 Ga old event of mafic magmatism in West Africa.  
2558 *Journal of Geophysical Research* 95, 17605–17629.  
2559 Abzalov, M.Z., Both, R.A., 1997. The Pechenga Ni–Cu deposit,  
2560 Russia: data on PGE and Au distribution and sulfur isotope  
2561 compositions. *Mineralogy and Petrology* 61, 119–143.  
2562 Åhäll, K.-L., Larson, S.-Å., 2000. Growth-related 1.85–1.55 Ga  
2563 magmatism in the Baltic Shield; a review addressing the tectonic  
2564 characteristics of Svecofennian TIB 1-related and Gothian  
2565 events. *GFF* 122, 193–206.  
2566 Alapieti, T., Lahtinen, J., 2002. Platinum-group element mineraliza-  
2567 tion in layered intrusions of northern Finland and the Kola

Peninsula, Russia. In: Cabri, L.J. (Ed.), *The Geology, Geochem- 2568*  
*istry, Mineralogy and Mineral Beneficiation of Platinum-group 2569*  
*Elements. CIM Special Volume, vol. 54, pp. 507–546. 2570*  
Alapieti, T., Kujanpää, J., Lahtinen, J.J., Papunen, H., 1989. The  
2571 Kemi stratiform chromitite deposit, northern Finland. *Economic 2572*  
*Geology* 84, 1057–1077. 2573  
Allen, R.L., Weihed, P., Svenson, S.-Å., 1996a. Setting of Zn–Cu– 2574  
Au–Ag massive sulfide deposits in the evolution and facies 2575  
architecture of a 1.9 Ga marine volcanic arc, Skellefte district, 2576  
Sweden. *Economic Geology* 91, 1022–1053. 2577  
Allen, R.L., Lundström, I., Ripa, M., Simeonov, A., Christofferson, 2578  
H., 1996b. Facies analysis of a 1.9 Ga, continental margin, 2579  
back-arc, felsic caldera province with diverse Zn–Pb–Ag–(Cu– 2580  
Au) sulfide and Fe oxide deposits, Bergslagen region, Sweden. 2581  
*Economic Geology* 91, 979–1008. 2582  
Allen, R.L., Weihed, P. and the Global VHMS Research Project 2583  
team, 2002. Global comparison of volcanic-associated massive 2584  
sulphide districts. In: Blundell, D.J., Neubauer, F., von Quadt, 2585  
A. (Eds.), *The Timing and Location of Major Ore Deposits in an 2586*  
*Evolving Orogen. Geological Society, London, Special Publica- 2587*  
*tions, vol. 204, pp. 13–37. 2588*  
Amelin, Y.V., Heaman, L.M., Semenov, V.S., 1995. U–Pb geo- 2589  
chronology of layered mafic intrusions in the eastern Baltic 2590  
Shield: implications for the timing and duration of Palaeo- 2591  
proterozoic continental rifting. *Precambrian Research* 75, 2592  
31–46. 2593  
Anderson, A.T., Morin, M., 1969. Two types of massif anorthosites 2594  
and their implications regarding the thermal history of the crust. 2595  
In: Isachsen, Y.W. (Ed.), *Origin of Anorthosites and Related 2596*  
*Rocks. New York State Museum Sciences Service Memoirs, 2597*  
*vol. 18, pp. 57–69. 2598*  
Andersson, M., Lie, J.E., Husebye, E.S., 1996. Tectonic setting of 2599  
post-orogenic granites within SW Fennoscandia based on deep 2600  
seismic and gravity data. *Terra Nova* 8, 558–566. 2601  
Arndt, N.T., 2003. Komatiites, kimberlites and boninites. *Journal of 2602*  
*Geophysical Research* 108 (B6), 2293, doi: 10.1029/ 2603  
2002JB002157. 2604  
Arndt, N.T., Albarède, F., Nisbet, E.G., 1997. Mafic and ultramafic 2605  
magmatism. In: de Wit, M.J., Ashwal, L.D. (Eds.), *Greenstone 2606*  
*Belts. Oxford Science Publications, Oxford, pp. 233–254. 2607*  
Ashwal, L.D., 1993. *Anorthosites. Springer-Verlag, Berlin, Heidel- 2608*  
*berg. 422 pp. 2609*  
BABEL Working Group, 1990. Evidence for Early Proterozoic plate 2610  
tectonics from seismic reflection profiles in the Baltic Shield. 2611  
*Nature* 348, 34–38. 2612  
Bailes, A.H., Galley, A.G., 1999. Evolution of the Paleoproterozoic 2613  
Snow Lake arc assemblage and geodynamic setting for asso- 2614  
ciated volcanic-hosted massive sulphide deposits, Flin Flon 2615  
Belt, Manitoba, Canada. *Canadian Journal of Earth Sciences* 2616  
36, 1789–1805. 2617  
Bark, G., Weihed, P., 2003. The new Lycksele–Storuman gold ore 2618  
province, northern Sweden; with emphasis on the Early Proter- 2619  
ozoic Fäboliden orogenic gold deposit. In: Eliopoulos, D.G., 2620  
et al., (Eds.), *Mineral Exploration and Sustainable Develop- 2621*  
*ment. Millpress, Rotterdam, pp. 1061–1064. 2622*  
Barley, M.E., Krapez, B., Groves, D.I., Kerrich, R., 1998. The Late 2623  
Archaean bonanza: metallogenic and environmental conse- 2624

- quences of the interaction between mantle plumes, lithospheric tectonics and global cyclicity. *Precambrian Research* 91, 65–90.
- 2627 Barnes, S.-J., Often, M., 1990. Ti-rich komatiites from northern Norway. *Contributions to Mineralogy and Petrology* 105, 42–54.
- 2630 Barnes, S.-J., Melezhik, V.A., Sokolov, S.V., 2001. The composition and mode of formation of the Pechenga nickel deposits, Kola Peninsula, northwestern Russia. *Canadian Mineralogist* 39, 447–471.
- 2634 Barnichon, J.-D., Havenith, H., Hoffer, B., Charlier, R., Jongmans, D., Duchesne, J.C., 1999. The deformation of the Egersund Ognå massif, South Norway: finite element modelling of diapirism. *Tectonophysics* 303, 109–130.
- 2638 Barrie, C.T., Hannington, M.D. (Eds.), *Volcanic-associated Massive Sulfide Deposits: Processes and Examples in Modern and Ancient Settings*. *Reviews in Economic Geology*, vol. 8, pp. 101–131.
- 2642 Barton, M.D., Johnson, D.A., 1996. Evaporitic-source model for igneous-related Fe oxide-(REE-Cu-Au-U) mineralization. *Geology* 24, 259–262.
- 2644 Bayanova, T.B., Smolkin, V.F., Levkovich, N.V., 1999. U–Pb geochronology study of Mount Generalskaya layered intrusion, northwestern Kola Peninsula, Russia. *Institution of Mining and Metallurgy, Transactions (Section B, Applied Earth Science)* 108, 83–90.
- 2650 Bergman, S., Kübler, L., Martinsson, O., 2001. Description of regional geological and geophysical maps of northern Norrbotten County. *Sveriges Geologiska Undersökning, Ba* 56 (110 pp.).
- 2654 Bergman Weihed, J., Bergström, U., Billström, K., Weihed, P., 1996. Geology and tectonic evolution of the Paleoproterozoic Boliden Au–Cu–As deposit, Skellefte District, northern Sweden. *Economic Geology* 91, 1073–1097.
- 2658 Berthelsen, A., Marker, M., 1986. 1.9–1.8 Ga old strike-slip megashears in the Baltic Shield, and their plate tectonic implications. *Tectonophysics* 128, 163–181.
- 2661 Bibikova, E., Skiöld, T., Bogdanova, S., Gorbatshev, R., Slabunov, A., 2001. Titanite–rutile thermochronometry across the boundary between the Archaean craton in Karelia and the Belomorian Mobile Belt, eastern Baltic Shield. *Precambrian Research* 105, 315–330.
- 2666 Billström, K., Martinsson, O., 2000. Links between epigenetic Cu–Au mineralizations and magmatism/deformation in the Norrbotten county, Sweden. In: Weihed, P., Martinsson, O. (Eds.), *Abstract Volume and Field Trip Guidebook, 2nd Annual GEODE-Fennoscandian Shield Field Workshop on Palaeoproterozoic and Archaean Greenstone Belts and VMS Districts in the Fennoscandian Shield 28 August to 1 September, 2000, Gällivare–Kiruna, Sweden*, Luleå University of Technology, Research Report, vol. 6, p. 6.
- 2675 Billström, K., Weihed, P., 1996. Age and provenance of host rocks and ores of the Paleoproterozoic Skellefte District, northern Sweden. *Economic Geology* 91, 1054–1072.
- 2678 Bjørlykke, A., Cumming, G.L., Krstic, D., 1990. New isotopic data from davidites and sulfides in the Bidjovagge gold–copper deposit, Finnmark, northern Norway. *Mineralogy and Petrology* 43, 1–21.
- Bogdanova, S.V., Pashkevich, V.B., Buryanov, V.B., Makarenko, I.B., Orlyuk, M.I., Skobelev, V.M., Starostenko, V.I., Legostaeva, O.V., 2004. The 1.80–1.74 Ga gabbro–anorthosite–rapakivi Korosten Pluton in the Ukrainian Shield: a 3-D geophysical reconstruction of deep structure. *Tectonophysics* 381, 5–27.
- Boher, M., Abouchami, W., Michard, A., Albarède, F., Arndt, N.T., 1991. Crustal growth in West Africa at 2.1 Ga. *Journal of Geophysical Research* 95, 17605–17629.
- Broman, C., Martinsson, O., 2000. Fluid inclusions in epigenetic Fe–Cu–Au ores in northern Norrbotten. *2nd Annual GEODE-Fennoscandian Shield Field Workshop on Palaeoproterozoic and Archaean Greenstone Belts and VMS Districts in the Fennoscandian Shield*. Luleå University of Technology, Research Report, vol. 6, 7 pp.
- Card, K.D., 1990. A review of the Superior Province of the Canadian Shield, a product of Archean accretion. *Precambrian Research* 48, 99–156.
- Cawthorn, R.G., 1996. *Layered igneous rocks*. Development in Petrology Elsevier Science, Amsterdam. 531 pp.
- Charlier, B., 2005. Fennoscandian Shield — Rogaland anorthosite province. *Ore Geology Reviews* (this volume).
- Charlier, B., Duchesne, J.C., 2003. Whole-rock geochemistry of the Bjerkreim–Sokndal layered series: bearing on crystallization processes of cumulus rocks. *NGU Special Publication* 9, 35–37.
- Cliff, R.A., Rickard, D., Blake, K., 1990. Isotope systematics of the Kiruna magnetite ores, Sweden: Part I. Age of the ore. *Economic Geology* 85, 1770–1776.
- Condie, K.C., 1999. *Archean Crustal Evolution*. Elsevier Science B.V., Amsterdam. 420 pp.
- Condie, K.C., 2004. Precambrian superplume events. In: Eriksson, P.G., Altermann, W., Nelson, D.R., Mueller, W.U., Catuneanu, O. (Eds.), *The Precambrian Earth: Tempos and Events*. Elsevier Science B.V., Amsterdam, pp. 163–173.
- de Wit, M.J., Hart, R.A., Hart, R.J., 1987. The Jamestown ophiolite complex, Barberton mountain belt: a section through 3.5 Ga oceanic crust. *Journal of African Earth Sciences* 6, 681–730.
- Duchesne, J.C., 1996. Liquid ilmenite or liquidus ilmenite: a comment on the nature of ilmenite vein deposit. In: Demaiffe, D. (Ed.), *Petrology and Geochemistry of Magmatic Suites of Rocks in the Continental and Oceanic Crusts*. ULB-MRAC, Bruxelles, pp. 73–82.
- Duchesne, J.C., 1999. Fe–Ti deposits in Rogaland anorthosites (South Norway): geochemical characteristics and problems of interpretation. *Mineralium Deposita* 34, 182–198.
- Duchesne, J.C., Bingen, B., 2001. The Rogaland anorthosite province: an introduction. In: Duchesne, J.C. (Ed.), *The Rogaland Intrusive Massifs, an Excursion Guide*, NGU Report, vol. 29. Geological Survey of Norway, pp. 13–24.
- Duchesne, J.C., Hertogen, J., 1988. Le magma parental du lopolithe de Bjerkreim–Sokndal (Norvège méridionale). *Comptes Rendus de l’Académie des Sciences, Série II* 306, 45–48 (Paris).
- Duchesne, J.C., Schiellerup, H., 2001. The iron–titanium deposits in the Rogaland anorthosite Province. In: Duchesne, J.C. (Ed.), *The Rogaland Intrusive Massifs: an Excursion Guide*, NGU Report, vol. 029, pp. 56–75.

- 2739 Duchesne, J.C., Liégeois, J.P., Vander Auwera, J., Longhi, J., 1999. 2796  
 2740 The crustal tongue melting model and the origin of massive 2797  
 2741 anorthosites. *Terra Nova* 11, 100–105. 2798  
 2742 Edfelt, Å., Martinsson, O., 2004. The Tjårrojåkka Fe-oxide and Cu– 2799  
 2743 Au occurrences, northern Sweden — products of one ore form- 2800  
 2744 ing event? IAVCEI General Assembly 14–19 November 2004, 2801  
 2745 Pucón, Chile. Abstract volume (CD-ROM). 2802  
 2746 Edfelt, Å., Martinsson, O., 2003. Fennoscandian Shield — iron 2803  
 2747 oxide copper–gold deposits. *Ore Geology Reviews* (this 2804  
 2748 volume). 2805  
 2749 Edfelt, Å., Broman, C., Martinsson, O., 2004. A preliminary fluid 2806  
 2750 inclusion study of the Tjårrojåkka IOCG-occurrence, Kiruna 2807  
 2751 area, northern Sweden. *GFF* 126, 148. 2808  
 2752 Eilu, P., Weihed, P., 2003. Fennoscandian Shield — orogenic gold 2809  
 2753 deposits. *Ore Geology Reviews* (this volume). 2810  
 2754 Eilu, P., Sorjonen-Ward, P., Nurmi, P., Niiranen, T., 2003. A review 2811  
 2755 of gold mineralization styles in Finland. *Economic Geology* 98, 2812  
 2756 1329–1353. 2813  
 2757 Eilu, P., Pankka, H., Keinänen, V., Kortelainen, V., Niiranen, T., 2814  
 2758 Pulkkinen, E., in press. Characteristics of gold mineralisation in 2815  
 2759 the greenstone belts of northern Finland. Geological Survey of 2816  
 2760 Finland, Special Paper. 2817  
 2761 Ekdahl, E., 1993. Early Proterozoic Karelian and Svecofennian 2818  
 2762 Formations and the Evolution of the Raahe–Ladoga Ore Zone, 2819  
 2763 Based on the Pielavesi Area, Central Finland. *Bulletin*, vol. 373. 2820  
 2764 Geological Survey of Finland. 137 pp. 2821  
 2765 Emslie, R.F., Hamilton, M.A., Thiéroult, R.J., 1994. Petrogenesis of a 2822  
 2766 a Mid-Proterozoic anorthosite–mangerite–charnockite–granite 2823  
 2767 (AMCG) complex: isotopic and chemical evidence from the 2824  
 2768 Nain plutonic suite. *Journal of Geology* 102, 539–558. 2825  
 2769 Ettner, C.D., Bjørlykke, A., Andersen, T., 1993. Fluid evolution 2826  
 2770 and Au–Cu genesis along a shear zone: a regional fluid 2827  
 2771 inclusion study of a shear zone-hosted alteration and gold 2828  
 2772 and copper mineralization in the Kautokeino greenstone belt, 2829  
 2773 Finnmark, Norway. *Journal of Geochemical Exploration* 49, 2830  
 2774 233–267. 2831  
 2775 Ettner, D.C., Bjørlykke, A., Andersen, T., 1994. A fluid inclusion 2832  
 2776 and stable isotope study of the Proterozoic Bidjovagge Au–Cu 2833  
 2777 deposit, Finnmark, northern Norway. *Mineralium Deposita* 29, 2834  
 2778 16–29. 2835  
 2779 Foley, S.F., Buhre, S., Jacob, D.E., 2003. Evolution of the Archaean 2836  
 2780 crust by delamination and shallow subduction. *Nature* 421, 2837  
 2781 249–252. 2838  
 2782 Fram, M.S., Longhi, J., 1992. Phase equilibria of dikes associated 2839  
 2783 with Proterozoic anorthosite complexes. *American Mineralogist* 2840  
 2784 77, 605–616. 2841  
 2785 Francis, D., Ludden, J., Johnstone, R., Davis, W., 1999. Picrite 2842  
 2786 evidence for more Fe in Archaean mantle reservoirs. *Earth 2843*  
 2787 and Planetary Science Letters 167, 197–213. 2844  
 2788 Frietsch, R., 1977. The iron ore deposits in Sweden. In: Zitman, A. 2845  
 2789 (Ed.), *The Iron Ore Deposits of Europe and Adjacent Areas*. 2846  
 2790 Bundesanstalt für Geowissenschaft und Rohstoffe, Hannover, 2847  
 2791 pp. 279–293. 2848  
 2792 Frietsch, R., Tuisku, P., Martinsson, O., Perdahl, J.-A., 1997. Cu– 2849  
 2793 (Au) and Fe ore deposits associated with Na–Cl metasomatism 2850  
 2794 in Early Proterozoic rocks of northern Fennoscandia: a new 2851  
 2795 metallogenic province. *Ore Geology Reviews* 12, 1–34. 2852
- Gaál, G., 1972. Tectonic control of some Ni–Cu deposits in Finland. 2796  
 In: Gill, J.E. (Ed.), *Proceedings, International Geological Con- 2797*  
 gress, 24th session, Montreal 1972: Section 4, Mineral Deposits, 2798  
 pp. 215–224. 2799  
 Gaál, G., 1982. Proterozoic tectonic evolution and Late Svecokar- 2800  
 elian plate deformation of the central Baltic Shield. *Geologische 2801*  
*Rundschau* 71, 158–170. 2802  
 Gaál, G., 1985. Nickel metallogeny related to tectonics. In: Papu- 2803  
 nen, H., Gorbunov, G.I. (Eds.), *Nickel–Copper Deposits of the 2804*  
*Baltic Shield and Scandinavian Caledonides*, *Bulletin*, vol. 333. 2805  
 Geological Survey of Finland, pp. 143–155. 2806  
 Gaál, G., 1990. Tectonic styles of Early Proterozoic ore deposi- 2807  
 tion in the Fennoscandian Shield. *Precambrian Research* 46, 2808  
 83–114. 2809  
 Gaál, G., Gorbatshev, R., 1987. An outline of the Precam- 2810  
 brian evolution of the Baltic Shield. *Precambrian Research* 2811  
 35, 15–52. 2812  
 Geological Survey of Finland., 2004. *Ore Deposit Data Base*. 2813  
<http://www.gs.fi/explor/>. 2814  
 Goldfarb, R.J., Groves, D.I., Gardoll, S., 2001. Orogenic gold 2815  
 and geologic time: a global synthesis. *Ore Geology Reviews* 2816  
 18, 1–75. 2817  
 Goldstein, S.L., Arndt, N.T., Stallard, R.F., 1997. The history of a 2818  
 continent from Sm–Nd isotopes in Orinoco basin river sedi- 2819  
 ments and U–Pb ages of zircons from Orinoco river sand. 2820  
*Chemical Geology* 139, 271–298. 2821  
 Gorbatshev, R., Bogdanova, S., 1993. Frontiers in the Baltic 2822  
 Shield. *Precambrian Research* 64, 3–21. 2823  
 Gorbunov, G.I., Zagorodny, V.G., Robonen, W.I., 1985. Main fea- 2824  
 tures of the geological history of the Baltic Shield and the 2825  
 epochs of ore formation. In: Papunen, H., Gorbunov, G.I. 2826  
 (Eds.), *Nickel–Copper Deposits of the Baltic Shield and Scan- 2827*  
*dinavian Caledonides*, *Bulletin*, vol. 333. Geological Survey of 2828  
 Finland, pp. 17–41. 2829  
 Green, A.H., Melezhik, V.A., 1999. Geology of the Pechenga ore 2830  
 deposits; a review with comments on ore forming processes. In: 2831  
 Keays, R.R., Leshner, C.M., Lightfoot, P.C., Farrow, C.E.G. 2832  
 (Eds.), *Dynamic Processes in Magmatic Ore Deposits and 2833*  
*their Application to Mineral Exploration*. Geological Association 2834  
 of Canada, Short Course Notes, vol. 13, pp. 287–328. 2835  
 Grönholm, P., 1999. The mesothermal Saattopora copper–gold 2836  
 deposit in the Palaeoproterozoic Central Lapland greenstone 2837  
 belt, Northern Finland. In: Cook, N.J., Sundblad, K. (Eds.), 2838  
*Precambrian Gold in the Fennoscandian and Ukrainian Shields 2839*  
*and Related Areas*. Gold '99 Trondheim, Norway, 4–6 May 2840  
 1999. Geological Survey of Norway, Trondheim, p. 83. 2841  
 Groves, D.I., Goldfarb, R.J., Gebre-Mariam, M., Hagemann, S., 2842  
 Robert, F., 1998. Orogenic gold deposits: a proposed classi- 2843  
 fication in the context of their crustal distribution and rela- 2844  
 tionship to other gold deposit types. *Ore Geology Reviews* 13, 2845  
 1–28. 2846  
 Halkoaho, T., Pietikäinen, K., 1999. Ni and Au prospects of the 2847  
 Kuhmo and Suomussalmi greenstone belts. In: Papunen, H., 2848  
 Eilu, P. (Eds.), *Geodynamic Evolution and Metallogeny of the 2849*  
*Central Lapland, Kuhmo and Suomussalmi Greenstone Belts,* 2850  
*Finland*. Publication, vol. 42. Institute of Geology and Miner- 2851  
 alogy, University of Turku, pp. 60–63. 2852

- 2853 Halkoaho, T., Liimatainen, J., Papunen, H., Välimaa, J., 2000. 2910  
 2854 Exceptionally Cr-rich basalts in the komatiitic volcanic associa- 2911  
 2855 tion of the Archaean Kuhmo greenstone belt, eastern Finland. 2912  
 2856 *Mineralogy and Petrology* 70, 105–120. 2913  
 2857 Hallberg, A., 1994. The Enåsen gold deposit, central Sweden: 1. A 2914  
 2858 Paleoproterozoic high sulphidation epithermal gold mineraliza- 2915  
 2859 tion. *Mineralium Deposita* 29, 150–162. 2916  
 2860 Hamilton, M.A., Ryan, A.B., Emslie, R.F., Ermanovics, I.F., 1998. 2917  
 2861 Identification of Paleoproterozoic anorthositic and monzonitic 2918  
 2862 rocks in the vicinity of the Mesoproterozoic Nain plutonic suite, 2919  
 2863 Labrador: U–Pb evidence. Radiogenic Age and Isotopic Studies, 2920  
 2864 Current Research 1998-F, Report, vol. 11. Geological Survey of 2921  
 2865 Canada, pp. 23–40. 2922  
 2866 Hanski, E.J., 1992. Petrology of the Pechenga ferropicrites and 2923  
 2867 cogenetic Ni-bearing gabbro–wehrlite intrusions, Kola Penin- 2924  
 2868 sula, Russia. *Geological Survey Finland Bulletin* 367 (192 pp.). 2925  
 2869 Hanski, E.S., 1997. The Nuttito serpentinite belt, central Lapland: an 2926  
 2870 example of Paleoproterozoic ophiolitic mantle rocks in Finland. 2927  
 2871 *Ophioliti* 22, 35–46. 2928  
 2872 Hanski, E.S., Smolkin, V.F., 1989. Pechenga ferropicrites and other 2929  
 2873 Early Proterozoic picrites in the eastern part of the Baltic Shield. 2930  
 2874 *Precambrian Research* 45, 63–82. 2931  
 2875 Hanski, E., Huhma, H., Vaasjoki, M., 2001a. Geochronology of 2932  
 2876 northern Finland: a summary and discussion. *Special Paper*, vol. 2933  
 2877 33. Geological Survey of Finland, pp. 255–279. 2934  
 2878 Hanski, E., Huhma, H., Rastas, P., Kamenetsky, V.S., 2001b. The 2935  
 2879 palaeoproterozoic komatiite–picrite association of Finnish Lap- 2936  
 2880 land. *Journal of Petrology* 42, 855–876. 2937  
 2881 Haughton, D.R., Roeder, P.L., Skinner, B.J., 1974. Solubility of 2938  
 2882 sulfur in mafic magmas. *Economic Geology* 69, 451–467. 2939  
 2883 Hedström, P., Simeonov, A., Malmström, L., 1989. The Zinkgruvan 2940  
 2884 ore deposit, south-central Sweden: a Proterozoic, proximal Zn– 2941  
 2885 Pb–Ag deposit in distal volcanic facies. *Economic Geology* 84, 2942  
 2886 1235–1261. 2943  
 2887 Helovuori, O., 1979. The geology and zinc–copper deposits of the 2944  
 2888 Pyhäsalmi–Pielavesi district, Finland. *Economic Geology* 74, 2945  
 2889 1084–1101. 2946  
 2890 Herzberg, C., 1992. Depth and degree of melting of komatiite. 2947  
 2891 *Journal of Geophysical Research* 97, 4521–4540. 2948  
 2892 Hietanen, A., 1975. Generation of potassium poor magmas in the 2949  
 2893 northern Sierra Nevada and the Svecofennian of Finland. *Jour- 2950*  
 2894 *nal of Research, US Geological Survey* 3, 631–645. 2951  
 2895 Hill, R.E.T., 2001. Komatiite volcanology, volcanological setting 2952  
 2896 and primary geochemical properties of komatiite-associated 2953  
 2897 nickel deposits. *Geochemistry: Exploration, Environment, Ana- 2954*  
 2898 *lysis* 1, 365–381. 2955  
 2899 Hiltunen, A., 1982. The Precambrian Geology and Skarn Iron Ores 2956  
 2900 of the Rautuvaara Area, Northern Finland. *Bulletin*, vol. 318. 2957  
 2901 Geological Survey of Finland. 133 pp. 2958  
 2902 Hitzman, M.W., 2000. Iron oxide–Cu–Au deposits: what, where, 2959  
 2903 when, and why. In: Porter, T.M. (Ed.), *Hydrothermal Iron Oxide 2960*  
 2904 Copper–Gold and Related Deposits: A Global Perspective. Aus- 2961  
 2905 tralian Mineral Foundation, Adelaide, pp. 9–25. 2962  
 2906 Hitzman, M.W., Oreskes, N., Einaudi, M.T., 1992. Geological 2963  
 2907 characteristics and tectonic setting of Proterozoic iron 2964  
 2908 oxide (Cu–U–Au–REE) deposits. *Precambrian Research* 58, 2965  
 2909 241–287. 2966  
 Huhma, H., Cliff, R.A., Perttunen, V., Sakko, M., 1990. Sm–Nd 2910  
 and Pb isotopic study of mafic rocks associated with Early 2911  
 Proterozoic continental rifting; the Perapohja schist belt in 2912  
 northern Finland. *Contributions to Mineralogy and Petrology* 2913  
 104, 369–379. 2914  
 Huhma, H., Mänttäri, I., Vaasjoki, M., 1999. Dating the Finnish 2915  
 Archaean greenstone belts— isotope geology. In: Papunen, H., 2916  
 Eilu, P. (Eds.), *Geodynamic Evolution and Metallogeny of the 2917*  
 Central Lapland, Kuhmo and Suomussalmi Greenstone Belts, 2918  
 Finland. Joint Field Excursion and Workshop of GEODE, 11– 2919  
 16. September 1999, pp. 72–74. abstracts. 2920  
 Huhma, H., Mutanen, T., Whitehouse, M., 2004. Oldest rocks of the 2921  
 Fennoscandian Shield: the 3.5 Ga Siurua trondhjemite gneiss in 2922  
 the Archaean Pudasjärvi granulite belt, Finland. *GFF* 126, 10. 2923  
 Huhtala, T., 1979. The geology and zinc–copper deposits of the 2924  
 Pyhäsalmi–Pielavesi District, Finland. *Economic Geology* 74, 2925  
 1069–1083. 2926  
 Huppert, H.E., Sparks, S.J., Turner, J.S., Arndt, N.T., 1984. Empla- 2927  
 cement and cooling of komatiite lavas. *Nature* 309, 19–22. 2928  
 Inkinen, O., 1979. Copper, zinc, and uranium occurrences at Pahta- 2929  
 vuoma in the Kittilä greenstone complex, northern Finland. 2930  
*Economic Geology* 74, 1153–1165. 2931  
 Juhlin, C., Elming, S.-Å., Mellqvist, C., Öhlander, B., Weihed, P., 2932  
 Wikström, A., 2002. Crustal reflectivity near the Archaean– 2933  
 Proterozoic boundary in northern Sweden and the implications 2934  
 for the tectonic evolution of the area. *Geophysical Journal 2935*  
*International* 150, 180–197. 2936  
 Kähkönen, Y., Lahtinen, R., Nironen, M., 1994. Palaeoproterozoic 2937  
 supracrustal belts in southwestern Finland. *Guide*, vol. 37. 2938  
 Geological Survey of Finland, pp. 43–47. 2939  
 Karhu, J.A., 1993. Paleoproterozoic Evolution of the Carbon 2940  
 Isotope Ratios of Sedimentary Carbonates in the Fennoscandian 2941  
 Shield. *Bulletin*, vol. 371. Geological Survey of Finland. 2942  
 87 pp. 2943  
 Karsten, J.L., Klein, E.M., Sherman, S.B., 1996. Subduction zone 2944  
 geochemical characteristics in ocean ridge basalts from the 2945  
 southern Chile ridge: implications of modern ridge subduction 2946  
 systems for the Archean. *Lithos* 37, 143–161. 2947  
 Kilpeläinen, T., 1998. Evolution and 3D Modelling of Structural 2948  
 and Metamorphic Patterns of the Palaeoproterozoic Crust in the 2949  
 Tampere–Vammala Area, Southern Finland. *Bulletin*, vol. 397. 2950  
 Geological Survey of Finland. 124 pp. 2951  
 Kimura, G., Ludden, J.N., Desrochers, J.-P., Hori, R., 1993. A 2952  
 model of ocean-crust accretion for the Superior Province, 2953  
 Canada. *Lithos* 30, 337–355. 2954  
 Koark, H.J., 1962. Zur Altersstellung und Entstehung der Sulfiderze 2955  
 vom Typus Falun. *Geologische Rundschau* 52, 123–146. 2956  
 Koistinen, T., Stephens, M.B., Bogatchev, V., Nordgulen, Ø., Wen- 2957  
 nerström, M., Korhonen, J. (Eds.), 2001. Geological Map of the 2958  
 Fennoscandian Shield, Scale 1:2 000 000. Geological surveys of 2959  
 Finland, Norway and Sweden and the North-West Department 2960  
 of Natural Resources of Russia. ISBN: 951-690-810-1. 2961  
 Kontinen, A., 1998. The nature of the serpentinites, associated 2962  
 dolomite–skarn–quartz rocks and massive Co–Cu–Zn sulphide 2963  
 ores in the Outokumpu area, eastern Finland. In: Hanski, E., 2964  
 Vuollo, J. (Eds.), *International Ophiolite Symposium and Field 2965*  
*Excursion — Generation and Emplacement of Ophiolites* 2966

- 2967 Through Time. August 10–15, 1998, University of Oulu, Oulu,  
2968 Finland. Abstracts — Excursion Guide. Special Paper, vol. 26.  
2969 Geological Survey of Finland, p. 33.
- 2970 Kontinen, A., Paavola, J., Lukkarinen, H., 1992. K–Ar ages  
2971 of hornblende and biotite from Late Archaean rocks of  
2972 eastern Finland — interpretation and discussion of tectonic  
2973 implications. *Bulletin*, vol. 365. Geological Survey of Finland,  
2974 pp. 1–31.
- 2975 Kontoniemi, O., 1998. Geological setting and characteristics of the  
2976 Palaeoproterozoic tonalite-hosted Osikonmäki gold deposit,  
2977 southeastern Finland. Special Paper, vol. 25. Geological Survey  
2978 of Finland, pp. 39–80.
- 2979 Korja, A., 1995. Structure of the Svecofennian crust — growth and  
2980 destruction of the Svecofennian orogen. Ph.D. Thesis, Institute  
2981 of Seismology, University of Helsinki, Report S-31. 36 p.
- 2982 Korja, A., Korja, T., Luostro, U., Heikkinen, P., 1993. Seismic and  
2983 geoelectric evidence for collisional and extensional events in the  
2984 Fennoscandian Shield — implications for Precambrian crustal  
2985 evolution. *Tectonophysics* 219, 129–152.
- 2986 Korsman, K., Koistinen, T., Kohonen, J., Wennerström, M., Ekdahl,  
2987 E., Honkamo, M., Idman, H., Pekkala, Y. (Eds.), 1997. Suomen  
2988 kallioperäkartta — Berggrundskarta Över Finland — Bedrock  
2989 Map of Finland 1:1 000 000. Geological Survey of Finland,  
2990 Espoo, Finland.
- 2991 Korsman, K., Korja, T., Pajunen, M., Vinansalo, P.GGT/SVEKA  
2992 Working Group, 1999. The GGT/SVEKA Transect structure and  
2993 evolution of the continental crust in the Paleoproterozoic Sve-  
2994 cofennian orogen in Finland. *International Geological Reviews*  
2995 41, 287–333.
- 2996 Korvuo, E., 1997. The Saattopora gold ore and the Pahtavuoma Cu–  
2997 Zn–U occurrences in the Kittilä region, northern Finland. In:  
2998 Korhikoski, E., Sorjonen-Ward, P. (Eds.), *Research and*  
2999 *Exploration — Where do they Meet?* 4th Biennial SGA Meet-  
3000 *ing*, August 11–13, 1997, Turku, Finland. Excursion Guidebook  
3001 B1: Ore Deposits of Lapland in Northern Finland and Sweden.  
3002 Guide, vol. 43. Geological Survey of Finland, pp. 21–25.
- 3003 Kousa, J., Marttila, E., Vaasjoki, M., 1994. Petrology, geochemistry  
3004 and dating of Paleoproterozoic metavolcanic rocks in the Pyhä-  
3005 järvi area, central Finland. In: Nironen, M., Kähkönen, Y. (Eds.),  
3006 *Geochemistry of Proterozoic Supracrustal Rocks in Finland*.  
3007 Special Paper, vol. 19. Geological Survey of Finland, pp. 7–27.
- 3008 Kurki, J., Papunen, H., 1985. Geology and nickel–copper deposits  
3009 of the Kianta area, Suomussalmi. In: Papunen, H., Gorbunov,  
3010 G.I. (Eds.), *Nickel–Copper Deposits of the Baltic Shield and*  
3011 *Scandinavian Caledonides*. *Bulletin*, vol. 333. Geological Sur-  
3012 *vey of Finland*, pp. 155–164.
- 3013 Lahtinen, R., 1994. Crustal Evolution of the Svecofennian and  
3014 Karelian Domains during 2.1–1.79 Ga, with Special Emphasis  
3015 on the Geochemistry and Origin of 1.93–1.91 Ga Gneissic  
3016 Tonalites and Associated Supracrustal Rocks in the Rautalampi  
3017 Area, Central Finland. *Bulletin*, vol. 378. Geological Survey of  
3018 Finland. 128 pp.
- 3019 Lahtinen, R., Huhma, H., 1997. Isotopic and geochemical con-  
3020 straints on the evolution of the 1.93–1.79 Ga Svecofennian  
3021 crust and mantle in Finland. *Precambrian Research* 82, 13–34.
- 3022 Lahtinen, R., Korja, A., Nironen, M., 2003. Paleoproterozoic oro-  
3023 genic evolution of the Fennoscandian Shield at 1.92–1.77 Ga  
with notes on the metallogeny of FeOx–Cu–Au, VMS, and  
orogenic gold deposits. In: Eliopoulos, D.G., et al., (Eds.),  
*Mineral Exploration and Sustainable Development*. Millpress,  
Rotterdam, pp. 1057–1060.
- Lahtinen, R., Korja, A., Nironen, M., 2004. Paleoproterozoic oro-  
genic evolution of the Fennoscandian Shield at 1.92–1.77 Ga —  
the formation of a supercontinent. *GFF* 126, 27.
- Lahtinen, R., Korja, A., Nironen, M., 2005. Paleoproterozoic tec-  
tonic evolution. In: Lehtinen, M., Nurmi, P.A., Rämö, O.T.  
(Eds.), *Precambrian Geology of Finland — Key to the Evolution*  
*of the Fennoscandian Shield*. Elsevier Science, B.V., Amster-  
dam, pp. 481–532.
- Lehtonen, M., Airo, M.-L., Eilu, P., Hanski, E., Kortelainen, V.,  
Lanne, E., Manninen, T., Rastas, P., Räsänen, J., Virransalo, P.,  
1998. The Stratigraphy, Petrology and Geochemistry of the  
Kittilä Greenstone Area, Northern Finland: a Report of the  
Lapland Volcanite Project. Report of Investigation, vol. 140.  
Geological Survey of Finland. 144 pp. (in Finnish with English  
summary).
- Leshner, C.M., 1989. Komatiite-associated nickel sulfide depos-  
its. In: Whitney, J.A., Naldrett, A.J. (Eds.), *Ore Deposition*  
*Associated with Magmas*. *Reviews in Economic Geology*, vol.  
4, pp. 45–102.
- Leshner, C.M., Arndt, N.T., Groves, D.I., 1984. Genesis of komatiite-  
associated nickel sulfide deposits at Kambalda, Western Aus-  
tralia: a distal volcanic model. In: Buchanan, D.L., Jones, M.L.  
(Eds.), *Sulfide Deposits in Mafic and Ultramafic Rocks*. Insti-  
tute of Mining and Metallurgy, London, pp. 70–80.
- Lindblom, S., Broman, C., Martinsson, O., 1996. Magmatic–hydro-  
thermal fluids in the Pahtohavare Cu–Au deposit in greenstone  
at Kiruna, Sweden. *Mineralium Deposita* 31, 307–318.
- Lindskog, L., 2001. Relationships between Fe-oxide Cu/Au depos-  
its at Gruvberget—Kiruna District, northern Sweden. Unpub-  
lished B.Sc. Thesis, James Cook University, Townsville,  
Australia. 123 pp.
- Lindsley, D.H., 2003. Do Fe–Ti oxide magmas exist? *Geology*: yes;  
experiments: no! *NGU Special Publication* 9, 34–35.
- Lobach-Zhuchenko, S.B., Chekulaev, V.P., Sergeev, S.A., Levchen-  
kov, O.A., Krylov, I.N., 1993. Archaean rocks from southeast-  
ern Karelia (Karelian granite–greenstone terrain). *Precambrian*  
*Research* 62, 375–397.
- Longhi, J., Fram, M.S., Vander Auwera, J., Montieth, J.N., 1993.  
Pressure effects, kinetics, and rheology of anorthositic and  
related magmas. *American Mineralogist* 78, 1016–1030.
- Longhi, J., Vander Auwera, J., Fram, M., Duchesne, J.C., 1999.  
Some phase equilibrium constraints on the origin of Proterozoic  
(Massif) anorthosites and related rocks. *Journal of Petrology* 40,  
339–362.
- Lundqvist, T., Vaasjoki, M., Persson, P.-O., 1998. U–Pb ages of  
plutonic and volcanic rocks in the Svecofennian Bothnian  
Basin, central Sweden, and their implications for the Paleopro-  
terozoic evolution of the basin. *GFF* 120, 357–363.
- Lundström, I., 1987. Lateral variations in supracrustal geology  
within the Swedish part of the southern Svecofennian volcanic  
belt. *Precambrian Research* 35, 353–365.
- Luukkonen, E., 1992. Late Archaean and Early Proterozoic  
structural evolution in the Kuhmo–Suomussalmi terrain, east-

- ern Finland. *Annales Universitatis Turkuensis Series A*, II 78, 1–37.
- Mäki, T., 1986. Litho-geochemistry of the Pyhäsalmi zinc–copper–pyrite deposit, Finland. *Prospecting in Areas of Glaciated Terrain*. Symposium Proceedings, Sept. 1–2, 1986 Kuopio, Finland. Institution of Mining and Metallurgy, London, pp. 69–82.
- Mäkinen, J., 1987. Geochemical Characteristics of Svecokarelidic Mafic–Ultramafic Intrusions Associated with Ni–Cu Occurrences in Finland. *Bulletin*, vol. 342. Geological Survey of Finland. 109 pp.
- Makkonen, H.V., 1996. 1.9 Ga Tholeiitic Magmatism and Related Ni–Cu Deposition in the Juva Area, SE Finland. *Bulletin*, vol. 386. Geological Survey of Finland. (128 pp.)
- Manninen, T., Huhma, H., 2001. A new U–Pb zircon constraint from the Salla schist belt, northern Finland. *Special Paper*, vol. 33. Geological Survey of Finland, pp. 201–208.
- Mänttari, I., 1995. Lead Isotope Characteristics of Epigenetic Gold Mineralization in the Palaeoproterozoic Lapland Greenstone Belt, Northern Finland. *Bulletin*, vol. 381. Geological Survey of Finland. 70 pp.
- Marshall, B., Smith, J.V., Mancini, F., 1995. Emplacement and implications of peridotite-hosted leucocratic dykes, Vammala Mine, Finland. *Geologiska Föreningens i Stockholm Förhandlingar* 117, 199–205.
- Martinsson, O., 1997. Tectonic setting and metallogeny of the Kiruna greenstones. Ph.D. Thesis, Luleå University of Technology, Sweden, 19. 19 pp.
- Martinsson, O., 2001. Diversity and character of apatite iron ores and their relation to epigenetic Cu–Au deposits in the Norrbotten Fe–Cu–Au province, northern Sweden. *GSA Annual Meeting, Special session: Iron-Oxide(–Copper–Gold) Systems – Deposit Studies to Global Context*, Boston 4 November 2001, *GSA Website Abstracts with Programs*, vol. 33. [http://gsa.confex.com/gsa/2001AM/finalprogram/abstract\\_26785.htm](http://gsa.confex.com/gsa/2001AM/finalprogram/abstract_26785.htm).
- Martinsson, O., Weighed, P., 1999. Metallogeny of juvenile Palaeoproterozoic volcanic arcs and greenstone belts in rifted Archaean crust in the northern part of Sweden, Fennoscandian Shield. In: Stanley, C.J., et al., (Eds.), *Mineral Deposits: Processes to Processing*. A.A. Balkema, Rotterdam, pp. 1329–1332.
- Martinsson, O., Hallberg, A., Broman, C., Godin-Jonsson, L., Kisiel, T., Fallick, T., 1997. Viscaria — a syngenetic exhalative Cu-deposit in the Palaeoproterozoic Kiruna greenstones. In: Martinsson, O., 1997. Tectonic setting and metallogeny of the Kiruna greenstones. Ph.D. Thesis, Luleå University of Technology, Sweden, 19, ISSN:1402.
- Melezhik, V.A., 1996. The geology and ore deposits of the Pechenga greenstone belt. *IGCP Project 336, Field Conference And Symposium*, Rovaniemi, Finland, August 18–30, 1996; *Field Trip Guidebook: Part III*. Geological Survey of Norway, Trondheim. 91 pp.
- Melezhik, V.A., Hudson-Edwards, K.A., Green, A.H., Grinenko, L.N., 1994. The Pechenga area, Russia. 2. Nickel–copper deposits and related rocks. *Transactions, Institute of Mining and Metallurgy (Section B, Applied Earth Science)* 103, 146–161.
- Melezhik, V.A., Grinenko, L.N., Fallick, A.E., 1998. 2000-Ma sulfide concretions from the “Productive” Formation of the Pechenga greenstone belt, NW Russia: genetic history based on morphological and isotopic evidence. *Chemical Geology* 148, 61–94.
- Menard, T., Ridgway, C.K., Stowell, H.H., Leshner, C.M., 1999. Geochemistry and textures of metasomatic combs and orbicules in ultramafic rocks, Namew Lake, Manitoba. *Canadian Mineralogist* 37, 431–442.
- Mints, M.Y., Berzin, R.G., Zamozhnyaya, N.G., Stupak, Y.M., Suleimanov, A.K., Konilov, A.N., Babarina, I.I., 2001. Collision structures in the Early Precambrian crust of the eastern Baltic Shield: a geological interpretation of seismic data along profile 4B. *Doklady Earth Sciences* 379, 515–520.
- Mitrofanov, F.P., Bayanova, T.B., 1999. Duration and timing of ore-bearing Paleoproterozoic intrusions of Kola Province. In: Stanley, C.J., et al., (Eds.), *Mineral Deposits: Processes to Processing*. A.A. Balkema, Rotterdam, pp. 1275–1278.
- Mutanen, T., 1997. Geology and Ore Petrology of the Akanvaara and Koitelainen Mafic Layered Intrusions and the Keivitsa–Satovaara Layered Complex, Northern Finland. *Bulletin*, vol. 395. Geological Survey of Finland. 233 pp.
- Naldrett, A.J., 1989. Magmatic Sulfide Deposits. *Oxford Monographs on Geology and Geophysics*, vol. 14. Oxford University Press. 186 pp.
- Naldrett, A.J., 2001. World-class Ni–Cu–PGE deposits: key factors in their genesis. *Mineralium Deposita* 34, 227–240.
- Nelson, D.R., 2004. Episodic crustal growth during catastrophic global-scale mantle overturn events. In: Eriksson, P.G., Altermann, W., Nelson, D.R., Mueller, W.U., Catuneanu, O. (Eds.), *The Precambrian Earth: Tempos and Events*. Elsevier Science B.V., Amsterdam, pp. 180–183.
- Niiranen, T., Hanski, E., Eilu, E., 2003. General geology, alteration, and iron deposits in Palaeoproterozoic Misi region, northern Finland. *Bulletin*, vol. 75. Geological Society of Finland, pp. 69–92.
- Nironen, M., 1997. The Svecofennian Orogen: a tectonic model. *Precambrian Research* 86, 21–44.
- Nisbet, E.G., Cheadle, M.J., Arndt, N.T., Bickle, M.J., 1993. Constraining the potential temperature of the Archaean mantle: a review of the evidence from komatiites. *Lithos* 30, 291–307.
- Nuutilainen, J., 1968. On the Geology of the Misi Iron Ore Province, Northern Finland. *Annales Academiae Scientiarum Fennicae, Series A III, Geologica–Geographica*. 98 pp.
- Nyström, J.O., Henriquez, F., 1994. Magmatic features of iron ores of the Kiruna type in Chile and Sweden: ore textures and magnetite geochemistry. *Economic Geology* 89, 820–839.
- O’Brien, H.E., Nurmi, P.A., Karhu, J.A., 1993. Oxygen, hydrogen and strontium isotopic compositions of gold mineralization in the Late Archaean Hattu Schist Belt, eastern Finland. In: Nurmi, P., Sorjonen-Ward, P. (Eds.), *Geological Development, Gold Mineralization and Exploration Methods in the Late Archaean Hattu Schist Belt, Ilomantsi, Eastern Finland*. *Special Paper*, vol. 17. Geological Survey of Finland, pp. 291–306.
- Paludan, J., Hansen, U.B., Olesen, N.Ø., 1994. Structural evolution of the Precambrian Bjerkreim–Sokndal intrusion, South Norway. *Norsk Geologisk Tidsskrift* 74, 185–198.
- Pankka, H., 1992. Geology and mineralogy of Au–Co–U deposits in the Proterozoic Kuusamo volcanosedimentary belt, north-

- 3195 eastern Finland. Ph.D. Thesis, Michigan Technological Univer-  
3196 sity. 233 pp.
- 3197 Papunen, H., 1971. Sulfide mineralogy of the Kotalahti and Hitura  
3198 nickel–copper ores, Finland. *Annales Academiae Scientiarum*  
3199 *Fennicae, Series A, III* (109 pp.).
- 3200 Papunen, H., 1989. Platinum-group elements in metamorphosed  
3201 Ni–Cu deposits in Finland. In: Prendergast, M.D., Jones, M.J.  
3202 (Eds.), *Magmatic Sulphides — the Zimbabwe Volume*. Institu-  
3203 tion of Mining and Metallurgy, London, pp. 165–176.
- 3204 Papunen, H., 2003. Ni–Cu sulfide deposits in mafic–ultrama-  
3205 fic orogenic intrusions. Examples from the Svecofennian  
3206 areas, Finland. In: Eliopoulos, D.G., et al., (Eds.), *Mineral*  
3207 *Exploration and Sustainable Development*. Millpress, Rotter-  
3208 dam, pp. 551–554.
- 3209 Papunen, H., Gorbunov, G.I. (Eds.), *Nickel–Copper Deposits of the*  
3210 *Baltic Shield and Scandinavian Caledonides*. Bulletin, vol. 333.  
3211 Geological Survey of Finland. 394 pp.
- 3212 Papunen, H., Vormaa, A., 1985. Nickel deposits in Finland, a review.  
3213 In: Papunen, H., Gorbunov, G.I. (Eds.), *Nickel–Copper Deposits*  
3214 *of the Baltic Shield and Scandinavian Caledonides*, Bulletin,  
3215 vol. 333. Geological Survey of Finland, pp. 123–143.
- 3216 Papunen, H., Halkoaho, T., Tulenheimo, T., Liimatainen, J., 1998.  
3217 Excursion to the Kuhmo greenstone belt. In: Hanski, E., Vuollo,  
3218 J. (Eds.), *International Ophiolite Symposium and Field Excur-  
3219 sion; Generation and Emplacement of Ophiolites through Time;*  
3220 *Abstracts, Excursion Guide, Special Paper, vol. 26*. Geological  
3221 Survey of Finland, pp. 91–106.
- 3222 Parák, T., 1975. The origin of the Kiruna iron ores. *Sveriges*  
3223 *Geologiska Undersökning C 709* (209 pp.).
- 3224 Parman, S., Grove, T.L., Dann, J., 2001. The production of Barber-  
3225 ton komatiites in an Archean subduction zone. *Geophysical*  
3226 *Research Letters* 28, 2513–2516.
- 3227 Peltonen, P., 1990. Metamorphic olivine in picritic metavolcanics  
3228 from Southern Finland. Bulletin, vol. 62. Geological Society of  
3229 Finland, pp. 99–114.
- 3230 Peltonen, P., 1995a. Petrogenesis of ultramafic rocks in the Vam-  
3231 malla Nickel Belt: implications for crustal evolution of the Early  
3232 Proterozoic Svecofennian arc terrane. *Lithos* 34, 253–274.
- 3233 Peltonen, P., 1995b. Crystallization and re-equilibration of zoned  
3234 chromite in ultramafic cumulates, Vammala Ni-Belt, southwes-  
3235 tern Finland. *Canadian Mineralogist* 33, 521–535.
- 3236 Peltonen, P., 2005. Svecofennian mafic–ultramafic intrusions. In:  
3237 Lehtinen, M., Nurmi, P.A., Rämö, O.T. (Eds.), *The Precambrian*  
3238 *Bedrock of Finland — Key to the Evolution of the Fennoscandian*  
3239 *Shield*. Elsevier Science B.V., Amsterdam, pp. 411–446.
- 3240 Perring, C.S., Pollard, P.J., Dong, G., Nunn, A.J., Blake, K.L., 2000.  
3241 The Lightning Creek Sill Complex, Cloncurry District, North-  
3242 western Queensland: a source of fluids for the Fe oxide Cu–Au  
3243 mineralization and sodic–calcic alteration. *Economic Geology*  
3244 95, 1037–1089.
- 3245 Philpotts, A.R., 1967. Origin of certain iron–titanium oxide and  
3246 apatite rocks. *Economic Geology* 62, 303–315.
- 3247 Piirainen, P., 1988. The geology of the Archaean greenstone–gran-  
3248 itoid terrain in Kuhmo, eastern Finland. In: Marttila, E. (Ed.),  
3249 *Archaean Geology of the Fennoscandian Shield; Proceedings of*  
3250 *a Finnish–Soviet Symposium*. Special Paper, vol. 4. Geological  
3251 Survey of Finland, pp. 39–51.
- Porter, T.M., 2000. Hydrothermal iron-oxide copper–gold and  
related ore deposits. In: Porter, T.M. (Ed.), *Hydrothermal Iron*  
*Oxide Copper–Gold and Related Deposits: A Global Perspec-  
tive*. Australian Mineral Foundation, Adelaide, pp. 3–5.
- Poutiainen, M., Grönholm, P., 1996. Hydrothermal fluid evolution  
of the Paleoproterozoic Kutemajärvi gold telluride deposit,  
Southwest Finland. *Economic Geology* 91, 1335–1353.
- Poutiainen, M., Partamies, S., 2003. Fluid inclusion characteristics  
of auriferous quartz veins in Archean and Paleoproterozoic  
greenstone belts of eastern and southern Finland. *Economic*  
*Geology* 98, 1355–1369.
- Puchtel, I.S., Hofmann, A.W., Amelin, Y.V., Garbe Schonberg,  
C.D., Samsonov, A.V., Shchipansky, A.A., 1999. Combined  
mantle plume–island arc model for the formation of the 2.9 Ga  
Sumozero–Kenozero greenstone belt, SE Baltic Shield: isotope  
and trace element constraints. *Geochimica et Cosmochimica*  
*Acta* 63, 3579–3595.
- Puustinen, K., Saltikoff, B., Tontti, M., 1995. Distribution and  
Metallogenic Types of Nickel Deposits in Finland. Report of  
Investigation, vol. 132. Geological Survey of Finland. 38 pp.
- Räsänen, J., Huhma, H., 2001. U–Pb datings in the Sodankylä schist  
area, central Finnish Lapland. In: Vaasjoki, M. (Ed.), *Radiom-  
etric Age Determinations from Finnish Lapland and their*  
*Bearing on the Timing of Precambrian Volcano–Sedimentary*  
*Sequences*. Special Paper, vol. 33. Geological Survey of Fin-  
land, pp. 153–188.
- Rasilainen, K., 1991. Geochemistry and wall rock alteration at the  
Kangasjärvi massive sulphide deposit, Central Finland. In:  
Aufio, S. (Ed.), *Current Research 1989–1990*. Special Paper,  
vol. 12. Geological Survey of Finland, pp. 107–110.
- Rastas, P., Huhma, H., Hanski, E., Lehtonen, M.I., Härkönen, I.,  
Kortelainen, V., Mänttari, I., Paakkola, J., 2001. U–Pb isotopic  
studies on the Kittilä greenstone area, central Lapland, Finland.  
In: Vaasjoki, M. (Ed.), *Radiometric Age Determinations from*  
*Finnish Lapland and their Bearing on the Timing of Precam-  
brian Volcano–sedimentary Sequences*. Special Paper, vol. 33.  
Geological Survey of Finland, pp. 95–141.
- Rickard, D. (Ed.), 1986. The Skellefte Field, *Sveriges Geologiska*  
*Undersökning Ca, vol. 62*. 54 pp.
- Roberts, M., 2002. Architecture, geochemistry and dynamics of  
Palaeoproterozoic seafloor hydrothermal systems preserved in  
a high grade metamorphic terrane, Vihanti–Pyhäsalmi District,  
Central Finland. Ph.D. Thesis, James Cook University, Towns-  
ville, Australia. 407 pp.
- Robins, B., Wilson, J.R., 2001. The Bjerkeim–Sokndal layered  
intrusion. In: Duchesne, J.C. (Ed.), *The Rogaland Intrusive*  
*Massifs, an Excursion Guide*. NGU Report, vol. 29. Geological  
Survey of Norway, pp. 35–37.
- Romer, R.L., Martinsson, O., Perdahl, J.-A., 1994. Geochronology  
of the Kiruna iron ores and hydrothermal alterations. *Economic*  
*Geology* 89, 1249–1261.
- Russell, M.J., Arndt, N.T., 2005. Geodynamic and metabolic cycles  
in the Hadean. *Biogeosciences* 1, 591–624.
- Rutland, R.W.R., Skiöld, T., Page, R.W., 2001. Age of deformation  
episodes in the Palaeoproterozoic domain of northern Sweden,  
and evidence for a pre-1.9 Ga crustal layer. *Precambrian*  
*Research* 112, 239–259.



- 3309 Schärer, U., Wilmart, E., Duchesne, J.C., 1996. The short duration  
3310 and anorogenic character of anorthosite magmatism: U–Pb dat-  
3311 ing of the Rogaland complex, Norway. *Earth and Planetary*  
3312 *Science Letters* 139, 335–350.
- 3313 Schiellerup, H., Lambert, D.D., Prestvik, T., Robins, B., McBride,  
3314 J.S., Larsen, R.B., 2000. Re–Os isotopic evidence for a lower  
3315 crustal origin of massif-type anorthosites. *Nature* 405, 781–784.
- 3316 Scoates, J.S., Chamberlain, K.R., 1997. Orogenic to post-orogenic  
3317 origin for the 1.76 Ga Horse Creek anorthosite complex, Wyom-  
3318 ing, USA. *Journal of Geology* 105, 331–343.
- 3319 Slabunov, A.I., Bibikova, E.V., 2001. The meso- and neo-  
3320 Archaean of the Karelian and Belomorian provinces, Baltic  
3321 Shield (geology, isotope geochemistry and geodynamic recon-  
3322 structions). In: Cassidy, K.F., Dunphy, J.M., van Kranendonk,  
3323 M.J. (Eds.), *Fourth International Archaean Symposium; Extended Abstracts*. Australian Geological Survey Organisation  
3324 Record, pp. 359–361.
- 3325  
3326 Sleep, N.H., Windley, B.F., 1982. Archaean plate tectonics: con-  
3327 straints and inferences. *Journal of Geology* 90, 363–379.
- 3328 Sorjonen-Ward, P., 1993. An overview of structural evolution and  
3329 lithic units within and intruding the Late Archaean Hattu schist  
3330 belt, Ilomantsi, eastern Finland. In: Nurmi, P., Sorjonen-Ward, P.  
3331 (Eds.), *Geological Development, Gold Mineralization and*  
3332 *Exploration Methods in the Late Archaean Hattu Schist Belt*,  
3333 *Ilomantsi, Eastern Finland. Special Paper, vol. 17. Geological*  
3334 *Survey of Finland*, pp. 9–102.
- 3335 Sorjonen-Ward, P., Luukkonen, E., 2005. Archaean rocks. In: Leh-  
3336 tinten, M., Nurmi, P.A., Rämö, O.T. (Eds.), *Precambrian Geol-  
3337 ogy of Finland — Key to the Evolution of the Fennoscandian*  
3338 *Shield. Elsevier Science, B.V., Amsterdam*, pp. 19–99.
- 3339 Sorjonen-Ward, P., Nurmi, P., Härkönen, I., Pankka, H., 1992.  
3340 Epigenetic gold mineralization and tectonic evolution of a  
3341 Lower Proterozoic greenstone terrain in the northern Fennos-  
3342 candian (Baltic) Shield. In: Sarkar, S.C. (Ed.), *Metallogeny*  
3343 *Related to Tectonics of the Proterozoic Mobile Belts. Oxford*  
3344 *and IBH Publishing, New Delhi*, pp. 37–52.
- 3345 Sorjonen-Ward, P., Ord, A., Kontonen, A., Alt-Epping, P., Zhang,  
3346 Y., Kuronen, U., 2004. Geological constraints and numerical  
3347 simulations of the formation and deformation of the Outokumpu  
3348 Cu–Co–Ni–Zn–Au deposits. In: Muhling, J., et al., (Eds.), *Pred-  
3349 ictive Mineral Discovery under Cover. Extended Abstracts*,  
3350 *SEG Meeting, 27 September–1 October 2004. Perth, Western*  
3351 *Australia, Centre for Global Metallogeny, The University of*  
3352 *Western Australia. Publication, vol. 33*, pp. 285–288.
- 3353 Stein, M., Hofmann, A.W., 1994. Mantle plumes and episodic  
3354 crustal growth. *Nature* 372, 63–68.
- 3355 Stein, H., Morgan, J.W., Markey, R.J., Wiszniewska, J., 1998. A  
3356 Re–Os study of the Suwalki anorthosite massif. *Geophysical*  
3357 *Journal* 4, 111–114.
- 3358 Sundblad, K., 1994. A genetic reinterpretation of the Falun and  
3359 Ämmeberg ore types, Bergslagen, Sweden. *Mineralium Depos-  
3360 ita* 29, 170–179.
- 3361 Sundblad, K., 2003. Metallogeny of gold in the Precambrian of  
3362 northern Europe. *Economic Geology* 98, 1271–1290.
- 3363 Svetov, S.A., 2001. Archean high-MgO volcanism in east Fennos-  
3364 candia. In: Cassidy, K.F., Dunphy, J.M., van Kranendonk, M.J.  
3365 (Eds.), *Fourth International Archaean Symposium; Extended*  
*Abstracts. Australian Geological Survey Organisation Record*,  
pp. 199–201.
- Syme, E.C., Bailes, A.H., Price, D.P., Ziehlke, D.V., 1982. Flin Flon  
volcanic belt: geology and ore deposits at Flin Flon and Snow  
Lake, Manitoba. *Field Trip Guidebook, Geological Association*  
of Canada–Mineralogical Association of Canada Joint Meeting,  
Winnipeg. 90 pp.
- Thurston, P.C., Ayres, L.D., 2004. Archean and Proterozoic green-  
stone belts: setting and evolution. In: Eriksson, P.G., Altermann,  
W., Nelson, D.R., Mueller, W.U., Catuneanu, O. (Eds.), *The*  
*Precambrian Earth: Tempos and Events. Elsevier Science B.V.,*  
*Amsterdam*, pp. 311–333.
- Toplis, M., Corgne, A., 2002. An experimental study of element  
partitioning between magnetite, clinopyroxene and iron-bearing  
silicate liquids with particular emphasis on vanadium. *Contribu-  
tions to Mineralogy and Petrology* 144, 22–37.
- Tuisku, P., 1985. The origin of scapolite in the Central Lapland  
schist area, northern Finland, preliminary results. *Bulletin, vol.*  
*331. Geological Survey of Finland*, pp. 159–173.
- Vaasjoki, M., 2001. Three decades of U–Pb mineral analyses at the  
*Geological Survey of Finland. Special Paper, vol. 33. Geologi-  
cal Survey of Finland*, pp. 9–13.
- Vaasjoki, M., Sorjonen-Ward, P., Lavikainen, S., 1993. U–  
Pb age determinations and sulfide Pb–Pb characteristics  
from the Late Archaean Hattu schist belt, Ilomantsi,  
eastern Finland. In: Nurmi, P., Sorjonen-Ward, P. (Eds.), *Geo-  
logical Development, Gold Mineralization and Exploration*  
*Methods in the Late Archaean Hattu Schist Belt, Ilomantsi,*  
*Eastern Finland. Special Paper, vol. 17. Geological Survey of*  
*Finland*, pp. 103–131.
- Vaasjoki, M., Taipale, K., Tuokko, I., 1999. Radiometric ages and  
other isotopic data bearing on the evolution of Archaean crust  
and ore in the Kuhmo–Suomussalmi area, eastern Finland.  
*Bulletin, vol. 71. Geological Society of Finland*, pp. 155–176.
- Vander Auwera, J., Longhi, J., 1994. Experimental study of a  
jotunite (hypersthene monzodiorite): constraints on the parent  
magma composition and crystallization conditions ( $P, T, fO_2$ ) of  
the Bjerkreim–Sokndal layered intrusion. *Contributions to*  
*Mineralogy and Petrology* 118, 60–78.
- Vander Auwera, J., Longhi, J., Duchesne, J.C., 2003. Some results  
on the role of  $P, T$ , and  $fO_2$  on ilmenite composition. *NGU*  
*Special Publication* 9, 35–37.
- Vanhänen, E., 2001. Geology, Mineralogy and Geochemistry of the  
Fe–Co–Au–(U) Deposits in the Paleoproterozoic Kuusamo  
Schist Belt, Northeastern Finland. *Bulletin, vol. 399. Geological*  
*Survey of Finland*. 229 pp.
- Vivallo, W., Claesson, L.-Å., 1987. Intra-arc rifting and massive  
sulphide mineralization in an Early Proterozoic volcanic arc,  
Skellefte District, northern Sweden. In: Pharaoh, T.C., Beckin-  
sale, R.D., Rickard, D. (Eds.), *Geochemistry and Mineralization*  
*Of Proterozoic Volcanic Suites. Geological Society, London*,  
*Special Publications, vol. 33*, pp. 69–79.
- Vlaar, N.J., 1986. Archaean global dynamics. *Geologie en Mij-  
bouw* 65, 91–101.
- Vuollo, J.I., 1994. Paleoproterozoic basic igneous events in eastern  
Fennoscandian Shield between 2.45 Ga and 1.97 Ga, studied by  
means of dyke swarms and ophiolites in Finland. *Acta Univer-*  
3366  
3367  
3368  
3369  
3370  
3371  
3372  
3373  
3374  
3375  
3376  
3377  
3378  
3379  
3380  
3381  
3382  
3383  
3384  
3385  
3386  
3387  
3388  
3389  
3390  
3391  
3392  
3393  
3394  
3395  
3396  
3397  
3398  
3399  
3400  
3401  
3402  
3403  
3404  
3405  
3406  
3407  
3408  
3409  
3410  
3411  
3412  
3413  
3414  
3415  
3416  
3417  
3418  
3419  
3420  
3421  
3422

- 3423 sitatis Ouluensis, Series A, Scientiae Rerum Naturalium, A 250  
3424 (116 pp.).
- 3425 Wager, L.R., Brown, G.M., 1968. Layered Igneous Rocks. Oliver  
3426 and Boyd Ltd., London. 588 pp.
- 3427 Walker, R.J., Morgan, J.W., Hanski, E.J., Smolkin, V.F., 1997.  
3428 Re–Os systematics of Early Proterozoic ferropicrites,  
3429 Pechenga Complex, northwestern Russia: evidence for ancient  
3430 <sup>187</sup>Os-enriched plumes. *Geochimica et Cosmochimica Acta* 61,  
3431 3145–3160.
- 3432 Wanhainen, C., Broman, C., Martinsson, O., 2003. The Aitik Cu–  
3433 Au–Ag Deposit in Northern Sweden: a product of high salinity  
3434 fluids. *Mineralium Deposita* 38, 715–726.
- 3435 Ward, P., 1987. Early Proterozoic deposition and deformation at the  
3436 Karelian craton margin in southeastern Finland. *Precambrian  
3437 Research* 35, 71–93.
- 3438 Wasström, A., 1993. The Knaften granitoids of Västerbotten  
3439 County, northern Sweden. *Sveriges Geologiska Undersökning  
3440 C* 823, 60–64.
- 3441 Weihed, P., 2001. A review of Palaeoproterozoic intrusive hosted  
3442 Cu–Au–Fe-oxide deposits in northern Sweden. *Sveriges Geolo-  
3443 giska Undersökning C* 833, 4–32.
- 3444 Weihed, P., Eilu, P., 2005. Fennoscandian Shield — proterozoic  
3445 VMS deposits. *Ore Geology Reviews* (this volume).
- 3446 Weihed, P., Bergman, J., Bergström, U., 1992. Metallogeny and  
3447 tectonic evolution of the Early Proterozoic Skellefte District,  
3448 northern Sweden. *Precambrian Research* 58, 143–167.
- 3449 Weihed, P., Billström, K., Persson, P.-O., Bergman Weihed,  
3450 J., 2002. Relationship between 1.90–1.85 Ga accretionary  
3478 processes and 1.82–1.80 Ga oblique subduction at the  
Karelian craton margin, Fennoscandian Shield. *GFF* 124,  
163–180.
- Weihed, P., Bergman Weihed, J., Sorjonen-Ward, P., 2003. Struc-  
tural evolution of the Björkdal gold deposit, Skellefte district,  
northern Sweden: implications for Early Proterozoic mesother-  
mal gold in the late stage of the Svecofennian orogen. *Economic  
Geology* 98, 1291–1309.
- Williams, P.J., Guoyi, D., Pollard, P.J., Broman, C., Martinsson, O.,  
Wanhainen, C., Mark, G., Ryan, C.G., Mernagh, T.P., 2003. The  
nature of iron oxide–copper–gold ore fluids. Fluid inclusion  
evidence from Norrbotten (Sweden) and the Cloncurry district  
(Australia). In: Eliopoulos, D.G., et al., (Eds.), *Mineral Explora-  
tion and Sustainable Development*. Millpress, Rotterdam,  
pp. 1127–1130.
- Wilson, J.R., Robins, B., Nielsen, F., Duchesne, J.C., Vander  
Auwera, J., 1996. The Bjerkreim–Sokndal layered intrusion,  
Southwest Norway. In: Cawthorn, R.G. (Ed.), *Layered Intru-  
sions*. Elsevier Science B.V., Amsterdam, pp. 231–256.
- Wiszniewska, J., Claesson, S., Stein, H.J., Vander Auwera, J.,  
Duchesne, J.C., 2002. The north-eastern Polish anorthosite  
massifs: petrological, geochemical and isotopic evidence for a  
crustal derivation. *Terra Nova* 14, 451–460.
- Yngström, S., Nord, A.G., Åberg, G., 1986. A sulphur and  
strontium isotope study of the Aitik copper ore, northern  
Sweden. *Geologiska Föreningens i Stockholm Förhandlingar*  
108, 367–372.